

UNIVERSIDADE DE LISBOA  
INSTITUTO SUPERIOR TÉCNICO

Ambulatory sleep assessment from behavioural and  
physiological data

Alexandre João Borralho Domingues

Supervisor: Prof. João Miguel Sanches  
Co-Supervisor: Prof. Teresa Paiva

Thesis specifically prepared to obtain the PhD Degree in  
Biomedical Engineering

March 2014



# Abstract

This thesis deals with the problem of assessing sleep from a limited array of physiological variables, acquired in non-controlled environments across several days. The described methods are focused on the estimation of sleep and wakefulness states and on the automatic computation of sleep parameters.

So far the most accurate methodology in the diagnosis of sleep disorders is the Polysomnography, where a large number of physiological signals are acquired and analysed by the medical doctor at a sleep laboratory. However, this exam is very complex and uncomfortable to the subject, involving long set-up procedures, complex wiring and a lot of hardware, compromising the subject's mobility and sleep pattern.

The basis of this work consists on a set of statistical models and processing algorithms to characterize nocturnal activity and estimate the temporal pattern of sleep/wakefulness states. This core is expanded, including physiological data, namely Heart Rate and Breathing, to estimate a simplified Hypnogram and three common sleep parameters.

All the described algorithms are validated with real data acquired from recruited volunteers who performed a Polysomnography at a sleep laboratory.

The last topic of the thesis addresses the requirements, limitations and practicalities for the implementation of a portable sleep monitor, used to support the diagnosis of sleep disorders.

**Key-words:** Sleep, Actigraphy, Heart Rate Variability, Breathing, Sleep Parameters, Hypnogram, Portable Monitoring, Hidden Markov Models, Viterbi Algorithm, Classification.



# Resumo

Esta tese aborda o problema da avaliação do sono e seus parâmetros a partir de um conjunto limitado de variáveis fisiológicas, adquiridas em ambientes não controlados ao longo de vários dias. Os métodos descritos focam-se na estimativa dos estados de Sono e Vigília e no cálculo automático de um conjunto restrito de parâmetros do sono.

O exame padrão para a análise e diagnóstico de distúrbios do sono é a Polisomnografia, onde várias variáveis fisiológicas são adquiridas num laboratório do sono e posteriormente analisadas por técnicos especializados. No entanto, este exame é complexo e desconfortável para o sujeito, implicando um longo período de preparação e muito equipamento, afetando fortemente a mobilidade do sujeito e o seu padrão de sono.

Nesta tese, vários modelos estatísticos são propostos para descrever a actividade nocturna, fornecendo a base para um novo método de estimativa do padrão Sono/Vigília. Este algoritmo é em seguida melhorado, passando a integrar dados fisiológicos, nomeadamente a variabilidade cardíaca e a respiração, permitindo a estimativa de um Hipnograma simplificado e a computação automática de três parâmetros do sono.

Todos os algoritmos descritos são validados usando dados adquiridos de um conjunto de voluntários recrutados para realizar uma Polisomnografia.

Por último, os requisitos, limitações e questões práticas para a implementação de uma sistema portátil para monitorização do sono são discutidos.

**Palavras-chave:** Sono, Actigrafia, Variabilidade Cardíaca, Respiração, Parâmetros do Sono, Hipnograma, Monitorização Portátil, Cadeias de Markov, Algoritmo de Viterbi, Classificação.



# Contents

<b>Abstract</b>	<b>iii</b>
<b>Resumo</b>	<b>v</b>
<b>List of figures</b>	<b>ix</b>
<b>List of tables</b>	<b>xii</b>
<b>Acronyms</b>	<b>xv</b>
<b>1 Introduction</b>	<b>1</b>
1.1 Scope and Objectives . . . . .	1
1.2 Thesis Organization . . . . .	4
1.3 Contributions . . . . .	5
<b>2 Sleep</b>	<b>7</b>
2.1 Introduction . . . . .	7
2.1.1 Physiology . . . . .	8
2.1.2 Functions and Origins . . . . .	11
2.1.3 Sleep structure . . . . .	13
2.2 Sleep Pathologies and disorders . . . . .	15
2.3 Diagnosis . . . . .	18
2.3.1 Sleep interview and questionnaires . . . . .	18
2.3.2 Actigraphy . . . . .	19
2.3.3 Polysomnography . . . . .	21
2.3.4 Other methods . . . . .	22
<b>3 Pattern Recognition Background</b>	<b>25</b>
3.1 Introduction . . . . .	25
3.2 Classification . . . . .	26
3.2.1 Linear Discriminant classifier . . . . .	27
3.2.2 Support Vector Machines . . . . .	29
3.2.3 Parzen classifier . . . . .	36
3.3 Classifier performance metrics . . . . .	38
3.4 Hidden Markov Models and optimal state estimation . . . . .	41

## Contents

---

3.4.1	Hidden Markov Models . . . . .	43
3.4.2	Viterbi Algorithm . . . . .	44
<b>4</b>	<b>Behavioural data</b>	<b>49</b>
4.1	The role of Actigraphy in sleep medicine . . . . .	50
4.1.1	Assessment of sleep disorders . . . . .	50
4.1.2	Sleep diaries and Actigraphy . . . . .	51
4.1.3	General Actigraphy guidelines . . . . .	52
4.2	Sleep/Wakefulness estimation from Nocturnal Actigraphy . . . . .	52
4.2.1	Proposed method . . . . .	54
4.2.2	Pre-processing and movement detection . . . . .	55
4.2.3	Nocturnal Movement Characterization . . . . .	57
4.2.4	Feature extraction . . . . .	71
4.2.5	Main classification stage . . . . .	71
4.2.6	HMM regularization algorithm . . . . .	72
4.3	Experimental Results . . . . .	73
4.3.1	Data . . . . .	73
4.3.2	ACT data characterization . . . . .	74
4.3.3	<i>Sleep / Wakefulness</i> discrimination . . . . .	76
4.3.4	Final remarks . . . . .	79
4.4	Conclusions . . . . .	79
<b>5</b>	<b>Physiological data</b>	<b>81</b>
5.1	Autonomic Nervous System . . . . .	82
5.1.1	Structure . . . . .	83
5.1.2	Neurotransmitters . . . . .	83
5.1.3	Sympathovagal balance . . . . .	84
5.2	The Baroreflex . . . . .	84
5.3	Heart Rate Variability . . . . .	86
5.3.1	Origin of the frequency components . . . . .	88
5.3.2	Respiratory Sinus Arrhythmia and Mayer Waves . . . . .	90
5.4	The ANS and sleep . . . . .	91
5.5	Baroreflex Model . . . . .	93
5.5.1	Existing models . . . . .	93
5.5.2	Model description . . . . .	93
5.5.3	Active Orthostatic Test . . . . .	95
5.6	Conclusions . . . . .	97
<b>6</b>	<b>Automatic Sleep Staging</b>	<b>99</b>
6.1	Introduction . . . . .	99
6.2	Method overview . . . . .	101
6.3	Pre-processing . . . . .	102
6.3.1	Detection of QRS complexes and RR tachogram formation . . . . .	102

6.3.2	Actigraphy and RIP pre-processing . . . . .	102
6.4	Feature extraction . . . . .	102
6.4.1	RR features . . . . .	103
6.4.2	RIP features . . . . .	104
6.4.3	RR + RIP features . . . . .	104
6.4.4	ACT features . . . . .	104
6.5	Classification and Feature Selection . . . . .	108
6.6	Hypnogram and sleep parameter estimation . . . . .	109
6.7	Alternative sleep parameter estimation . . . . .	110
6.8	Experimental Results . . . . .	112
6.8.1	Data Sets . . . . .	112
6.8.2	Classifiers Performance . . . . .	113
6.8.3	Hypnogram estimation . . . . .	114
6.8.4	Sleep parameters estimation . . . . .	115
6.8.5	Final Remarks . . . . .	116
6.9	Conclusion . . . . .	118
<b>7</b>	<b>Portable sleep monitoring system</b>	<b>119</b>
7.1	Introduction . . . . .	119
7.2	Body Sensor Networks for health assessment . . . . .	120
7.3	Portable Sleep Monitoring . . . . .	122
7.4	Smart Sleep Monitor . . . . .	124
7.4.1	Structure . . . . .	125
7.4.2	Data acquisition . . . . .	125
7.4.3	Supporting software . . . . .	126
7.4.4	Other applications . . . . .	129
<b>8</b>	<b>Conclusions and Future Work</b>	<b>131</b>
8.0.5	Limitations and guidelines for portable sleep monitor applications . . .	133
<b>A</b>	<b>Actigraphy - Comparative methods</b>	<b>135</b>
A.1	Sadeh's algorithm . . . . .	135
A.2	Hedner's algorithm . . . . .	136
<b>B</b>	<b>International Classification of sleep disorders</b>	<b>137</b>
<b>Bibliography</b>		<b>158</b>



# List of Figures

2.1	The head of Hypnos . . . . .	7
2.2	Nathaniel Kleithman . . . . .	8
2.3	Sleep Regulation . . . . .	9
2.4	Sleep Wake transition . . . . .	11
2.5	EEG activity during sleep . . . . .	14
2.6	Typical Hypnogram . . . . .	15
2.7	Wrist Actigraph . . . . .	20
2.8	ACT data acquired over a 24h period . . . . .	20
2.9	PSG data . . . . .	22
3.1	Linear Discriminative classifier . . . . .	28
3.2	Linear Discriminative classifier:Regularization . . . . .	30
3.3	Support Vector Classifier - Linear Problem . . . . .	30
3.4	Non-linearly separable data . . . . .	33
3.5	SVM kernel trick . . . . .	35
3.6	Parzen density estimation . . . . .	38
3.7	Hidden Markov Model . . . . .	43
3.8	Viterbi algorithm - iterative process . . . . .	47
3.9	Viterbi algorithm - Optimal sequence . . . . .	47
4.1	Actigraphy data . . . . .	50
4.2	Fluxogram of the proposed SW estimation method . . . . .	56
4.3	Structure of the movement detector. . . . .	57
4.4	Determination of the optimal threshold for the movement detector. . . . .	58
4.5	Pre-processed Actigraphy data . . . . .	59
4.6	Length of nocturnal quietness and activity periods. . . . .	60
4.7	Histogram of nocturnal movement data . . . . .	61
4.8	Four different mixture distributions fitted to the ACT data . . . . .	66
4.9	Rayleigh Mixture Model fitted to nocturnal actigraphy . . . . .	67
4.10	AR coefficients - Sleep and Wakefulness . . . . .	70
4.11	RMM and AR features . . . . .	72
4.12	Posture and Movement . . . . .	76
5.1	Structure of the ANS . . . . .	82

## List of Figures

---

5.2	Central regulation of blood flow . . . . .	85
5.3	Heart Rate Variability . . . . .	87
5.4	HRV - Active Orthostatic Test . . . . .	89
5.5	Baroreflex Model . . . . .	94
5.6	Heart Block . . . . .	95
5.7	Active Orthostatic Test - Simulation . . . . .	97
5.8	Active Orthostatic Test - Results . . . . .	97
6.1	Fluxogram of the proposed method . . . . .	101
6.2	Pre-processed data . . . . .	103
6.3	Coupling of breathing and RR signal . . . . .	105
6.4	REM vs Non-REM features. . . . .	106
6.5	Sleep vs Wakefulness Features. . . . .	106
6.6	Rejection of ambiguous samples. . . . .	109
6.7	Estimated Hypnogram . . . . .	114
7.1	Body Sensor Network . . . . .	121
7.2	Structure of the proposed Smart Sleep Monitor . . . . .	125
7.3	Zephyr BioHarness chest strap . . . . .	125
7.4	Sleep monitor based on the BTalino board . . . . .	126
7.5	Sleep electronic Diary structure . . . . .	127
7.6	Dream electronic Diary structure . . . . .	127
7.7	Structure of the main SSM application and aspect of the data acquisition panel. . . . .	128
7.8	HRV differences under different breathing patterns. . . . .	129

# List of Tables

3.1	Support Vector Machine Kernels . . . . .	35
3.2	Confusion matrix . . . . .	39
4.1	Sleep/Wakefulness from Actigraphy: Performance review . . . . .	54
4.2	Rayleigh Mixture Models: Kullback-Leibler divergence . . . . .	66
4.3	Mixture Distributions: Weights and Parameters . . . . .	68
4.4	Actigraphy data: Statistical characterization . . . . .	74
4.5	Naive classifiers performance . . . . .	75
4.6	Performance of MSD algorithm . . . . .	77
4.7	Algorithm performance comparison . . . . .	78
5.1	Model gain factors and time delay parameters used in the simulation. . . . .	96
6.1	List of significant features . . . . .	107
6.2	Performance of the individual classifiers . . . . .	113
6.3	Misclassification and rejection ratios of the binary classifiers . . . . .	114
6.4	Performance of the Hypnogram estimation algorithm. Detection rates for the three considered states with different percentages of rejection. . . . .	115
6.5	HMM parameters - Transition matrix . . . . .	115
6.6	Hierarchical classification. . . . .	116
6.7	Estimated Sleep Parameters . . . . .	117
6.8	Sleep Parameters - Regularization . . . . .	118
7.1	Sampling rate for different physiological signals. . . . .	121

## **List of Tables**

---

# Acronyms

<b>AASM</b> American Academy of Sleep Medicine.	<b>MCS</b> Main Classification Stage.
<b>Acc.</b> Accuracy.	<b>MD</b> Movement Detector.
<b>ACT</b> Actigraphy.	<b>MhD</b> Mahalanobis Distance.
<b>ALS</b> Anterolateral System.	<b>ML</b> Maximum Likelihood.
<b>ANS</b> Autonomous Nervous System.	<b>MSD</b> Movement based State Detection.
<b>AOT</b> Active Orthostatic Test.	<b>MSLT</b> Multiple Sleep Latency Test.
<b>AR</b> Autoregressive model.	<b>MWT</b> Maintenance of Wakefulness Test.
<b>BP</b> Blood Pressure.	<b>NREM</b> Non-REM.
<b>BSN</b> Body Sensor Networks.	<b>NREM<sub>p</sub></b> Non-REM sleep percentage.
<b>CNS</b> Central Nervous System.	<b>NTS</b> Nucleus Tractus Solitarius.
<b>CO</b> Cardiac Output.	<b>OSA</b> Obstructive Sleep Apnea.
<b>CPAP</b> Continuous Positive Airway Pressure.	<b>PAT</b> Peripheral Arterial Tone.
<b>DeD</b> Dream electronic Diary.	<b>PDF</b> Probability Distribution Function.
<b>DS</b> Dynamic Stabilization.	<b>PSG</b> Polysomnography.
<b>ECG</b> Electrocardiography.	<b>PVT</b> Psychomotor Vigilance Task.
<b>EEG</b> Electroencephalography.	<b>RAS</b> Reticular Activating System.
<b>EMG</b> Electromyography.	<b>REM</b> Rapid Eye Movement.
<b>EOG</b> Electrooculography.	<b>REM<sub>p</sub></b> REM sleep percentage.
<b>GSR</b> Galvanic Skin Response.	<b>RF</b> Rejection Factor.
<b>HMM</b> Hidden Markov Model.	<b>RIP</b> Respiratory inductance plethysmography.
<b>HR</b> Heart Rate.	<b>RMM</b> Rayleigh Mixture Model.
<b>HRV</b> Heart Rate Variability.	<b>ROC</b> receiver operating characteristic.
<b>ICSD</b> International Classification of Sleep Disorders.	<b>RSA</b> Respiratory Sinus Arrhythmia.
<b>KL</b> Kullback-Leibler divergence.	<b>RSBD</b> REM Sleep Behavior Disorder.
<b>LDC</b> Linear Discriminant Classifier.	<b>SAN</b> Sinoatrial Node.
<b>MAP</b> Mean Arterial Pressure.	<b>SCN</b> Suprachiasmatic Nucleus.
	<b>SE</b> Sleep Efficiency.
	<b>SeD</b> Sleep electronic Diary.
	<b>Sens.</b> Sensitivity.

## **Acronyms**

---

**SOL** Sleep Onset Latency.

**Spec.** Specificity.

**SSM** Smart Sleep Monitor.

**SVM** Support Vector Machine.

**SW** Sleep / Wakefulness.

**SWS** Slow Wave Sleep.

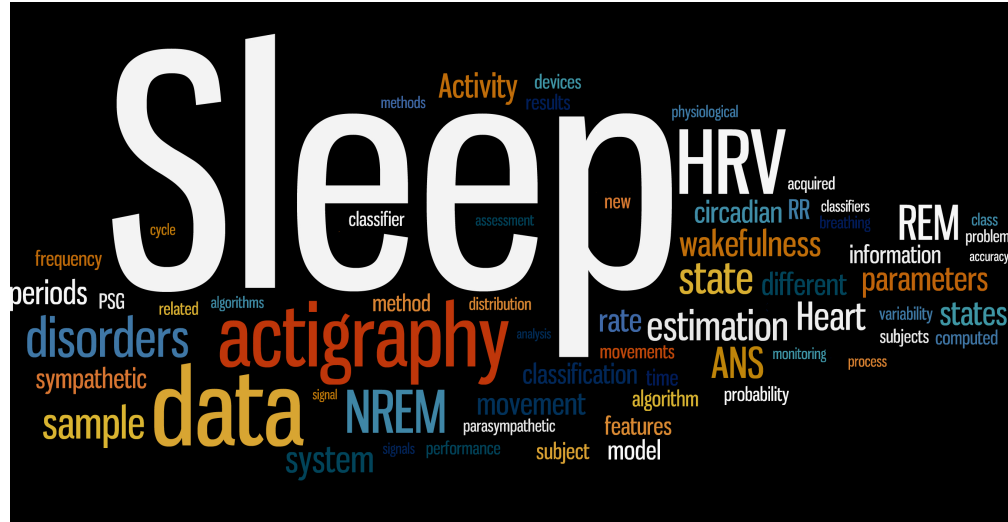
**TST** Total Sleep Time.

**TVAM** Time-Variant Autoregressive Model.

**VLPO** ventrolateral pre-optic nucleus.

**WASO** Wake after Sleep Onset.

# 1 Introduction



## 1.1 Scope and Objectives

Sleep is increasingly recognized as a major issue in public health [3]. Deficient sleep has been related to motor vehicle accidents, industrial disasters, medical errors, decreased productivity and efficiency. It has been identified as a risk factor to many health problems, such as diabetes, depression, obesity and cardiovascular diseases [33, 1]. In a study from 2010 nearly 30% of adults reported an average of less than 6 hours of sleep per day [2], it is believed that, in the US alone, 50 to 70 million people suffer from sleep disorders. Due to its high prevalence in western countries, some authors refer to sleep disorders as a *public health epidemic*.

The increasing burden of sleep disorders and sleep deprivation, together with the limited capacity of health care systems, demands for the adoption of new strategies to minimize the impact of this epidemic. They include the promotion of the awareness in general public to the impact of sleep disorders and the validation and development of new technologies, supporting the existing tools for diagnosis and treatment of sleep disorders.

So far, the most accurate method in the diagnosis of sleep disorders is the Polysomnography (PSG) [3], an exam performed in a sleep laboratory, under controlled conditions, where several physiological signals are acquired to be later analysed by the medical doctor.

However, this exam is very complex, uncomfortable for the patient and has high associated

## **Chapter 1. Introduction**

---

costs, since it involves a lot of hardware and wiring and requires specially adapted installations and trained personnel. Besides compromising the mobility of the subject and interfering with his daily routine, the PSG lacks the ability to perform long term monitoring.

The generalized tendency in western countries to adopt portable and low cost diagnosis solutions, enabling people to "take health care home", has increased the demand for reliable, accurate and portable devices for sleep monitoring. The existing solutions include portable PSGs and a wide range of physiological data recorders, such as blood pressure and Holter monitors, temperature sensors, among others.

Other useful means of diagnosis involve monitoring the behavioural patterns of the patient during his circadian cycle. It can be done using sleep and dream diaries and Actigraphy (ACT). The main advantage of behavioural information is that it can be easily acquired over long periods of time, overcoming one of the limitations of the PSG.

However, the information extracted from single sources of data is limited. A reliable solution must support multi-modal data and robust algorithms to extract the relevant information and provide useful indicators for the clinician.

The great diversity of sleep disorders, which can be radically different in their nature, implies an initial screening process that determines if the subject is indicated for a PSG or for simpler monitoring solutions, such as the above mentioned diaries or ACT.

The purpose of this thesis is to explore the viability of new methods for the assessment of sleep, namely, the use of data easily acquired by portable devices in order to extract indicators and parameters, complementing the standard tools in sleep medicine. The final objective is to provide an intermediate solution between the PSG and the existent portable monitors, providing a robust screening tool for sleep disorders while releasing some of the patient load from the sleep labs. The proposed system includes a small array of physiological data sensors, a set of algorithms responsible for processing the multi-modal data and a supporting portable platform such as a smartphone or tablet.

The research problem starts with the identification of appropriate sources of data, keeping in mind the use of a minimum amount of physiological data, acquired in a continuous basis with light and portable equipment. Then, an adequate classification framework is developed that extracts discriminative features and combines them in a well designed scheme.

The following physiological and behavioural sources of data were selected, and addressed in the thesis, for their reported relevance in the scope of sleep disorders and widespread availability in commercial portable biosignal recorders:

- [Actigraphy] data, measured by an actigraph sensor located at the non dominant wrist of the patient. It reflects the activity of the patient during the day and, more important, during the night.

Several analysis methods are reported in the literature with different agreement rates. The relevance of wrist ACT in the scope of sleep disorders is well established and doc-

umented e.g. in the reviews [4, 5]. The characterization of the circadian cycle [6, 7] and identification of certain disorders such as circadian phase shifts [8] are accurately detected with ACT, but a reliable and accurate estimation of the *Sleep* and *Wakefulness* states is still an open issue and an active field of research.

- [ECG], from which the Heart Rate (HR) and RR intervals are extracted. The Heart Rate Variability (HRV) is known to be related with the activity of the sympathetic and parasympathetic branches of the Autonomous Nervous System (ANS) [9] which in its turn is deeply connected with sleep. An in depth review of the standard measures and physiological interpretation of HRV is made in [10].

Fluctuations in autonomic nervous activity are related to changes in sleep regulation during sleep stages. Analysis of the variability and temporal organization of heartbeat fluctuations across sleep stages, in both young and elderly subjects, were found to exhibit the same ordering and values across sleep stages, forming a robust stratification pattern [11]. A recent review by Stein et al. [12] summarizes the fluctuations observed in healthy adults and subjects suffering a wide range of disorders, including sleep Apnea, periodic limb movements, insomnia, sleep deprivation, among others.

The application of HRV for automatic sleep staging has already been addressed by some authors, recent papers include the work in [13] where the authors achieve an accuracy of 85% in the estimation of *Sleep* and *Wakefulness* states in children, and in [14] the authors use an extended set of features together with a Hidden Markov Model (HMM) and achieve an accuracy of 79% in the discrimination of Rapid Eye Movement (REM) and Non-REM (NREM) states.

- [Breathing] waveform is intimately related to HRV and the ANS. The Respiratory Sinus Arrhythmia (RSA) is a naturally occurring variation in heart rate present during every breathing cycle. While the origin of the RSA is still not fully understood, it is widely used as an index of cardiac vagal function [15].

In [16] the authors show that different sleep stages lead to distinct autonomic regulations of breathing. REM stages are characterized by rapid and irregular breathing, the opposite effect is observed in NREM stages, leading to the well described high frequency components of the HRV during these states.

- [Sleep and Dream diaries] where the patient maintains a register of his activities during the day and night. These diaries are easily implemented and kept for long periods. They are essential tools in sleep medicine evaluation [17, 18].

Other considered sources, although discarded for the applications in this thesis, include the **central temperature**, from which the melatonin secretion can be indirectly estimated and **oxygen saturation** which is mainly needed in apnea conditions.

## **1.2 Thesis Organization**

This thesis is organized as follows: In this chapter, after the problem has been introduced and the thesis structure described, a small description of each chapter is made followed by the listing of the main original contributions.

**Chapter 2** introduces the central topic of the thesis: Sleep. A general overview of its physiology, functions and structure is given, followed by the description of the different sleep disorders categories included in the international classification. The chapter ends with a brief introduction to the available diagnosis means.

**Chapter 3** describes the pattern recognition tools used in the structure of the described algorithms. The mathematical formalism of the used classifiers are presented followed by the discussion of the performance metrics. Finally, HMMs are introduced together with the adopted optimal state sequence estimation algorithm - the Viterbi Algorithm.

**Chapter 4** deals with behavioural data, relevant in the context of sleep. A new approach for nocturnal ACT processing is proposed based on the assumption that the nature of movements recorded during wakefulness and sleep is different. A complete statistical characterization of the data is made and integrated in a HMM supported algorithm in order to estimate sleep and wakefulness states throughout the night.

**Chapter 5** starts with an overview of the ANS and its role in sleep regulation. The relevance of HRV and Respiratory inductance plethysmography (RIP) for sleep assessment is justified based on physiology, reflecting the activity of the ANS. In the end of the chapter, model for the Baroreflex is proposed, where its main components, the heart, vasculature, baroreceptors and ANS, are mathematically described based on physiology. Real data, acquired from a set of volunteers performing an Active Orthostatic Test (AOT), is used to test the model. It is shown that the model is able to reproduce the control mechanisms controlling the Blood Pressure (BP) during an AOT.

**Chapter 6** presents a novel algorithm designed to estimate a simplified 3 state hypnogram (Wakefulness/REM/NREM) and compute a limited set of sleep parameters. The algorithm uses a multi-modal data set, including Electrocardiography (ECG), ACT and RIP. The developed algorithms are tested using a database composed by 20 PSG exams, performed on healthy volunteers, specifically created for this purpose.

**Chapter 7** presents the structure of a portable sleep monitoring system. The requirements of such a system are discussed together with the implementation practicalities. Finally, the elements of the existing prototype are presented.

**Chapter 8** provides a general overview of the obtained results and discusses their significance. Particular attention is given to some of the topics only briefly explored in this thesis and pointers to future research are given.

### **1.3 Contributions**

The elaboration of this thesis required a multi-disciplinary approach. A particular effort was made to support the developed algorithms and models with the physiology underlying the processes. The main contributions of this thesis are the following:

- a new algorithm for Sleep/Wakefulness discrimination from nocturnal activity data. This algorithm incorporates a set of statistical models, describing nocturnal movements recorded using ACT, and a temporal dependence between states.
- a novel model for the ANS and baroreflex that takes into account the physiology of the involved structures. The model is used to explains the long established HRV frequency bands of operation of both branches of the ANS.
- a new algorithm, integrating multi-modal data, that automatically estimates a simplified 3 state hypnogram and several sleep parameters.
- a smartphone based portable system, that integrates the developed algorithms and dream/sleep diaries, allowing long term sleep monitoring with automatically estimation of sleep parameters.
- a new database, built specifically in the scope of this work, consisting of several PSG and ACT exams performed on healthy subjects.

This thesis is based on material from the following papers:

#### **International journals:**

- A. Domingues, T. Paiva and J. M. Sanches. Hypnogram and Sleep parameter estimation from activity and cardiovascular data. *Transactions on Biomedical Engineering*, doi:10.1109/TBME.2014.2301462, 2014. (accepted for publication)
- A. Domingues, T. Paiva and J. M. Sanches. Sleep and Wakefulness State Detection in Nocturnal Actigraphy Based on Movement Characterization. *Transactions on Biomedical Engineering*, vol.61, no.2, pp.426 - 434, 2014.
- A. Domingues, T. Paiva and J. M. Sanches. Statistical Characterization of Actigraphy Data for Sleep/Wake Assessment, *International Journal of Bioelectromagnetism*, Vol. 15, No. 1, pp. 13-19, 2013

#### **International Conference:**

- A. Domingues, T. Paiva, J. Sanches, Sleep parameter estimation from portable data. *Sleep Medicine*, Vol. 14, p. e108, 2013.

## **Chapter 1. Introduction**

---

- A. Domingues, T. Paiva, J. M. Sanches. An actigraphy heterogeneous mixture model for sleep assessment. *34rd Annual International IEEE EMBS Conference* (EMBC 2012), Boston, US, 2012.
- A. Domingues, T. Paiva, J. M. Sanches. Statistical Characterization of Actigraphy Data for Sleep/Wake Assessment. *7<sup>th</sup> International Workshop on Biosignal Interpretation* (BSI2012). Como, Italy, July 2-4, 2012
- A. Ondrej, A. Domingues, T. Paiva, J. M. Sanches. Statistical Characterization of Actigraphy Data during Sleep and Wakefulness States. *32rd Annual International IEEE EMBS Conference* (EMBC 2010), Buenos Aires, Argentina, 2010
- A. Domingues, A. Ondrej, T. Paiva, J. M. Sanches. Automatic Annotation of Actigraphy Data for Sleep Disorder Diagnosis Purposes. *32rd Annual International IEEE EMBS Conference* (EMBC 2010), Buenos Aires, Argentina, 2010

### **National Conference:**

- A. Domingues, T. Paiva, J. M. Sanches. Automatic sleep parameter computation from Activity and Cardiovascular data. *19<sup>a</sup> Conferência Portuguesa de Reconhecimento de Padrões* (RecPad 2013), Lisboa, Portugal, November 1, 2013.
- A. Stembitska, A. Domingues, J. M. Sanches. A mathematical model of the baroreflex physiology: model parameters measurement. *19<sup>a</sup> Conferência Portuguesa de Reconhecimento de Padrões* (RecPad 2013), Lisboa, Portugal, November 1, 2013.
- A. Domingues, T. Paiva, J. M. Sanches. Actigraphy movement classification for sleep/wakefulness discrimination. *18<sup>a</sup> Conferência Portuguesa de Reconhecimento de Padrões* (RecPad 2012), Coimbra, Portugal, October 26, 2012.
- A. Stembitska, A. Domingues, J. M. Sanches. An incremental linear model for the dynamics of the sinoatrial node. *18<sup>a</sup> Conferência Portuguesa de Reconhecimento de Padrões* (RecPad 2012), Coimbra, Portugal, October 26, 2012.
- M. Cânovas , A. Domingues, J. M. Sanches. Ream Time HRV with smartphone. *17<sup>a</sup> Conferência Portuguesa de Reconhecimento de Padrões* (RecPad 2011), Porto, Portugal, 2011.
- A. Domingues, T. Paiva, J. M. Sanches. Sleep and Wakefulness activities: are they intrinsically different? *17<sup>a</sup> Conferência Portuguesa de Reconhecimento de Padrões* (RecPad 2011), Porto, Portugal, 2011.
- A. Domingues, A. Ondrej, T. Paiva, J. M. Sanches. Sleep detection from Actigraphy data. *16<sup>a</sup> Conferência Portuguesa de Reconhecimento de Padrões* (RecPad 2010), Vila Real, Portugal, Oct 2010.

# 2 Sleep

## 2.1 Introduction

Sleep has a fundamental role in human life, throughout his life a typical human will spend approximately 30% of his time sleeping.

The familiar yet mysterious nature of sleep has always fascinated humans. In many ancient cultures, sleep and in particular, dreams, played an important role in the society, as they were considered to bring valuable information. Dreams were looked to for information about hunting, as in some Eskimo and African societies, but also for insights regarding political decisions and ways of healing physical and psychological ills.

Greek mythology is particularly rich in references to sleep. Hypnos, the God of Sleep, was described as an intangible young man with wings attached to his temples or shoulders. He was the father of four other gods, all related with dreams and their creation. One of the most significant visions reported in the old testament, is the message received by the apostle Peter in his dreams, promoting equality among men.

The list of references to sleep and dreams and their influence in the humanity is long, but despite its great significance in human and animal life, our knowledge about how and why we sleep is still far from complete.

Although Neuroscientists can now explain many behaviours based on neurological mechanisms, several questions remain unanswered. Until the 20<sup>th</sup> century, sleep was regarded as a passive phenomenon, simply characterized by the lack of conscience. The lack of technology strongly restricted the accessible information regarding the central nervous system and brain processes underlying the mechanisms for the generation of sleep and wakefulness states.

The partial overcome of the technological limitation throughout the last century led to the



Figure 2.1: The head of Hypnos, the personification of sleep according to Greek Mythology, displayed in the British Museum

accumulation of a large body of knowledge, which, in its turn, revealed another critical factor: **the high complexity of the problem.**

### 2.1.1 Physiology

Sleep is intrinsically connected with biological rhythms, which can be found in animals, plants, fungi and even some kinds of bacteria. These rhythms are commonly divided based on their period: *Infradian rhythms* have periods longer than 24 hours, such as the menstrual cycle, hibernation and migration cycles; *Ultradian rhythms*, refer to cycles with shorter periods such as blinking, heart beats and bowel activity. Cycles having a period of approximately 24 hours are called *Circadian cycles* and include the sleep-wake and body temperature cycles.

The empirical association between the period of circadian cycles and the duration of a day is natural, however, the regulation of the cycle is far more complex. The biological clock regulating these cycles is, in fact, independent of external stimuli, thus being referred to as an *endogenous rhythm*.

The first experiment attempting to separate the endogenous clock from responses to external influences dates back to 1729, when the French scientist Jean-Jacques d'Ortous observed that 24 hour patterns in the movement of the leaves of the plant *Mimosa pudica* continued, even when the plants were kept in constant darkness.



Figure 2.2: Nathaniel Kleithman and Bruce Richardson after 32 days of isolation in the Mammoth Cave, Kentucky.

In 1938, Russian scientist Nathaniel Kleithman spent 32 days in the Mammoth Cave in Kentucky trying to adjust his circadian cycle to a 28 hour cycle. Although the results of the study were not fully conclusive, it motivated further studies such as the one by the German sleep researcher, Jurgen Aschoff, who placed a group of people in a sun-free environment and, by monitoring urine output and body temperature, proved that circadian sleep cycles were not dependent on environmental cues such as sunlight or darkness.

In humans, the central endogenous circadian rhythm generator is located in the Suprachiasmatic Nucleus (SCN), a small region of the hypothalamus situated directly above the optic chiasm [19].

Although the fundamental periods of human circadian rhythms are not exactly 24 hours, they synchronize with the day-night cycle due to external stimuli, called *Zeitgebers*. The main external Zeitgeber is bright light, which is sensed by a small fraction of retinal ganglion cells and conducted to the SCN via the retinohypothalamic tract. The cells of the SCN are then responsible for the synchronization of hormone secretion, core temperature and sleep-wake cycles mediated by various effector systems on the Central Nervous System (CNS), as shown in Figure 2.3

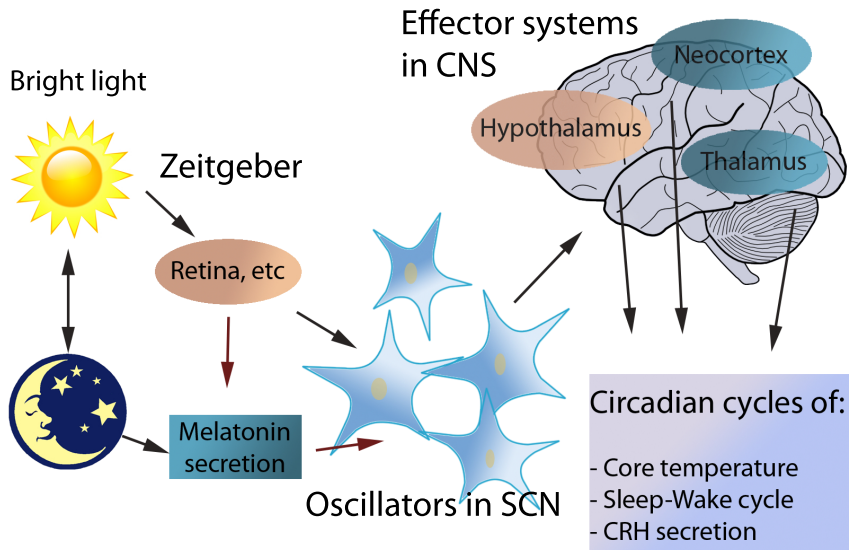


Figure 2.3: Circadian rhythm generation and regulation in the SCN (adapted from [19]).

The mechanisms that control and regulate the reciprocal operation of the sleep-wakefulness cycle are still not fully understood. The concept of sleep homeostasis was introduced by Alexander Borbély in 1980 and described as the "*regulated balance between sleep and waking. Homeostatic mechanisms counteract deviations from an average reference level of sleep.*" This idea was later used as a base to model the regulation of sleep and wakefulness. The **two-process model of sleep regulation**, proposed by Borbély in 1982 [20, 21] states that the sleep-wakefulness cycle is controlled by two processes: a sleep dependent homoeostatic process (Process S) and a sleep-independent circadian process (Process C):

- Process S is dependent on the duration of sleep and wakefulness periods, increasing with the duration of the wakefulness periods (increasing sleepiness) and decreasing during sleep (decreasing the necessity to sleep).
- Process C is the circadian rhythm generated in the SCN, determining the rhythmic propensity to sleep and wakefulness.

According to the two-process model, the timing and structure of sleep are determined by the interaction of the two processes process, determining the cyclic occurrence of sleep during the night period.

Several hypothesis have been proposed for the physiological mechanism that leads to sleep and waking-up. An earlier theory, the Passive Theory, supported that the excitatory areas of the upper brain stem, the Reticular Activating System (RAS), would get fatigued along the day leading to sleep. The discovery that lesions in certain parts of the brain lead to a state of excessive sleepiness, comatose states or inability to sleep has supported the idea that sleep is

## Chapter 2. Sleep

---

an active inhibitory process, controlled by several centres in the brain. It is now accepted that sleep and wake are controlled by a complex interaction between sleep centres (sleep-agonists) and arousal centres (sleep-antagonists) in the brain. The SCN acts as a central convergence point, altering and relaying the information from the sleep and arousal centres.

In general, the firing rate of **sleep antagonist** centres is maximized during wakefulness state, decreasing with sleepiness.

- The RAS, also known as Reticular Formation due to its main structure, is a major region in the brain involved in many different activities, including arousal.
- The *Raphé nucleus* is a subregion of the Reticular Formation associated to arousal [22] with connections to several brain areas including the SCN.
- The *Locus Coeruleus*, also contained within the Reticular Formation, is also implicated in arousal and waking functions [23, 24] with indirect connections to the SCN.
- The *Tuberomammillary Nucleus*, like the other arousal centres, decreases firing with decreased arousal and has the particularity of being the only part of the brain using Histamine as neurotransmitter [25] thus mediating the drowsiness induced by anti-allergic (anti-histamine) drugs.
- Finally, the *Perifornical Lateral Hypothalamus*, the source of Orexin in the mammalian brain. Orexin is a neurotransmitter that regulates arousal, wakefulness, and appetite [26], its influence is well studied in narcolepsy, in which the sufferer briefly loses muscle tone caused by a lack of orexin in the brain.

The *pineal gland* [23, 24] is a hormone based **sleep agonist** that produces and discharges Melatonin directly to the bloodstream. The activity of the *pineal gland* is highly related with the light levels in the surrounding environments, with Melatonin secretion increasing with decreasing levels of light intensity. By circulating in the bloodstream, the Melatonin causes an effect wherever there is a receptor for it. One of the major receptors of Melatonin in the brain is the SCN.

The pre-optic area of the Hypothalamus is also a known sleep-agonist centre, more specifically two small regions, the *medial pre-optic nucleus* and the ventrolateral pre-optic nucleus (VLPO). The hypnotogenic effect of the pre-optic area is thought to be due to the many efferent inhibitory projection to the RAS and possibly to the SCN.

The role of the VLPO in the sleep-wake cycle has been given particular attention in recent years due to its sensibility to Adenosine [27]. Adenosine is directly linked to the energy metabolism of the cells, an increase in neuronal activity enhances energy consumption thus increasing the extracellular concentration of Adenosine, which, in its turn is known to inhibit neuronal activity [28]. During Hypoxia and Ischemia periods, the concentration of Adenosine also increases, this mechanism is believed to have evolved in order to limit brain damage, by drastically reducing the neuronal activity. It has been shown that prolonged wakefulness states

lead to an increase in Adenosine concentrations that only decrease during slow-wave sleep [27]. This fact, together with the observation that Adenosine actively induces sleep [29, 30] supports the role of Adenosine as a "sleep factor", *a factor that accumulates during waking and puts animals and humans to sleep* [31].

The idea of a sleep inducing substance that accumulates during wakefulness has already been suggested by Pappenheimer *et al.* in 1975 [32], who identified a substance accumulating in sleep deprived goats. This substance was referred as *sleep-promoting substance* or *S factor* [33].

The existence of sleep and arousal centres in the brain, their complex interplay, together with the existence of a sleep factors, provides new insight regarding the two-process model of sleep regulation. Figure 2.4 summarizes the mechanisms involved in the sleep-wake cycle..

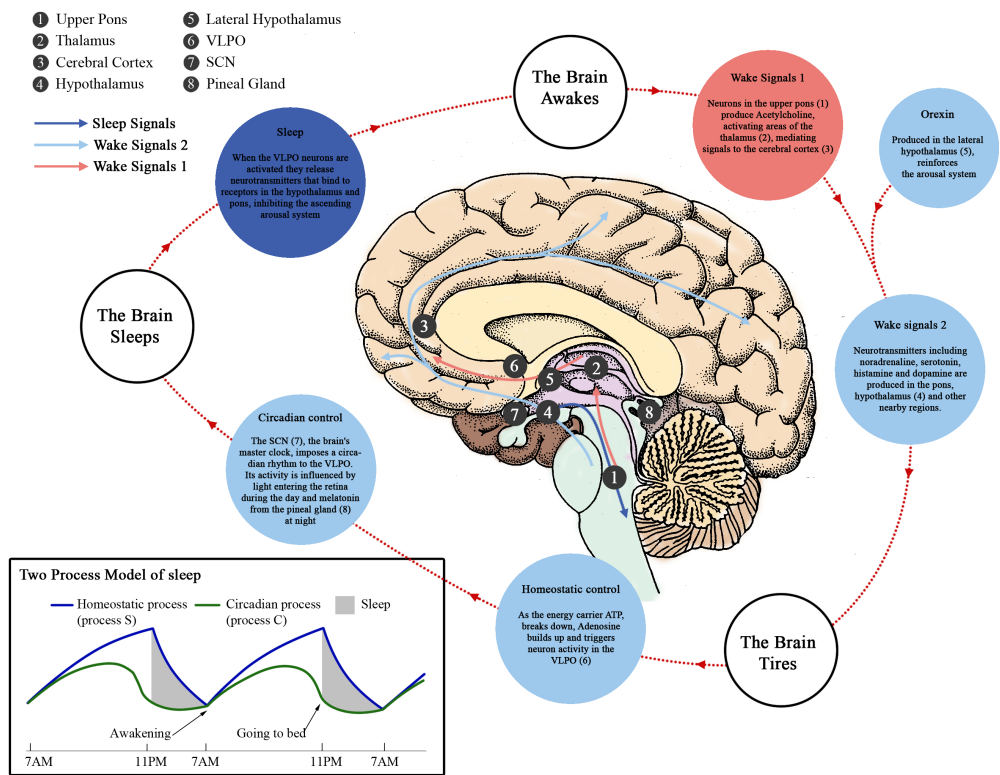


Figure 2.4: Control of the circadian sleep-wake cycle and the two-process model of sleep regulation (bottom)(adapted from [34]).

### 2.1.2 Functions and Origins

The role of sleep in the maintenance of life is closely connected with its origins. Several mechanisms provide clues to its evolutionary advantage.

## Chapter 2. Sleep

---

A commonly accepted theory for its origin is related with energy conservation, inherent to rest/sleep states [35]. Some authors suggest that the temperature regulatory function of the hypothalamus supports that sleep evolved from a primitive mechanism designed to maintain temperature homeostasis [36]. This hypothesis is consistent with phylogenetic and ontogenetic associations between sleep and endothermy, suggesting that sleep evolved in conjunction with endothermy to offset its high energetic cost [37] and with the evidence that some groups of neurons in the hypothalamus have a dual function, being involved in both temperature regulation and sleep. These dual functioning neurons may be the *living evidence of an ancient transition, from mere temperature maintenance to actual sleep* [38]. The correlation between sleep and energy saving strategies have now been extended for ectothermic animals [39].

The enhancement and maintenance of synaptic capability provide another theory for the evolutionary advantage of sleep. Roffwarg et al. [40] related the repetitive excitation of neural circuits, observed in REM sleep, with circuit development and maintenance. This hypothesis provided the foundation for the Dynamic Stabilization (DS) paradigm [41].

According to this model, frequent synaptic activation enhances synaptic strength in neural circuits, storing inherited information and information acquired through experience. DS can occur either through regular functional use or by way of spontaneous oscillatory neural activity. Since these spontaneous activations do not actually trigger the performance of a function, this is the type of DS that is believed to happen in the brain during sleep.

Some authors [42] propose that DS during sleep might have evolved from DS during rest, this fact is supported by the absence of a sleep cycle in some cold-blooded vertebrates having fairly complex brains. According to J. L. Kavanau [41] the growing brain complexity led to an increased need of neuronal circuit development, maturation, fine-tuning, and maintenance which conflicted with neural activities of rest. The conflict between extensive sensory input processing and increasing DS needs provided selective pressure for the evolution of sleep.

The evolution of sleep as a mechanism of synaptic capability enhancement is aligned with its function in metabolic homeostasis. The role of Adenosine in the sleep cycle, addressed in the previous section, supports this hypothesis. In a recent paper by Xie *et al.* [43] the authors show that the restorative function of sleep, is a consequence of the enhanced removal of potentially neurotoxic waste products, that accumulate in the awake central nervous system.

The harmful effects of sleep deprivation on humans and animals is well documented [33, 44]. A rat deprived from sleep will lose the ability to maintain body temperature and die in approximately three weeks, without any evidence of physiological damage [45]. In humans, sleep deprivation or bad sleep hygiene has been related with a propensity to develop diabetes and insulin resistance [46]. The deficit of sleep has been shown to increase the risk of hypertension, affecting particularly women [47, 48].

Increased cardiovascular risk has also been connected with impaired sleep, although the exact process is not known, it is believed to be related with the endogenous circadian clock and its influences on the heart rate [49] and with the influence of sleep in the body's inflammatory

processes [50].

Sleep also has an important role in the maintenance of cognitive and motor functions. In [51] the authors observed that the performance of a driver under strong sleep deprivation is similar to the performance under the influence of alcohol. In [52] the authors show that cumulative nocturnal sleep debt has a dynamic and escalating analog in cumulative daytime sleepiness with strong repercussions on the subjects psicomotor performance.

Hormonal secretion is also closely connected to sleep. The growth hormone (also known as somatotropin or somatropin), secreted during the first stages of sleep, is connected to protein synthesis, growth, bone mineralization, muscular mass increase, immune system stimulation, among others [33]. Other hormones secreted during sleep include prolactine and cortisol in the late stages of sleep.

The risk of obesity has also been related to sleep. Many studies indicate that subjects sleeping less than 5 or 6 or more than 9 hours per day have an increased risk of obesity [33].

The list of risk factors associated to sleep is long, and often correlated, other harmful effects of chronic sleep privation include increased fatigue, depression, anxiety and cancer.

### 2.1.3 Sleep structure

In the third decade of the 20<sup>th</sup> century, German neurologist Hans Berger made the first Electroencephalography (EEG) recordings in humans, calling it *Elektrenkephalogramm* [53].

The discovery of EEG allowed new insights into the nature of sleep. Initial observations recognized distinct amplitude and frequency signatures on sleep and wakefulness states. The high frequency, low amplitude EEG waves, characteristic of wakefulness would progressively be replaced by lower frequency and higher amplitude waves, supposedly following deeper states of sleep.

In the beginning of the decade of 1950, Aserinsky and Kleitman observed the existence of cyclic periods of complete ocular quiescence during sleep, referring to them as "NEM" or "No Eye Movement" periods. Further observations gave emphasis not to the "NEM" periods, but to the approximately twenty minute long periods, of vigorous ocular activity, including saccadic-like eye movements, observed every hour during sleep. This observation marked the discovery of REM sleep. [54, 55].

REM sleep accounts for approximately 20 to 25% of sleep time, with the first period occurring between 60 to 90 minutes after sleep onset. It is characterized by the occurrence of rapid and random movement of the eyes, complete skeletal muscle atonia with sporadic strong muscular contractions. Low voltage EEG activity is abundant, with frequent occurrence of sawtooth waves, and great similarity with Wakefulness EEG activity. REM sleep is marked by strong autonomic variability, reflected in changes of heart rate, breathing frequency and blood pressure [33]. The hypothalamus temperature rises but the thermoregulation mechanisms are disabled, thus leaving the body subject to environmental temperature variations.

Two categories, tonic and phasic, are occasionally distinguished in REM sleep. The distinction

## Chapter 2. Sleep

---

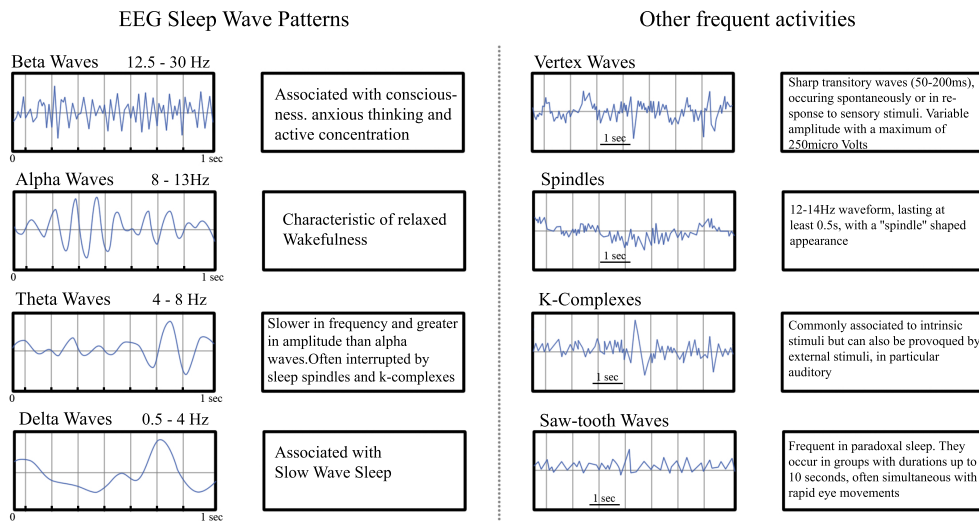


Figure 2.5: Different types of EEG activity during sleep.

is mainly based on the distribution of the eye movements that tend to occur in clusters (phasic) separated by episodes of relative quiescence (tonic).

The mental activity of human REM sleep is associated with emotional and vivid dreams that can be remembered in approximately 80% the times when waking up from this state [56]. For this reason, REM sleep is often referred to as *Oniric sleep*. REM sleep can be roughly characterized as an active brain inside a paralyzed body, for this reason, French Professor Michel Jouvet used the term *paradoxical sleep* to describe it.

NREM sleep accounts for approximately 75 to 80% of sleep time and is divided in 3 distinct phases, N1, N2 and N3, which can be roughly associated with the depth of sleep.

The EEG pattern during NREM sleep is commonly described as synchronous with predominance of low frequencies (Theta and Delta), with characteristic waveforms such as sleep spindles, K-complexes, and high voltage slow waves.

During N1 phase, alpha activity, characteristic of Wakefulness, decreases, being replaced by theta activity. Periods of mixed alpha-theta frequency patterns are common in this phase. Electromyography (EMG) activity decreases and Electrooculography (EOG) shows slow rolling eye movements. Vertex sharp waves are common in the end of N1 stage. Sleep is easily discontinued during stage 1 by external stimuli.

During N2 phase the EEG activity is mainly composed by Theta activity with moderate amplitude with frequent K-complexes and sleep spindles. In this phase, slow eye movements are non-existent and average breathing and heart rates are lower than in Wakefulness. In this phase, sleep is harder to interrupt, stimuli similar to the ones in N1 normally give origin to evoked K-complex but no awakening.

The N3 phase, formerly subdivided in N3 and N4, is also known as Slow Wave Sleep (SWS). High amplitude Delta waves are present in more than 20% of the time with occasional sleep

spindles and k-complexes. No eye movements are registered and muscle tone is reduced.

Besides REM and NREM periods, nocturnal sleep is also marked by small periods of Wakefulness. Sleep related Wakefulness is characterized by persistent Alpha rhythm often corrupted by muscular artefacts, related with posture changes.

Although there is a high intra and inter subject variability in sleep, it is possible to describe a typical structure for nocturnal sleep on healthy individuals. Sleep onset occurs a few minutes after lights out and marks the transition from Wakefulness to N1 stage, in this stage the subject is very sensible to external stimuli. After 1–7 minutes, stage N2 follows and after approximately 20 minutes the subjects enters SWS phase, remaining in this phase for a long period of time (20 – 60 minutes). The progression of sleep stages might be intermittently interrupted by changes in body posture or partial arousals. After the first SWS period, the subject returns to N2, then N1 and a small arousal episode might occur before the first REM episode. The first REM episode is typically small, 1 – 5 minutes, and marks the end of the first sleep cycle, lasting approximately 90 to 110 minutes. The REM-NREM cycle usually repeats 4 to 5 times, with a similar structure. While stage N3 is more prevalent at the beginning of the night (usually during the first NREM-REM cycles), REM sleep is usually of short duration during the initial NREM-REM cycles and lengthens in subsequent cycles [33, 56].

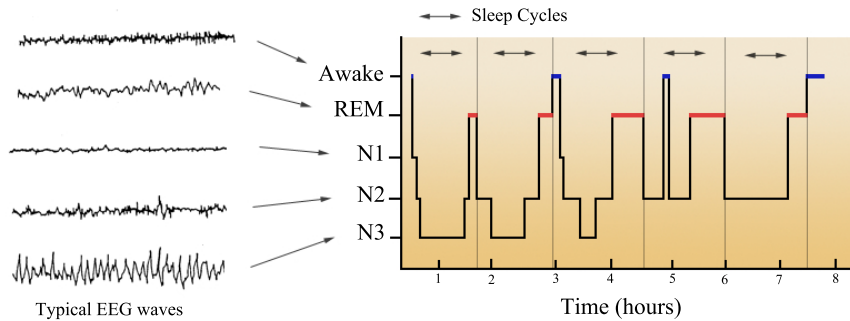


Figure 2.6: The typical hipnogram is composed by approximately 5 REM-NREM cycles (right). Each sleep phase is characterized by a dominant EEG frequency (left).

## 2.2 Sleep Pathologies and disorders

A **Sleep Disorder** or somnopathy is a general term used to define a disorder of sleep patterns, that may be severe enough to interfere with a person's normal physical, mental and emotional functioning. The great variability in symptoms and complaints associated to the different Sleep Disorders lead to the necessity of a systematic approach to organize clinical information and a standard classification scheme for Sleep Disorders.

The International Classification of Sleep Disorders (ICSD), produced by the American Academy of Sleep Medicine, in association with the European Sleep Research Society, the Japanese

## **Chapter 2. Sleep**

---

Society of Sleep Research, and the Latin American Sleep Society, is the authoritative text for clinicians to access information about sleep disorders, criteria for diagnosis and other relevant information imperative for the treatment of their patients. The first version of the ICSD was approved in 1997 and later revised in 2005 (ICSD-2 [57]).

Due to the varied nature of sleep disorders and since the pathophysiology of many disorders is still unknown, the latest version of ICSD uses a complex organization, combining descriptions based on symptoms (e.g. insomnia), pathophysiology (e.g. circadian rhythms disorders) and body systems (e.g., breathing disorders) [44, 33].

The following subsections briefly introduce the eight main categories of sleep disorders included in the ICSD-2, for a detailed list of sleep disorders refer to Table B.1 on Appendix B, for a complete description of each group, consult the original document of the International Classification of Sleep Disorders [57].

### **Insomnias**

This category includes a group of disorders that are characterized by a repeated difficulty with sleep initiation, duration or consolidation and a repetitive lack of sleep quality, that occurs even in friendly environments with adequate conditions, opportunity and time.

The patient typically reports some form of daytime impairment, such as: fatigue or malaise; lack of attention, concentration or memory impairment; social or vacational dysfunction; irritability or mood disturbances; daytime sleepiness, poor motivation and energy; proneness for errors or accidents at work or while driving; tension, headaches and concerns about sleep. The ICSD considers two type of Insomnias, i) primary, when the disorder is not attributable to any medical, psychiatric, or environmental cause and ii) secondary, when the disorders can be associated to other sleep perturbation, medical or psychiatric diseases or dependence on medication.

### **Sleep Related Breathing disorders**

Sleep Related Breathing disorders are characterized by disordered respiration during sleep and include a long list of syndromes with different origins. The sleep related breathing disorders are divided in 4 main groups: *Central Sleep Apnea Syndromes*, *Obstructive Sleep Apnea*, *Sleep-Related Hypoventilation/Hypoxemic Syndromes* and *Other Sleep-Related Breathing Disorders*.

### **Hypersomnias of Central Origin**

The hypersomnia disorders are those in which the primary complaint is daytime sleepiness (defined as the inability to stay alert and awake during the major waking episode) and the cause of the primary symptoms is not disturbed nocturnal sleep (including sleep related breathing disorders) or misaligned circadian rhythms.

Hypersomnias are commonly associated to Narcolepsy but also include other disorders such

## **2.2. Sleep Pathologies and disorders**

---

the Recurrent Hypersomnia, Idiopathic Hypersomnias, Behaviorally Induced Insufficient Sleep Syndrome, Hypersomnias due to medical conditions or drug or substance abuse, among others.

### **Circadian Rhythm sleep disorders**

The circadian rhythm sleep disorders share a common underlying chronophysiological base. The main feature is a persistent or recurrent pattern of sleep disturbance, which is primarily due to alteration of the circadian time-keeping system or a misalignment between the individual's circadian rhythm and external influences that affect the timing of sleep.

Circadian rhythm sleep disorders can be classified as *primary*, that include the common Delayed and Advanced Sleep Phase syndromes, among others and *Behaviorally Induced Circadian Rhythm Sleep Disorders*, which include work and lifestyle related disturbances.

The criteria for the diagnosis of circadian rhythm disorders are the existence of persistent and recurrent sleep pattern disruption/alteration; excessive daytime sleepiness and/or insomnia and a direct association between the sleep disturbances and social/occupational activities.

### **Parasomnias**

Parasomnias are a category of sleep disorders that involve abnormal physical or experimental events that occur during sleep, entering sleep or during arousals. They consist of abnormal sleep-related movements, behaviours, emotions, perceptions, dreaming, and autonomic nervous system manifestations.

The three major divisions for this group are the i) *Disorders of Arousal from NREM Sleep*, including sleepwalking, nocturnal terrors and Confusional Arousals, ii) *Parasomnias Usually Associated with REM sleep* such as the Recurrent Isolated Sleep Paralysis and REM Sleep Behavior Disorder (RSBD) and iii) *Other parasomnias* having no specific relations.

### **Sleep-related Movement disorders**

Sleep-related Movement disorders are mainly characterized by movements that occur during sleep or near sleep onset.

The movements are typically simple and stereotyped, such as short limb twitches. An exception to this characterization is Restless Legs Syndrome, also known as Willis-Ekbom disease, which was included in this category in ICSD-2 due to the close association with Periodic Limb Movement Disorder.

The main difference between Sleep-related Movement disorders and other movement related disorders, e.g. Parasomnias, is that the latter involves complex and goal-directed movement. Another condition for inclusion is that the movement during sleep must be significantly different than during wakefulness, e.g. Sleep-related bruxism.

### Isolated Symptoms

Most of disorders in this group were previously classified as "proposed sleep disorders". Others generally tended to come from various classifications within the parasomnias. According to the ICSD-2 committee, the symptoms included in this group did not have enough scientific basis for decisions regarding whether they were pathological disorders and so it was hard to classify them elsewhere. Common disorders included in this group are Snoring, Sleep Talking and Long/Short Sleepers.

### Other Sleep Disorders

This category includes all the disorders that could not be classified elsewhere by the ICSD-2 Committee. They are defined as *a sleep disorder that overlaps many of the other categories; domains that have new sleep disorders that might be discovered during the lifetime of ICSD-2; and situations in which a category might fulfil the need for sleep disorder diagnoses while insufficient data are available* [57].

## 2.3 Diagnosis

Throughout their lives, every person will likely suffer some kind of sleep disturbance, although not necessarily pathological.

The high incidence of sleep disturbances, common to all races and socio-economic classes, leads to a biased general opinion on what is considered healthy sleep. Thus, many subjects spend their lives with undiagnosed sleep disorders, as they accept those patterns to be normal, never seeking medical care.

The warning signs for disturbed sleep include daytime dysfunctions, such as sleepiness and lack of concentration but also difficulty falling asleep and abnormal nocturnal behaviours. Any of these common complaints may be caused by sleep disorders, such as sleep deprivation, poor sleep hygiene, insomnia, sleep apnea, restless legs syndrome and parasomnias.

The following subsections briefly present the main methods for sleep disorders diagnosis, for an in-depth description please refer to Paiva et. al. [33, pp. 60–182].

### 2.3.1 Sleep interview and questionnaires

The diagnosis process starts with a comprehensive history of the subject, with particular emphasis on sleep but not limited to it. Detailed information on the subjects routine during a typical day often provides clues, as well as the review of medical history, medication, social and family history. A common source of valuable information is the bed-partner, who can provide non-biased insight on the subjects habits and behaviours during the night and day.

Due to the high variability sleep disorders there is no standard physical examination for sleep disorders and the examination is normally tailored to the specific complaints of the subject.

The evaluation of the sleep habits of the subject is fundamental for the initial diagnosis: A subject that sleeps 5 hours per night and complaints about daytime sleepiness is probably suffering of sleep deprivation; A person that systematically goes to bed late at night and has difficulty waking up, feeling rested when sleeping with no time restrictions, suggests a delayed sleep phase syndrome.

The sleep interview or sleep anamnesis is thus a way to collect important cues from the reported habits and complaints that, together, point toward a possible disorder.

The maintenance of a log or diary is a helpful tool in the evaluation of the subjects habits. The most common diaries are the Sleep, Insomnia and Dream diaries.

In the sleep diary, completed over at least 1 or 2 weeks, the subject registers the main events of the daily routine, such as waking up, going to bed, main meals, complaints such as headaches and sleepiness and activities such as sports. These diaries can give the clinician a tremendous amount of information and help the patient realize the necessary improvements by correlating complaints with specific habits. Several sleep diaries structures have been proposed, the most commonly used is the *Karolinska Sleep Diary* [58] which was tested and validated.

The Insomnia diary [59] is kept over at least a week and is composed by several questions regarding schedules, habits and sleep quality. The clinician uses the given information to estimate several parameters including sleep latency, total sleep time, sleep efficiency, among others.

The dream diaries can be written, pictorial or even voice based. As the name implies, the subject maintains a descriptive report of his dreams together with emotional content and intensity.

Several validated sleep questionnaires are commonly used in sleep medicine to assess various parameters. The sleep anamnesis is often performed using the *Sleep Questionnaire and Assessment of Wakefulness* [60], the *Sleep Disorders Questionnaire* [61] and *Sleep Eval* [62]. Other questionnaires target specific parameters such as the quality of sleep (e.g. *Pittsburgh Sleep Quality Index* [17]) and sleepiness (e.g. *Stanford Sleepiness Scale* [63] and *Epworth Sleepiness Scale*[64]) and even specific disorders such as Insomnia, Apnea, Narcolepsy, etc.

Questionnaires and diaries allow the clinician to gather useful information about the subject without significant interference in his life. It is an effective and low cost solution to gain insight into possible sleep disorders.

### 2.3.2 Actigraphy

Sleep Actigraphy is a simple yet powerful technique that allows behavioural information to be acquired, across several days, in a non-cumbersome way. A wrist Actigraph (see Figure 2.7) is basically a 3D accelerometer that continuously monitors human activity, saving the informa-

tion on an internal memory.



Figure 2.7: Wrist Actigraph.

Wrist ACT has received particular attention since the publication, by the *American Sleep Disorders Association*, of the guidelines for its application in clinical environment [65, 66]. Its relevance in the scope of sleep disorders is well documented in several reviews [4, 5, 3, 66], the conclusions are consistent, showing that wrist ACT is a reliable method to assess sleep in healthy populations, having a marked performance decrease in the presence of sleep disorders.

It has a particular relevance monitoring circadian rhythm sleep disorders [6, 7] and in the diagnosis of delayed/advanced sleep phase syndromes. ACT is also a valuable tool to obtain estimates of some sleep parameters, such as sleep efficiency and fragmentation [67], although with some limitations.

The main limitation of ACT is the general tendency to overestimate sleep periods, particularly relevant during daytime with activities such as watching TV or working in a computer, and during the night in the presence of some specific sleep disorders, such as Insomnia, whose subjects tend to stay still even while awake.

Figure 2.8 shows a typical segment of ACT data over a 24 hour period, the rest and activity periods along the circadian cycle are clearly distinguishable.

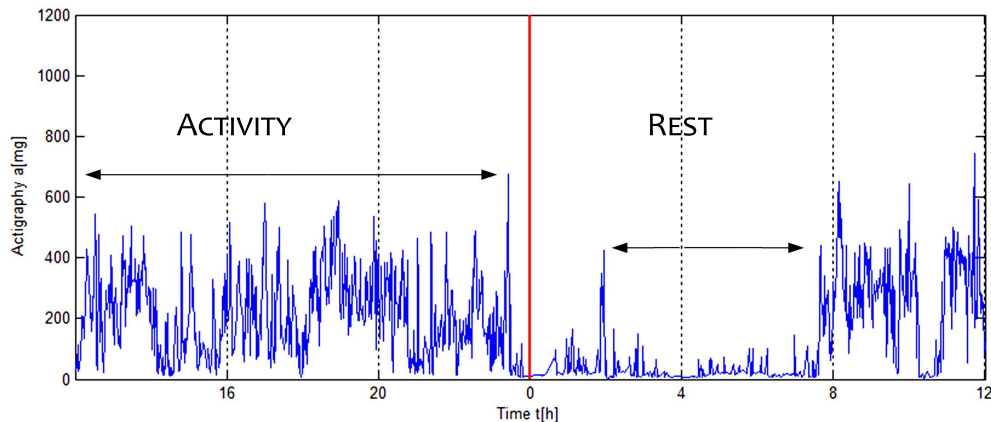


Figure 2.8: ACT data acquired over a 24h period. Rest and activity periods are clearly distinguishable.

Several strategies can be used to mitigate these limitations. The simultaneous use of ACT with sleep diaries [68] and its combination with other sources of physiological data [69] has been shown to improve the reliability of the acquired information.

The development of robust algorithms to process ACT data is an active field of research that is extensively discussed in Chapter 4 and an integrating part of Chapter 6.

### 2.3.3 Polysomnography

The description of a system specifically designed to accurately record and study the patterns of sleep dates back to 1937 [70]. This setup was limited to the recording of EEG but over time more physiologic variables were added, giving rise to modern Polysomnography. A standard PSG typically monitors EEG, EOG, EMG, ECG, respiratory airflow and effort, oxymetry, among others.

The high complexity of this exam, on which a large amount of data is acquired under supervised and controlled conditions, is both the reason of its great reliability, unmatched by any other exam, and the source of its main disadvantages.

Although the PSG is currently the gold standard for sleep disorders diagnosis, it involves some discomfort to the subject, it uses a large array of complex equipment and requires highly trained personnel during the exam, leading to high associated costs.

#### Indications

PSG is the gold standard exam for sleep disorders diagnosis, it is indicated for a large range of symptoms including daytime fatigue or sleepiness, complaints of insomnia, hypersomnia, atypical behaviours during the night such as sleep walking and snoring, among others.

The American Academy of Sleep Medicine (AASM) is responsible for the periodic publication of the "practice parameters for the indications for polysomnography and related procedures", with guidelines for the general use of PSG, different configurations and recommendations for specific disorders, the most recent edition dates back to 2005 [71]. Other complete revision of PSG usage principles can be found in [72].

#### Procedure

Given the wide variety of symptoms and disorders for which a PSG is indicated, its configuration is normally adapted according to the specific requirements. Although the montage used for a given subject may vary depending on the sleep laboratory and clinician, the baseline PSG follows a set of standards defined by the AASM.

The standards defined in [71] classify different types of PSG depending on the number and type of recorded variables, the inclusion of EEG channels and the presence, or not, of a trained technician.

The standard PSG typically includes: central and occipital EEG leads, based on the international 10/20 system; two EOG leads placed slightly above and below the exterior corner of each eye, with a common reference; an EMG lead placed below or over the chin; EMG leads placed over the anterior tibialis muscles and at least 3 ECG leads.

The respiration is usually monitored using a nasal thermistor and/or a nasal cannula pressure transducer and the respiratory effort is measured with Respiratory inductance plethysmography or with impedance pneumography. Finally, pulse oxymetry is also commonly used to

## Chapter 2. Sleep

---

monitor oxygen saturation throughout the night.

Standard PSG, can also include video recording, being referred to as video-polysomnography, which is useful in the case of parasomnias with complex behaviours and in the diagnosis of epilepsy.

The PSG is usually performed in a sleep laboratory with the supervision of a trained technician but unsupervised versions exist, where the subject takes the equipment home. Both methods have advantages and disadvantages.

### Interpretation

Following the polysomnogram acquisition, a trained technician or *scorer* reviews all the data and scores each 30 seconds epoch according to the criteria set by the AASM [73].

The resulting hypnogram is used to compute several sleep parameters, such as the Sleep Onset Latency (SOL), Sleep Efficiency (SE), REM and NREM percentages, etc.

The respiratory signals are screened looking for abnormal breathing related events, such as apneas and hypopneas

The scorer also looks for arrhythmias, seizure activity, bruxism, periodic limb movements and other atypical findings.

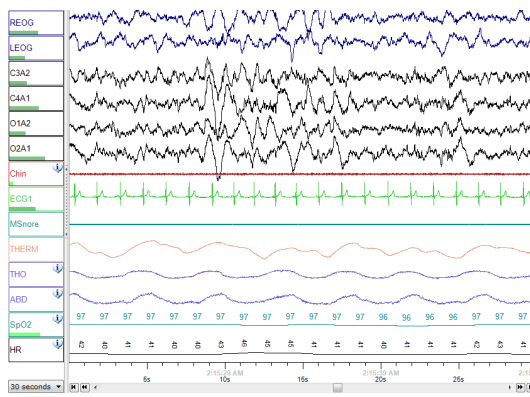


Figure 2.9: One epoch (30s) of PSG data.

Processing PSG data is thus a complex and time consuming procedure that requires highly trained technicians. Although most manufacturers provide software for automatic sleep staging, their performances are still far from the desirable accuracy and reliability.

### 2.3.4 Other methods

Other methods of diagnosis are available when the prognosis points to certain disorders, or when the subject has specific complaints. Reports of excessive daytime sleepiness and fatigue are common at sleep clinics, the evaluation of these symptoms can be performed with several tests, among which the Multiple Sleep Latency Test (MSLT) and the Maintenance of Wakefulness Test (MWT)[74] are the most used.

The MSLT is the standard tool to diagnose narcolepsy and idiopathic hypersomnia and measures how fast a subject falls asleep, in a quiet environment during the day. The MWT measures a subject's ability to stay awake in a quiet, dark room for a period of time, it is typically performed on subjects diagnosed with conditions causing daytime sleepiness such as sleep apnea. Another test designed to assess sleep debt, highly correlated with deteriorated alertness and

declined psycho-motor skills, is the Psychomotor Vigilance Task (PVT). A sustained-attention, reaction-timed task that measures the speed with which subjects respond to a visual stimulus. The Oxford Sleep Resistance test is an alternative to the MWT, where the subject is asked to press a button after a certain stimulus, unlike the PVT, the reaction time is not fundamental, as the test only assesses if the subject is able to remain awake in quiet conditions.

Pupillometry, consisting in the measurement of pupil diameter variations along the day, is commonly used in hypersomnolent patients. Although it has been shown to be a reliable tool to assess sleepiness it is typically not as accurate as the MSLT [75].

The previously described methods are simpler than the gold standard PSG but are mostly constrained to a sleep lab and do not provide much information. Portable solutions, which the subject can take home, also exist. The portable PSG and the Holter monitor are the two most common devices for home monitoring, although the latest is not necessarily related to sleep assessment.

The portable PSG is a simpler version of the standard PSG, the main advantage is that the subject is not restricted to the lab conditions and can sleep in the comfort of his own bed. On the other hand, this portable nature implied that any malfunction of electrode misplacement will not be corrected, which might compromise the validity of the exam. Finally, although the portable PSG allows accurate portable monitoring, it has the same limitation of the standard PSG in what concerns sleep variability across several nights, since the exam is only performed over 1 or 2 nights.

A more complete discussion of portable systems for sleep monitoring is presented in Chapter 7.



# 3 Pattern Recognition Background

## 3.1 Introduction

The field of pattern recognition can be generally defined as a way of making inferences from a given set of data. The considered problems extend across areas with very different natures and can be roughly grouped into *classification*, *parameter estimation* and *state estimation*. The heterogeneous nature of problems dealt by pattern recognition techniques led to a multitude of mathematical tools that are often general enough to be adapted to new problems.

Some algorithms described throughout this thesis, namely the inference of sleep states and sleep parameters, are classical examples of pattern recognition problems. This chapter introduces the mathematical tools that support these algorithms, in particular the ones from Chapters 4 and 6.

The presented material is restricted to the specific tools used in this thesis with and to the required adaptations, when relevant. An exhaustive description of pattern recognition areas and tools is thus outside the scope of this chapter.

This chapter starts by introducing the problem of classification, followed by a detailed description of the classifiers supporting the developed algorithms, namely the Linear Discriminant Classifier (LDC), Support Vector Machine (SVM) and the Parzen classifier.

The performance metrics, used in the evaluation of the algorithms are then discussed. This subject is of particular interest since the usage of proper metrics is fundamental for an unbiased assessment of the algorithms performance.

Finally, the main concepts behind HMMs are described together with the Viterbi algorithm, used for optimal state estimation. HMMs are of particular interest since they are able to model state sequences with temporal dependency, which is the case in sleep state sequence estimation.

## 3.2 Classification

In machine learning and statistics, classification is generally characterized as way to identify a class or label to which a given observation or sample belongs.

In this thesis, the term classification is used in the context of *supervised learning*. This is, a group of labelled data is used to infer a discriminative rule which then allows new, unlabelled data, to be classified into one of the considered classes.

Consider the following set of input or training data,

$$\mathbf{X} = \begin{bmatrix} x_{1,1} & x_{1,2} & \cdots & x_{1,N} \\ x_{2,1} & x_{2,2} & \cdots & x_{2,N} \\ \vdots & \vdots & \ddots & \vdots \\ x_{M,1} & x_{M,2} & \cdots & x_{M,N} \end{bmatrix} \quad (3.1)$$

with labels

$$\mathbf{c} = \begin{bmatrix} c_1, & c_2, & \cdots & c_N \end{bmatrix} \quad (3.2)$$

where  $N$  is the number of training **samples**,  $M$  the number of **features** describing the data and  $c_i$  represents the **class** to which the  $i^{th}$  sample belongs. For the sake of simplicity, in the following sections only two class (binary) problems are considered and  $c_i \in \{-1, 1\}$ .

The general problem of classification is to find a function

$$f : \mathbf{X} \rightarrow \mathbf{c} \quad (3.3)$$

which allows new data to be mapped to the correct class.

Often,  $f$  does not exist due to insufficient information or simply due to the nature of the data, in this case we search for  $f^* : \mathbf{X} \rightarrow \mathbf{c}$  which maximizes the probability of correctly mapping each new sample.

Throughout the development of this thesis several classifiers were tested. However, only the 3 classifiers yielding the best performances and integrating the final versions of the algorithms are described below.

### 3.2.1 Linear Discriminant classifier

A linear classifier, as the name implies, separates the samples to be classified using a linear decision boundary. The general form for a linear discriminant can be represented as

$$y(\mathbf{x}_i) = \begin{bmatrix} w_1 & w_2 & \dots & w_M \end{bmatrix} \begin{bmatrix} x_{1,i} \\ x_{2,i} \\ \vdots \\ x_{M,i} \end{bmatrix} + w_0 \quad (3.4)$$

$$= \mathbf{w}^T \mathbf{x}_i + w_0 \quad (3.5)$$

where  $y$  is the linear discriminant,  $\mathbf{x}_i = [x_{1,i} \dots x_{M,i}]$  is the  $i^{th}$  sample to be classified (consisting of  $M$  features),  $\mathbf{w} = [w_1 \dots w_M]$  a column vector of  $M$  regression weights and  $w_0$  a bias. The binary classifier labels each new sample according to the side of the hyperplane where it falls, the classifier is thus given by

$$f(\mathbf{x}_i) = \text{sign}(\mathbf{w}^T \mathbf{x}_i + w_0). \quad (3.6)$$

The family of linear classifiers is extensive and includes, among others, the *Naive Bayes classifier*, *logistic regression*, the *perceptron*, the SVM and the LDC also commonly known as *Fisher's Linear Discriminant*.

Linear Discriminant Analysis, or in the classifier form, LDC, is a classification method originally developed in 1936 by Fisher [76]. It is simple and mathematically robust, often producing models whose accuracy is as good as more complex methods.

Let us consider a two class discrimination problem, where each class  $C \in \{c_1, c_2\}$  follows a bivariate normal distribution (i.e. each sample is described by two features), with mean

$$\boldsymbol{\mu}_k = \frac{1}{N_k} \sum_{n \in c_k} \mathbf{x}_n \quad (3.7)$$

and  $N^k$  is the number of samples on the  $k^{th}$  class.

The optimal vector of regression weights can be found, for example, maximizing  $\mathbf{w}^T (\boldsymbol{\mu}_2 - \boldsymbol{\mu}_1)$ , subject to  $\|\mathbf{w}\| = 1$  leading to

$$\mathbf{w} \propto (\boldsymbol{\mu}_2 - \boldsymbol{\mu}_1) \quad (3.8)$$

However, if the two classes are not isotropic, the result will most likely not be optimal as shown

in Figure 3.1 A).

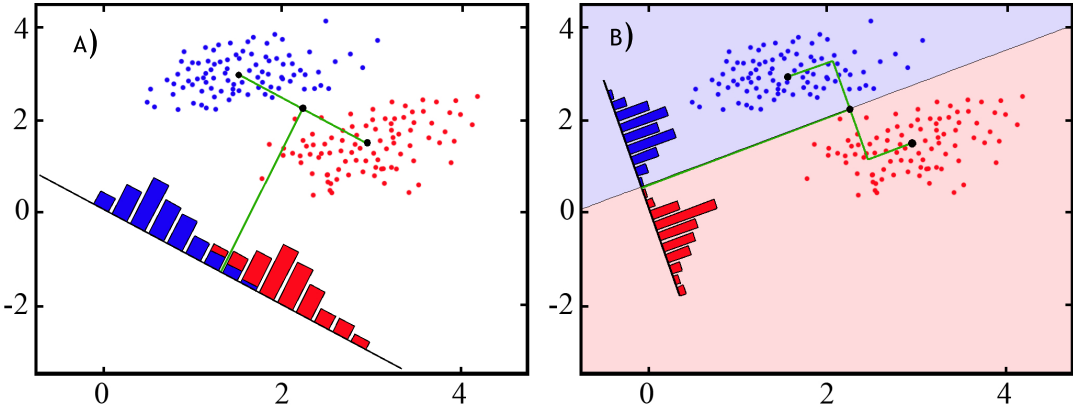


Figure 3.1: Linear Discriminative classifier (or Fisher linear classifier), assuming a binary classification problem where each sample is described by 2 features. A) Assuming isotropic normal distributions, the discriminative functions achieves sub-optimal conditions. B) By projecting the samples in a 1D space, after rotating the axis taking into account the variance of the two classes, the discriminative functions achieves the optimal condition. The classifier will map all samples in the red area in Class 2 and all samples in the blue area in class 1.

By projecting the data into a 1D subspace, the means can be redefined as

$$\mu_k = \mathbf{w}^T \boldsymbol{\mu}_k \quad (3.9)$$

and the within-class variance for each class  $c_k$  becomes

$$\sigma_k^2 = \frac{1}{N_k} \sum_{y_n \in c_k} (y_n - \mu_k)^2. \quad (3.10)$$

The Fisher criterion [76], defined as

$$J(\mathbf{w}) = \frac{(\mu_2 - \mu_1)^2}{\sigma_1^2 + \sigma_2^2} \quad (3.11)$$

can now be rewritten as

$$J(\mathbf{w}) = \frac{\mathbf{w}^T \mathbf{S}_b \mathbf{w}}{\mathbf{w}^T \mathbf{S}_w \mathbf{w}} \quad (3.12)$$

where

$$\mathbf{S}_b = (\boldsymbol{\mu}_2 - \boldsymbol{\mu}_1)(\boldsymbol{\mu}_2 - \boldsymbol{\mu}_1)^T \quad (3.13)$$

$$\mathbf{S}_w = \sum_{n \in c_1} (\mathbf{x}_n - \boldsymbol{\mu}_1)(\mathbf{x}_n - \boldsymbol{\mu}_1)^T + \sum_{n \in c_2} (\mathbf{x}_n - \boldsymbol{\mu}_2)(\mathbf{x}_n - \boldsymbol{\mu}_2)^T \quad (3.14)$$

are the between-class and within-class variances, respectively.

The optimal coefficients are finally obtained maximizing  $J(\mathbf{w})$ , which is maximized to

$$\mathbf{w} \propto \mathbf{S}_w^{-1}(\boldsymbol{\mu}_2 - \boldsymbol{\mu}_1). \quad (3.15)$$

The estimated coefficients vector can now be applied to the expression in (3.6) to obtain the optimal LDC classifier.

In order to allow an extra degree of freedom in the computation of the optimal LDC, two regularization parameters were included. After the computation of the within class variance matrix,  $\mathbf{S}_w$ , two parameters  $R$  and  $S$  ( $0 \leq R, S \leq 1$ ) are used to manipulate this matrix according to the Matlab expression

$$\tilde{\mathbf{S}}_w = (1 - R - S)\mathbf{S}_w + R \begin{bmatrix} S_w^{1,1} & \dots & 0 \\ \vdots & \ddots & \vdots \\ 0 & \dots & S_w^{M,M} \end{bmatrix} + S \frac{1}{M} \sum_{i=1}^M \mathbf{S}_w^{i,i} \begin{bmatrix} 1 & \dots & 0 \\ \vdots & \ddots & \vdots \\ 0 & \dots & 1 \end{bmatrix} \quad (3.16)$$

Figure 3.2 shows the effect of independently changing these parameters. In Chapter 4 this property is used to optimize the classifier toward a specific object function.

### 3.2.2 Support Vector Machines

Support vector machine classifiers, provide a non-probabilistic classification structure which is robust to large sets of data and can learn both simple and highly complex classification models. Although the first references in the literature date back to the 1960's the generalized use of SVM did not happen until the publication, of the paper *A Training Algorithm for Optimal Margin Classifiers*[77], by Boser *et al.* in 1992.

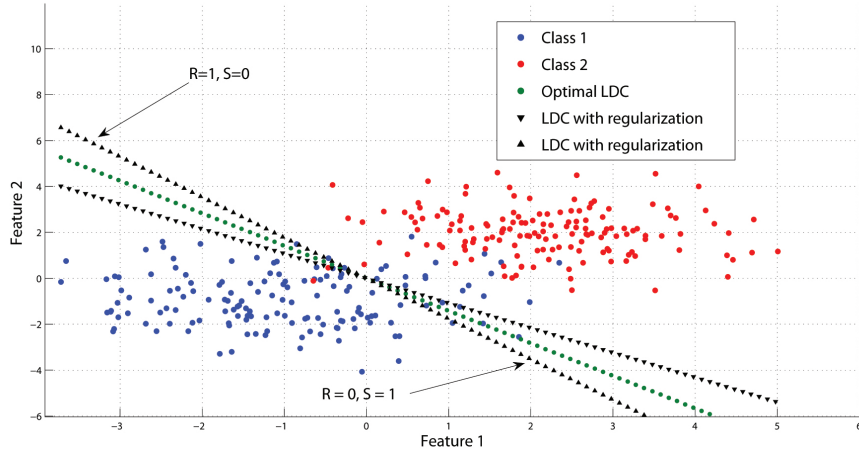


Figure 3.2: Effect of the regularization parameters in the optimal LDC. The dark dotted lines were obtained with  $\{R=0, S=1\}$  and  $\{R = 1, S=0\}$ .

### Linear SVM

The SVM belongs to the class of linear classifiers. As seen in the previous section, the general idea is to find a linear decision surface, or hyperplane, that separates the different classes. Consider a 2 class classification problem, similar to the one explored in the previous sec-

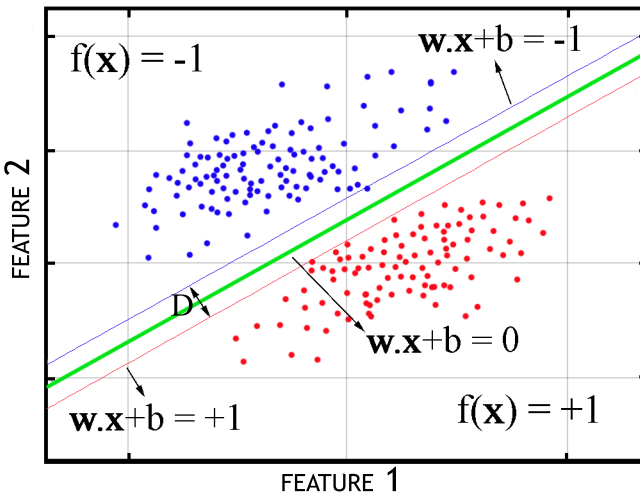


Figure 3.3: Support Vector Classifier - Linear Problem

tion, where each training sample is a vector with the 2 features characterizing the data and  $c_i \in \{-1, 1\}$ . The data, shown in Figure 3.3, is clearly linearly separable, in fact, an infinite number of hyperplanes exist able to separate the data.

In SVM the proper decision surface is found by maximizing the distance  $D$  or *margin*, between the border line samples also called *support vectors*.

The optimal hyperplane takes the form  $\mathbf{w}\mathbf{x} + w_0 = 0$  (see Eq. 3.5). The hyperplanes containing the support vectors are described by  $\mathbf{w}\mathbf{x} + w_1 = -1$ , for class 1, and  $\mathbf{w}\mathbf{x} + w_2 = 1$ , for class 2. The general expression for the distance,  $D$ , between two parallel hyperplanes is given by

$$D = \frac{|w_1 - w_2|}{\|\mathbf{w}\|} \quad (3.17)$$

$$= \frac{2}{\|\mathbf{w}\|} \quad (3.18)$$

The distance between the 2 hyperplanes can thus be maximized solving

$$\hat{D} = \arg \min_{\mathbf{w}, w_0} \|\mathbf{w}\| \quad (3.19)$$

since this expression depends on the norm of  $\mathbf{w}$ , involving a square root, the optimization is difficult to solve. The expression is typically rewritten in an equivalent form as

$$\hat{D} = \arg \min_{\mathbf{w}, w_0} \frac{1}{2} \sum_{i=1}^M w_i^2 \quad (3.20)$$

This minimization is performed under the constraint that every training sample must fall within the proper side of the hyperplane, expressed as

$$\mathbf{w}\mathbf{x}_i + b \leq -1 \quad \text{if } c_i = -1 \quad (3.21)$$

$$\mathbf{w}\mathbf{x}_i + b \geq +1 \quad \text{if } c_i = +1 \quad (3.22)$$

which can be rewritten as

$$c_i(\mathbf{w}\mathbf{x}_i + b) - 1 \geq 0 \quad (3.23)$$

### Primal form

The minimization of the quadratic objective function in 3.20, subject to the linear constraint in 3.23, is a convex quadratic programming optimization problem with  $M$  variables  $w_i, i = [1, \dots, M]$  where  $M$  corresponds to the number of features in the considered problem. This formulation of the optimization problem is called the *primal formulation of linear SVMs*.

### Dual form

The previous optimization problem can be solved applying the method of Lagrange multipliers [78]. The Lagrangian is defined as

$$L(\mathbf{w}, w_0, \boldsymbol{\alpha}) = \frac{1}{2} \sum_{i=1}^M w_i^2 - \sum_{i=1}^N \alpha_i [c_i(\mathbf{w}\mathbf{x}_i - w_0) - 1] \quad (3.24)$$

where  $\boldsymbol{\alpha}$  are the Lagrange multipliers. The expression in 3.24 must be minimized with respect to  $\{\mathbf{w}, w_0\}$  and, simultaneously, require that the derivative with respect to  $\boldsymbol{\alpha}$  is zero under the constraint  $\alpha_i \geq 0$ .

The optimization of 3.24 implies that the samples where  $c_i(\mathbf{w}\mathbf{x}_i - w_0) - 1 > 0$  must correspond to  $\alpha_i = 0$ . The remaining few samples with  $\alpha_i > 0$  are the *support vectors*, which lie on the margin and satisfy  $c_i(\mathbf{w}\mathbf{x}_i - w_0) = 1$ .

Setting the derivatives of  $L(\mathbf{w}, w_0, \boldsymbol{\alpha})$  with respect to  $\{\mathbf{w}, w_0\}$  to 0 we obtain

$$\frac{\partial L(\mathbf{w}, w_0, \boldsymbol{\alpha})}{\partial w_0} = 0 \rightarrow \sum_{i=1}^N \alpha_i c_i = 0 \quad (3.25)$$

$$\frac{\partial L(\mathbf{w}, w_0, \boldsymbol{\alpha})}{\partial \mathbf{w}} = 0 \rightarrow \mathbf{w} = \sum_{i=1}^N \alpha_i c_i \mathbf{x}_i \quad (3.26)$$

(3.27)

By replacing the previous expressions in equation 3.24 we obtain the *dual formulation of linear SVMs*.

The constrained optimization problem is now expressed as

$$\underset{\boldsymbol{\alpha}}{\operatorname{argmax}} \sum_{i=1}^N \alpha_i - \frac{1}{2} \sum_{i,j=1}^N \alpha_i \alpha_j c_i c_j \mathbf{x}_i \mathbf{x}_j \quad (3.28)$$

subject to

$$\alpha_i \geq 0 \quad (3.29)$$

$$\sum_{i=1}^N \alpha_i c_i = 0 \quad (3.30)$$

The solution of the previous problem leads to the optimal classifier in the form of

$$f(\mathbf{x}) = \text{sign}\left(\sum_{i=1}^N \alpha_i y_i \mathbf{x}_i \mathbf{x} + w_0\right). \quad (3.31)$$

Here, the vector of optimal coefficients,  $\mathbf{w}$ , is defined in terms of  $\alpha$  as

$$\mathbf{w} = \sum_{i=1}^N \alpha_i c_i \mathbf{x}_i \quad (3.32)$$

The dual form is the preferred method to optimize the SVM since the number of free parameters to estimate is bounded by the number of support vectors and not by the number of features.

### Soft margin SVM

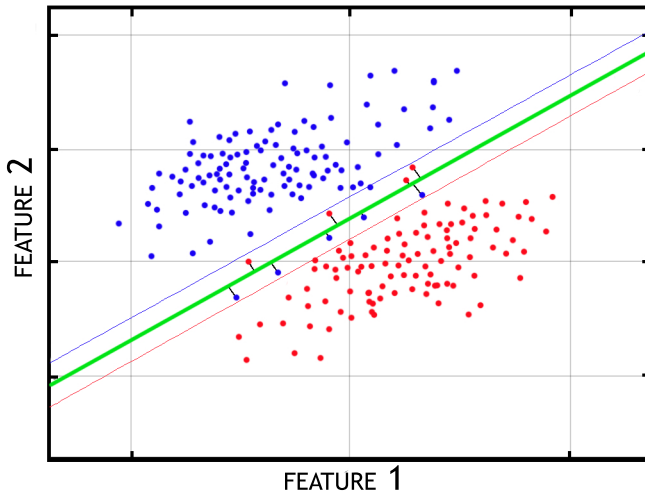


Figure 3.4: Soft-margin linear SVM

The classification problem shown in Figure 3.3 illustrates an optimal scenario, where the data is completely linearly separable, however in most problems this is not the case.

The presence of outliers, noisy measurements or the inherent nature of the data, often creates small non-linearities, as illustrated in Figure 3.4.

SVMs deal with this problem by creating a "slack" variable  $\phi \geq 0$  for each sample, which can be interpreted as the distance to the optimal hyperplane. The value of  $\phi$  will thus be positive if the sample is miss-classified or 0 if the sample is on the correct side of the optimal hyperplane.

### Chapter 3. Pattern Recognition Background

---

The *primal formulation* of the optimization problems becomes

$$\arg \min_{\boldsymbol{w}} \frac{1}{2} \|\boldsymbol{w}\|^2 + C \sum_{i=1}^N \phi_i \quad (3.33)$$

subject to

$$c_i(\boldsymbol{w}\boldsymbol{x}_i + w_0) \geq 1 - \phi_i \quad (3.34)$$

for  $i = [1, \dots, N]$ , and the *dual formulation*

$$\arg \max_{\boldsymbol{\alpha}} \sum_{i=1}^N \alpha_i - \frac{1}{2} \sum_{i,j=1}^N \alpha_i \alpha_j c_i c_j \boldsymbol{x}_i \boldsymbol{x}_j \quad (3.35)$$

subject to

$$0 \leq \alpha_i \leq C \quad (3.36)$$

$$\sum_{i=1}^N \alpha_i c_i = 0 \quad (3.37)$$

#### Kernel trick

In the examples given so far, only linearly or almost linearly separable data was considered. In the cases where a linear decision surface does not exist, such as in the classification problem shown in Figure 3.5 a), SVM maps the data to a higher dimensional space, where the separating decision surface is found. The function that projects the data into the new space is called the kernel.

The kernel function  $\Phi$  transforms a  $\mathbb{R}^M$  space into a higher dimension, this operation corresponds to a dot product in the feature space

$$K(\boldsymbol{x}_i, \boldsymbol{x}_j) = \Phi(\boldsymbol{x}_i)\Phi(\boldsymbol{x}_j) \quad (3.38)$$

The model parameters  $\boldsymbol{w}$  become

$$\boldsymbol{w} = \sum_{i=1}^N \alpha_i c_i \Phi(\boldsymbol{x}_i) \quad (3.39)$$

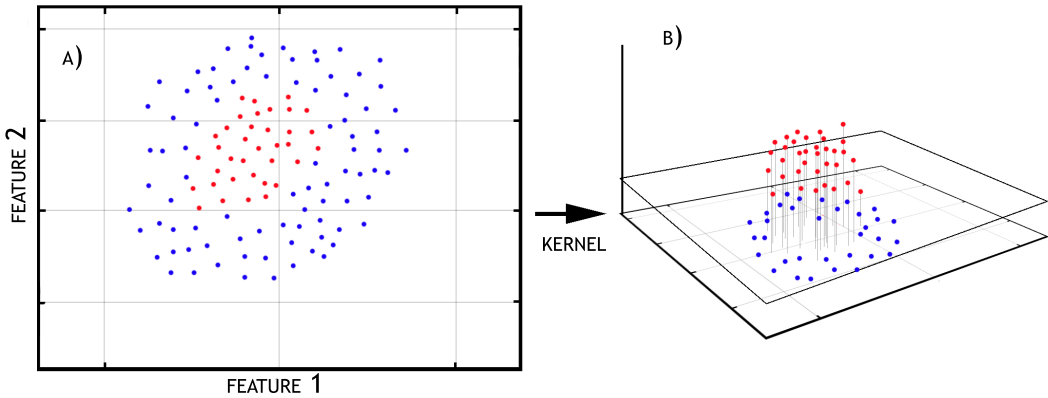


Figure 3.5: a) Data is not linearly separable in the input space. b) data becomes linearly separable in the feature space, obtained by a kernel.

and the optimal classifier function

$$f(\mathbf{x}) = \text{sign}(\mathbf{w}\Phi(\mathbf{x}) + b) \quad (3.40)$$

$$= \text{sign}\left(\sum_{i=1}^N \alpha_i c_i \Phi(\mathbf{x}_i)\Phi(\mathbf{x}) + w_0\right) \quad (3.41)$$

$$= \text{sign}\left(\sum_{i=1}^N \alpha_i c_i K(\mathbf{x}_i, \mathbf{x}) + w_0\right) \quad (3.42)$$

The kernel  $\Phi$  does not need to be explicitly known, as long as the function  $K(., .) : R^N \times R^N \rightarrow R$  can be defined.

Examples of common kernels are shown on Table 3.1. Several kernels were tested for the

$K(\mathbf{x}_i \mathbf{x}_j)$	Kernel
$\mathbf{x}_i \mathbf{x}_j$	Linear
$\exp(-\gamma \ \mathbf{x}_i - \mathbf{x}_j\ ^2)$	Gaussian
$\exp(-\gamma \ \mathbf{x}_i - \mathbf{x}_j\ )$	Exponential
$(p + \mathbf{x}_i \mathbf{x}_j)^q$	Polynomial

Table 3.1: Examples of common kernels used in SVM.

application described in the following chapters, the 2<sup>nd</sup> order Polynomial kernel was selected due to it's highest performance.

### 3.2.3 Parzen classifier

The Parzen classifier is a non-parametric classification method supported by the Parzen-windows density estimation, proposed by Emanuel Parzen [79] in 1962.

The Parzen-window density estimation can be considered as a data-interpolation technique, given a finite number  $N$  of observations of a random variable  $\mathbf{x} = [x_1, \dots, x_N]$ , the method allows the estimation of the Probability Distribution Function (PDF)  $P(x)$  from which the observations were derived. The method works by superposing a *kernel* function on each training observation,  $x_i$  and estimate a PDF from the contribution of each.

The method relies on the fact that the probability  $P$  that a sample falls in a hypercube  $R$ , centred on a given sample  $x$ , is given by

$$P = \int_R p(x) dx \quad (3.43)$$

If the region  $R$  is small enough the probability can be rewritten as

$$P = \int_R p(x) dx \approx p(x) \int_R = p(x)V \quad (3.44)$$

where  $V$  is the volume of region  $R$ .

If  $k$  samples of  $\mathbf{x}$  fall within region  $R$

$$P = \frac{k}{N} \quad (3.45)$$

Thus  $p(x)$  becomes

$$p(x) = \frac{k/N}{V} \quad (3.46)$$

$$= \frac{k}{NV} \quad (3.47)$$

Defining  $h$  as the length of the edge of the hypercube, it follows that  $V = h^2$  for a 2-D square and  $V = h^3$  for a 3-D cube.

The number of samples  $k$  falling inside region  $R$  can be assessed defining

$$\phi\left(\frac{x_i - x}{h}\right) = \begin{cases} 1 & \text{if } \frac{|x_{i,k} - x_k|}{h} \leq \frac{1}{2}, k = \{1, 2\} \\ 0 & \text{if otherwise} \end{cases} \quad (3.48)$$

which indicates whether sample  $x_i$  is inside the region, and iterating over all samples as

$$k = \sum_{i=1}^N \phi\left(\frac{x_i - x}{h}\right) \quad (3.49)$$

Replacing the value of  $k$ , from 3.49 in the expression for  $p(x)$  from 3.46, we obtain the Parzen probability density estimation expression, given by

$$\begin{aligned} p(x) &= \frac{k}{NV} \\ &= \frac{1}{N} \sum_{i=1}^N \frac{1}{h^d} \phi\left(\frac{x_i - x}{h}\right) \end{aligned} \quad (3.50)$$

where  $\phi(\cdot)$  is the window function, or *kernel* in the  $d$ -dimensional space, such that

$$\int \phi(\cdot) = 1 \quad (3.51)$$

The kernel function is typically unimodal. It is also itself a PDF, making it simple to guarantee that the estimated function  $P(\cdot)$  satisfies the properties of a PDF. The Gaussian PDF is a popular kernel for Parzen-window density estimation and it is used in the classification problems in this thesis. It is infinitely differentiable and thereby lending the same property to the Parzen-window PDF estimate  $P(X)$ . Using 3.50, the Parzen-window estimate with a Gaussian kernel becomes

$$P(x) = \frac{1}{n} \sum_{i=1}^n \frac{1}{(h\sqrt{2\pi})^d} \exp\left(-\frac{1}{2}\left(\frac{x-x_i}{\sigma}\right)^2\right) \quad (3.52)$$

where  $\sigma$  is the standard deviation of the Gaussian PDF along each dimension. Figure 3.6 illustrates the estimation of the PDF of a random variable with an unknown distribution.

The Parzen window density estimation can be used as a base to design several classifiers. A simple implementation, used in this thesis, assumes an invariant gaussian kernel and is supported by the estimation of the optimal probability density functions  $\hat{p}(x|C_j)$  where  $C_j$  refers to class  $j$ .

The classification rule is based on the maximum a posteriori, given a new sample to be classified, the optimal class  $\hat{C}$  is chosen applying the following rule

$$\hat{C} = \arg \max_C p(x|C)P(C) \quad (3.53)$$

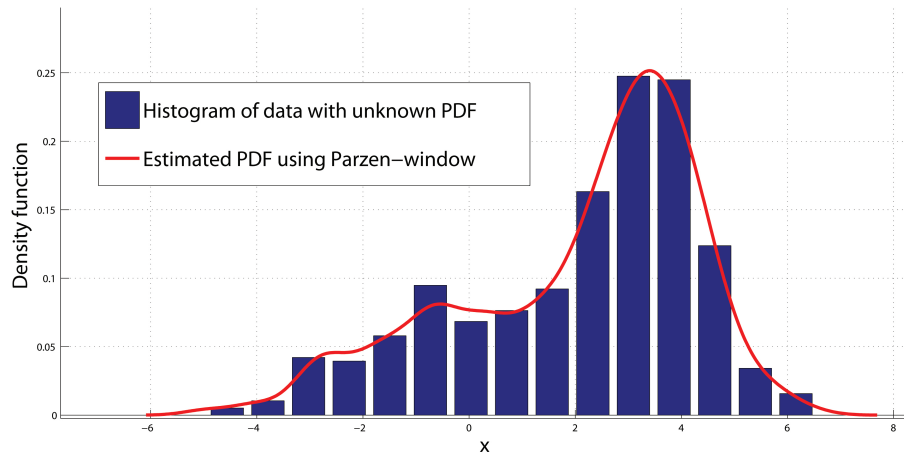


Figure 3.6: Parzen density estimation. (Blue) The histogram represents random data with an unknown probability distribution function; (Red) The estimated probability distribution function using Parzen-window density estimation with a Gaussian kernel.

where  $p(x|C_j)$  represents a non-parametric estimate of the PDF of class  $j$ .

### 3.3 Classifier performance metrics

In the design of a new classifier it is essential to take into account the requirements of the specific problem. In real life, classification problems such as the one shown in Figure 3.1 are unfortunately rare and the design of the classifier requires the definition of acceptable error rates for each class.

For example, a binary classifier that marks patients as positive/negative for a certain disease, must ensure that all, or almost all the pathological patients are properly detected, even if that implies that some healthy patients are miss-classified. On the other hand, a classifier designed to identify a subject so that he/she can have access e.g. to a building, must guarantee that the subject to whom is given clearance is in fact who he claims to be, even if that subject is denied access some times.

The specific prerequisites for different classifiers led to the definition of a large range of metrics to assess their performances, each giving relevance to the most important evaluation parameters. On the other hand, different metrics are often hard to compare, even when dealing with classifiers of the same nature. While the direct comparison of different classifiers/methods is important, the most critical issue lies on the fact that some metrics often hide relevant information, as explained below.

This section starts by briefly presenting the most common methods for classifier performance assessment, Accuracy (Acc.) Sensitivity (Sens.) and Specificity (Spec.), followed by Cohen's Kappa and the G-mean.

### Classical metrics

The classification performance of a given classification system is often represented using a confusion matrix, which contains information about true and predicted classes. The confusion matrix for a binary classifier is shown in Table 3.2, where

		<i>Predicted class</i>	
		Class 1	Class 2
<i>True class</i>	Class 1	TP	FN
	Class 2	FP	TN

Table 3.2: Confusion matrix for a binary classification problem.

- **TP** refers to the number of **true positives**: Samples from Class 1 correctly classified.
- **TN** refers to the **true negatives**: Samples from Class 2 correctly classified.
- **FP** refers to the **false positives**: Samples from Class 2, miss-classified as Class 1.
- **FN** refers to the **false negatives**: Samples from Class 1, miss-classified as Class 2.

The classical classifier performance metrics are derived from the confusion matrix as

$$\text{Accuracy} = \frac{\text{TP} + \text{TN}}{\text{TP} + \text{TN} + \text{FP} + \text{FN}} \quad (3.54)$$

$$\text{Sensitivity} = \frac{\text{TP}}{\text{TP} + \text{FN}} \quad (3.55)$$

$$\text{Specificity} = \frac{\text{TN}}{\text{TN} + \text{FP}} \quad (3.56)$$

Acc. reveals the overall performance of the classification system, Sens. relates with the capability of the system to properly identify samples from Class 1 and Spec. with the system's capability to identify samples from Class 2.

These metrics can be used not only to assess the performance of the classifier but also to fine tune the classifier performance to the specific requirements, by adjusting parameters or changing the optimized objective functions. A common tool for this adjustments, although not used in this thesis, is the receiver operating characteristic (ROC) curve, a plot of the Sens. as a function of 1-Spec..

### Chapter 3. Pattern Recognition Background

---

Other commonly used metrics include

$$\text{PPV} = \frac{\text{TP}}{\text{TP} + \text{FP}} \quad (3.57)$$

$$\text{NPV} = \frac{\text{TN}}{\text{TN} + \text{FN}} \quad (3.58)$$

where PPV or *precision* refers to the *positive predictive value*, i.e. given a sample predicted as Class 1, PPV is the probability of that sample actually belonging to Class 1. NPV or *negative predictive value* answers the opposite questions, given a sample predicted as Class 2, how probable is that the sample actually belongs to Class 2.

### G-mean

Consider a highly unbalanced classification problem, where most samples belong to Class 1, and the following hypothetical confusion matrix

$$\text{cm} = \begin{bmatrix} 320 & 20 \\ 20 & 20 \end{bmatrix} \quad (3.59)$$

The global Acc. is  $\approx 90\%$ , the Sens.  $\approx 94\%$  and the Spec.=  $50\%$ . This example shows that the Acc. alone is not able to properly describe the performance of the classifier. In fact, although the global accuracy is approximately 90% the capability of the classifier to detect Class 2 is only 50%, which is equivalent to chance.

In unbalanced classification problems, such as the ones involving Sleep/Wakefulness or REM/NREM, different metrics are required to properly assess and compare classifiers performances.

Such a metric is the *geometric mean* (G-mean) formulated as

$$\text{G-mean} = \sqrt{\text{Sensitivity} \times \text{Specificity}} \quad (3.60)$$

Applying this metric to the previous confusion matrix we obtain a G-mean of  $\approx 69\%$  which is significantly lower than the global accuracy.

### Cohens K-index

Cohen's kappa statistic, or k-index [80], is commonly used as a statistical measure of inter-rater agreement. It is generally accepted to be more robust to assess classification performance than the simple Acc., in part due to the integration, on its formulation, of the agreement

occurring by chance.

K-index can be used to compare the ability of different raters to classify subjects into one of several groups. It can also be used to assess the agreement between alternative methods of categorical assessment when new techniques are under study. In the context of this thesis, it is used to assess the agreement between the true class and the class predicted by a classifier.

It is computed from the observed and expected frequencies on the diagonal of a confusion matrix. Suppose that there are  $N$  samples belonging to  $C$  distinct classes. Let  $f_{ij}$  denote the number of samples belonging to the  $i^{th}$  Class and classified as Class  $j$ .

The observed proportional agreement between the True and the Predicted classes is defined as

$$p_0 = \frac{1}{N} \sum_{i=1}^C f_{ii} \quad (3.61)$$

which is equivalent to the Acc. expressed in 3.54 for a 2 class problem. The expected agreement by chance is

$$p_e = \frac{1}{N^2} \sum_{i=1}^C f_{i+} f_{+i} \quad (3.62)$$

where  $f_{i+}$  is the total for the  $i^{th}$  row and  $f_{+i}$  is the total for the  $i^{th}$  column of the confusion matrix.

The kappa statistic is finally given by

$$k = \frac{p_0 - p_e}{1 - p_e} \quad (3.63)$$

k-index values can range from  $-1.0$  to  $1.0$ , with  $-1.0$  indicating perfect disagreement below chance,  $0.0$  indicating agreement equal to chance, and  $1.0$  indicating perfect agreement above chance.

k-index is used in this thesis as an alternative for the G-mean, it is computed when relevant for comparison with values reported in the literature.

## 3.4 Hidden Markov Models and optimal state estimation

The classifiers described in the previous sections aim are designed to infer information based on a set of features extracted from a single sample. However, on sequences of data, the

assumption of independent samples is too constrained. The statistical dependence among samples, for example on an image or in a temporal sequence such as the case of sleep states, may bear critical information. A process where the current state is dependent on previous states on a non-deterministic way, is called a stochastic model. The probability of a given state, here defined as  $w$ , is expressed as

$$P(w_n|w_{n-1}, w_{n-2}, \dots, w_1). \quad (3.64)$$

However given a process with  $S$  possible states, the estimation of such a conditional probability distribution implies that the statistics of  $S^{n-1}$  past histories are known, thus leading to highly complex problem.

A **Markov Model** is a stochastic model that assumes the Markov property, i.e., the conditional probability distribution of future states depends only on the current state and not on the past states. The condition probability of the current state becomes

$$P(w_n|w_{n-1}, w_{n-2}, \dots, w_1) \approx P(w_n|w_{n-1}). \quad (3.65)$$

This is called a first-order Markov assumption, the probability of observing given state on instant  $n$  depends exclusively on the state observed on instant  $n - 1$ . While this restriction might seem limited for some applications it has proven to be a good approximation in many problems.

The previous concept can be extended to higher orders, for example, a second-order Markov process models state  $w_n$  as being dependent exclusively on states  $w_{n-1}$  and  $w_{n-2}$ . However, by omission, the expression *Markov Model* always refers to a first-order Markov Model, which is the type used in this thesis. The joint probability of a sequence of states on a Markov Model is thus represented as

$$P(w_1, \dots, w_n) = \prod_{i=1}^n P(w_i|w_{i-1}) \quad (3.66)$$

The expression in 3.66 implies that in order to compute the probabilities of all possible sequences only  $S^2$  statistics must be known. These statistics are organized in a  $S \times S$  square matrix called **transition matrix**,  $\mathbf{P} = \{p_{i,j}\}$ .

Each entry of the transition matrix corresponds to the probability of moving from state  $i$  to state  $j$ , i.e.  $p_{i,j} = P(w_j|w_i)$ . Since the probability of moving from state  $i$  to any other state is 1, this matrix is a right stochastic matrix so that

$$\sum_i p_{i,j} = 1 \quad (3.67)$$

### 3.4.1 Hidden Markov Models

So far, it was assumed that the states modelled by the Markov Model were easily observed. However this is often not the case, several processes have hidden states which generate a series of correlated observations.

For example, a sonar does not know the exact position of an object, but it listens to the echo produced by it. In the context of sleep, it is impossible to know the exact sleep state on which a subject is, but it is possible to infer related information from that state based on physiological signals readings.

A HMM [81] is thus a Markov Model in which the system being modelled has unobserved or *hidden* states . They are an important tool in pattern recognition, having applications in several areas including spacial and temporal pattern recognition such as speech, handwriting, gesture recognition, musical score following and bioinformatics among others.

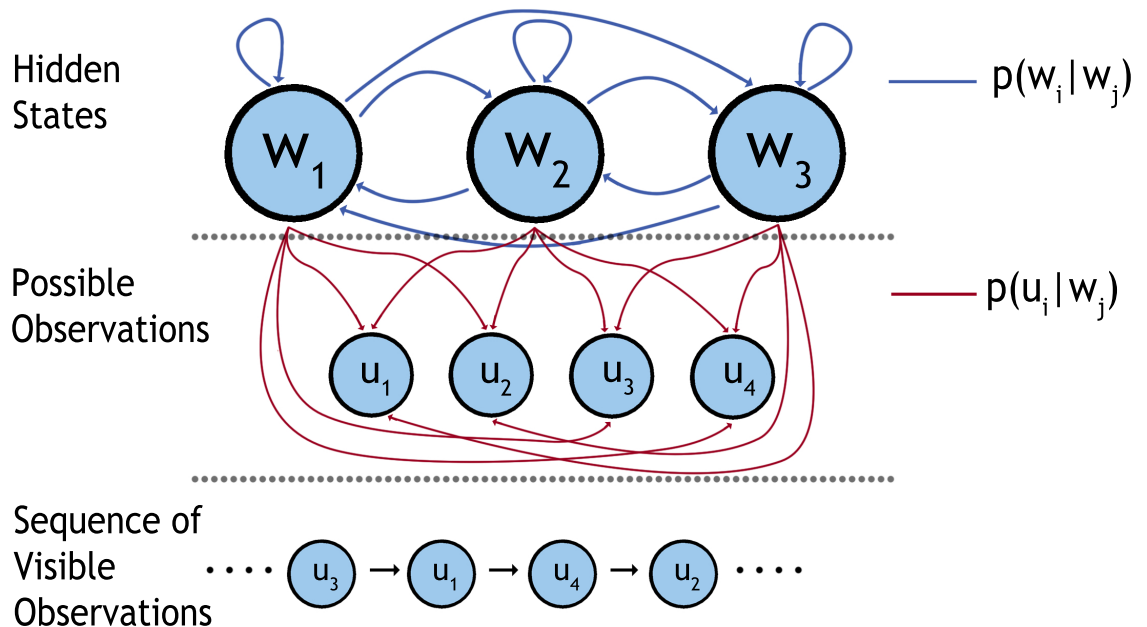


Figure 3.7: Hidden Markov Model.

HMM can be extended from Markov Models by defining an emission matrix  $\mathbf{U} = \{u_{i,j}\}$  where  $u_{i,j} = P(u_i | w_j)$  is the probability of state  $w_j$  emitting an observation  $u_i$ . The joint probability in 3.66 can now be re-written using Bayes Rule as

$$P(w_1, \dots, w_n | u_1, \dots, u_n) = \frac{P(u_1, \dots, u_n | w_1, \dots, w_n)P(w_1, \dots, w_n)}{P(u_1, \dots, u_n)} \quad (3.68)$$

Figure 3.7 summarizes the structure of a HMM, the process follows a sequence of states that are not directly observable, however the transition probability between states is known and each state emits a finite set of observations with a probability associated to each state.

### 3.4.2 Viterbi Algorithm

Assuming a system, modelled using a HMM, three problems are usually considered.

The first deals with training the model parameters, i.e. given a model structure, a sequence of states and respective observations, finding the model parameters that best fit the data. This problem is usually solved with *Maximum Likelihood Estimation*, *Viterbi training* or the *Baum-Welch* algorithm(closely related with the forward-backward algorithm).

The second deals with the problem of evaluating the probability of a given sequence of observations being produced by a particular model. This problem is usually solved using the *forward algorithm*, the *backwards algorithm* or the *Forward-Backward algorithm*. The Forward-Backward algorithm combines a forward step and a backward step to get the probability of being at each state at a specific time. Doing this for all time steps can therefore give a sequence of individually most likely states at each time (although not guaranteed to be a valid sequence, since it considers the individual state at each step, and it can happen that the probability  $p(w_n|w_{n-1}) = 0$  in the transition model).

The last problem deals with estimating the most likely sequence of states given a set of observations and a trained model. This problem is solved using the **Viterbi Algorithm** [82], which is used several times in this thesis and detailed below.

The general idea is to find the optimal sequence of states  $\hat{\mathbf{w}}$  that maximizes the posterior probability  $P(\mathbf{w}|\mathbf{u})$ , this maximization is written as

$$\hat{\mathbf{w}} = \arg \max_{\mathbf{w}} P(\mathbf{w}|\mathbf{u}) \quad (3.69)$$

Solving this problem by "brute-force" would involve searching for all possible sequences, in the order of  $N^S$  (where  $N$  is the number of observations), which would become impossible for relatively small state vector lengths.

The probability  $P(\mathbf{w}|\mathbf{u})$  can be re-written using the Bayes theorem in terms of the observation likelihood,  $P(\mathbf{u}|\mathbf{w})$ , the prior distribution of the states,  $P(\mathbf{w})$ , and the marginal distribution on the observations,  $P(\mathbf{u})$ , as

$$P(\mathbf{w}|\mathbf{u}) = \frac{P(\mathbf{u}|\mathbf{w})P(\mathbf{w})}{P(\mathbf{u})} \quad (3.70)$$

### 3.4. Hidden Markov Models and optimal state estimation

---

Assuming that the observations are independent (each observation depends only on the current state), the observation likelihood can be re-written as

$$\begin{aligned}
 P(\mathbf{u}|\mathbf{w}) &= P(u_N, u_{N-1}, \dots, u_1 | w_N, w_{N-1}, \dots, w_1) \\
 &= P(u_N|w_N)P(u_{N-1}|w_{N-1})\dots P(u_1|w_1) \\
 &= \prod_{n=1}^N P(u_n|w_n)
 \end{aligned} \tag{3.71}$$

The probability of observing the state vector sequence,  $P(\mathbf{w})$ , can also be re-written considering the 1st-order Markov property and the model transition probabilities

$$\begin{aligned}
 P(\mathbf{w}) &= P(w_N, w_{N-1}, \dots, w_1) \\
 &= P(w_N|w_{N-1}, \dots, w_1)P(w_{N-1}|w_{N-2}, \dots, w_1)\dots P(w_2|w_1)P(w_1) \\
 &= P(w_N|w_{N-1})P(w_{N-1}|w_{N-2})\dots P(w_2|w_1)P(w_1) \\
 &= \prod_{n=2}^N P(w_n|w_{n-1})P(w_1)
 \end{aligned} \tag{3.72}$$

The expression in 3.70 can now be re-written as

$$P(\mathbf{w}|\mathbf{u}) = \frac{\prod_{n=2}^N P(u_n|w_n)P(w_n|w_{n-1})P(w_1)}{P(\mathbf{u})} \tag{3.73}$$

The term in the denominator of expression 3.73, the marginal distribution of observations, is normally very hard to compute, however it can be shown that this term is constant, depending only on the model parameters and not changing the maximization process. Thus, the expression in 3.69 may now be written as

$$\begin{aligned}
 \hat{\mathbf{w}} &= \arg \max_{\mathbf{w}} P(\mathbf{w}|\mathbf{u}) \\
 &\approx \arg \max_{\mathbf{w}} P(\mathbf{u}|\mathbf{w})P(\mathbf{w}) \\
 &\approx \arg \max_{\mathbf{w}} P(\mathbf{u}, \mathbf{w}) \\
 &\approx \arg \max_{\mathbf{w}} \prod_{n=2}^N P(u_n|w_n)P(w_n|w_{n-1})P(w_1)
 \end{aligned} \tag{3.74}$$

The extremely small probabilities associated to the computation of the previous expression often lead to underflow problems in computational implementations, it is thus generally

### Chapter 3. Pattern Recognition Background

---

easier to maximize the log probability

$$\hat{\mathbf{w}} = \arg \max_{\mathbf{w}} \sum_{n=2}^N \log(P(u_n|w_n)) + \log(P(w_n|w_{n-1})) + \log(P(w_1)) \quad (3.75)$$

The maximization in 3.75 can be performed with a simple iterative implementation.

Suppose, as an example, a 3 state HMM. The idea is, at each time step  $n$ , find the paths that lead to each state  $w_j, j \in \{1, 2, 3\}$  from the possible old states  $w'_j$  (the notation  $w' = w(n-1)$  is used for simplification).

For each new state, only the path coming from the previous state with the largest probability is kept, this is, for each possible state the following is computed:

$$v_j^n = \max \begin{cases} v_1^{n-1} + \log P(w_j|w_1) + \log P(u_i|w_j) \\ v_2^{n-1} + \log P(w_j|w_2) + \log P(u_i|w_j) \\ v_3^{n-1} + \log P(w_j|w_3) + \log P(u_i|w_j) \end{cases} \quad (3.76)$$

or in a more compact form:

$$v_j^n = \max \left( v_{w'}^{i-1} + \log P(w_j|w') + \log P(u_i|w_j) \right) \quad (3.77)$$

where  $V = \{v_j^n\}, j \in \{1, 2, 3\}, n \in \{1, \dots, N\}$  and  $v_j^n$  corresponds to the maximum cumulative log-probability achieved in the transition from state  $w'$  to  $w_j$  at instant  $n$ .

By recursively maximizing the joint probability for each possible new state the posterior probability of the entire sequence of states is maximized. Figure 3.8 illustrates one single step of this iterative process.

### 3.4. Hidden Markov Models and optimal state estimation

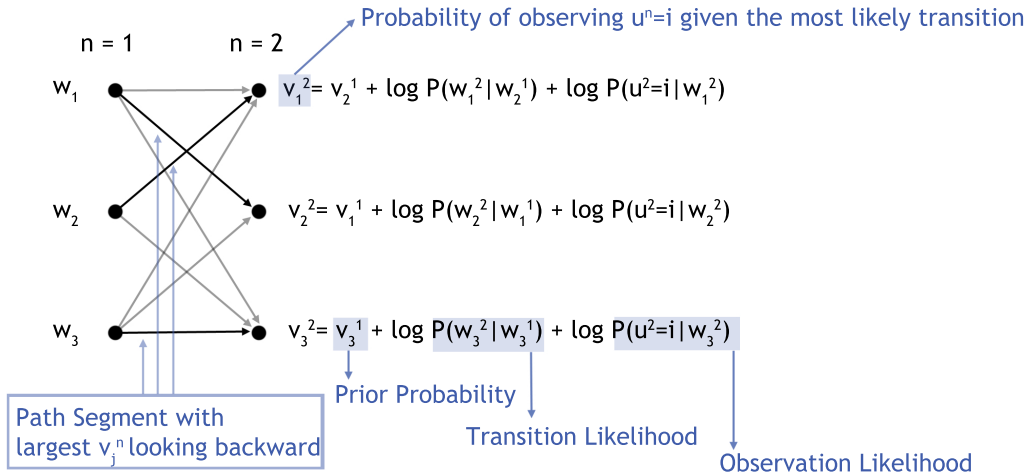


Figure 3.8: One step of the iterative implementation of the Viterbi algorithm.

At each time step  $n$ , the running sum of log-probabilities,  $v_{1,2,3}^{n-1}$ , is used as the prior probability. Then, all the (possible) transitions that lead to each state are examined, keeping only the transitions that yield the highest new log-probabilities  $v_{1,2,3}^n$ . Together with matrix  $V$  a second matrix  $K$  is updated on every iteration, keeping the most likely transition for each state on each time step.

This iterative process runs until the final observation is reached. Then, the state that yields the highest log-probability is selected and matrix  $K$  is used to trace back the most likely sequence of hidden states.

This process is illustrated in Figure 3.9, with the most probable sequence highlighted in blue.

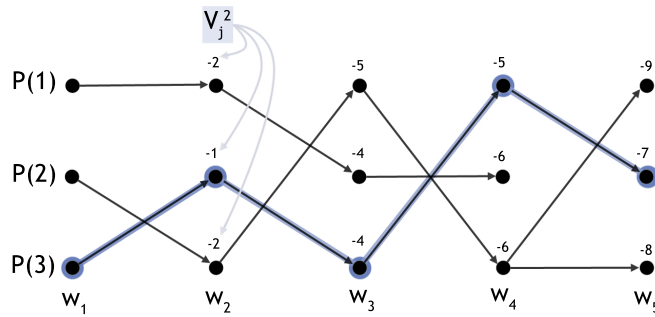


Figure 3.9: The optimal state sequence is found by backtracking the most likely transitions on each time step, starting from the state that yields the highest log-probability



## 4 Behavioural data

Poor sleep habits, or sleep hygiene, is a common problem often connected to sleep disorders. Irregular schedules and routines, lack of exercise, drug over-usage, nocturnal over-stimulation with activities such as TV, computers or strong meals, are some of the extrinsic factors that may lead to sleeping problems. Monitoring the behavioural patterns of subjects suffering from sleep disturbances is thus a common practice in sleep medicine, using tools such as diaries, questionnaires and ACT, as seen in Chapter 2.

The main advantage of these methods is their capability of long term monitoring, enabling the detection of trends often hidden to short-term methods such as the PSG. Other advantages arise from their relative simplicity, they are cheap and allow the subject to perform his daily life without any kind of disruption, leading to no *first night effects* [83].

The acquired behavioural data can be analysed to provide information considering two distinct periods. The first considers the complete day, or one full circadian cycle, as the unit of analysis. By looking at data from several consecutive days it is possible to identify trends in the subjects routine, such as circadian phase shifts, enabling the correlation between daily events and sleep quality/quantity.

The second approach focus on the nocturnal periods, or sleep periods, although not always coincident. Here, the goal is to assess sleep in a more traditional way, such as with the PSG, computing parameters such as the SOL and SE.

While commercial algorithms typically consider and analyse the two periods, the reliability of behavioural data is known to be significantly better in the detection of disorders that manifest along several circadian cycles.

This chapter starts with an overview of the usage of behavioural data, in particular Sleep Diaries and ACT, in the characterization of the circadian cycle. Then the problem of estimating Sleep and Wakefulness periods from nocturnal ACT is addressed. The estimation of a two state hypnogram from ACT is an active field of research, with many interesting nuances that are often neglected.

## 4.1 The role of Actigraphy in sleep medicine

The role of ACT in the study of sleep and circadian rhythms [67, 4, 84, 5] and the practice parameters [85, 66, 65] have been extensively discussed in several reviews. Regular updates take into account the advances in the algorithms and sensor technology, which currently offer several weeks of continuous monitoring. Figure 4.1 shows a 6 days segment of ACT data,

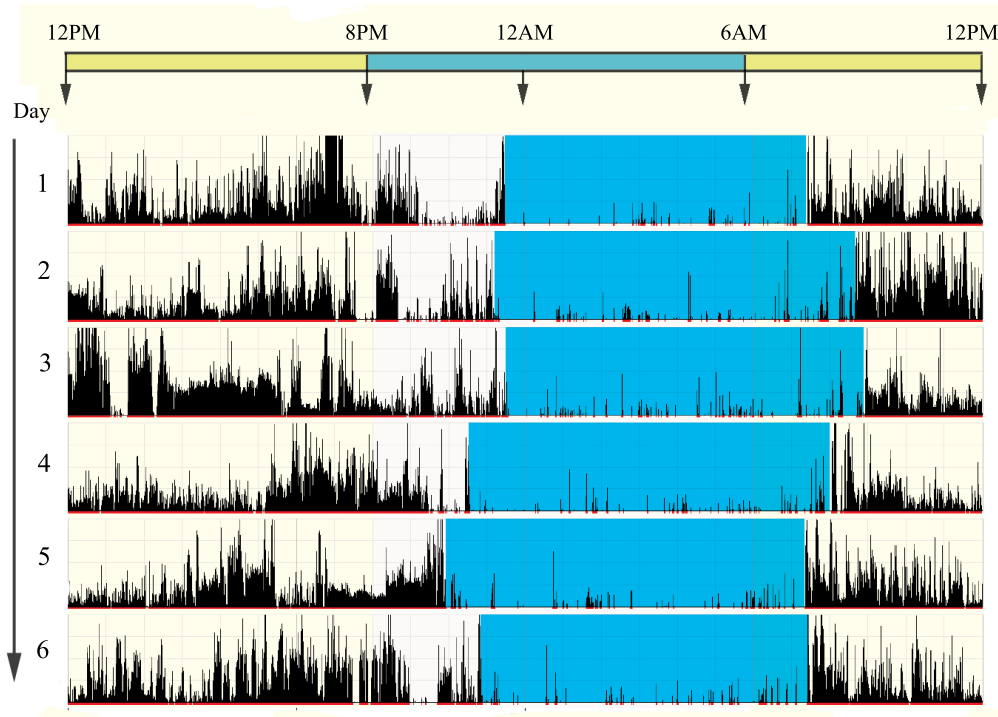


Figure 4.1: Actigraphy data acquired along 6 consecutive days. The estimated sleep periods are marked in blue.

with the automatically estimated sleep periods marked in blue. Despite the limitations in the precise estimation of Sleep / Wakefulness (SW), discussed in the next section, the level of activity along the circadian cycle can immediately be inferred from the acquired data. In addition to provide a quick insight regarding the length and activity during sleep periods, the data can be used to determine circadian cycles. It is thus particularly useful for recording rhythms, specially since it is very difficult to record PSG for 24 hours and almost impossible to record for more than 24 hours.

### 4.1.1 Assessment of sleep disorders

Validation studies, supported by PSG data, have shown that ACT has reasonable validity and reliability in the assessment of sleep in healthy subjects. Sadeh et al. [67] concluded that validation studies with normal individuals reached agreement rates as high as 90%. On the other hand, the validity of ACT in special populations, in individuals with poor sleep or with

## 4.1. The role of Actigraphy in sleep medicine

---

sleep related disorders is more questionable. The most common reported issue is the low specificity of ACT, leading to a poor ability of detecting wakefulness within sleep periods.

In the case of subjects suffering with **Insomnia**, earlier reports [67, 4, 84] suggested very limited reliability of ACT for sleep assessment due to its tendency to overestimate sleep time, resulting in lower estimated SOL and Wake after Sleep Onset (WASO). Mainly due to the subjects efforts to fall asleep, leading to long motionless periods while awake.

However, this conclusion is not unanimous, as shown by the heterogeneity in the reported results. Later studies such as the ones performed by Lichstein et al. [86], with a large population and by Sánchez et al. [87], found no significant differences between PSG and ACT derived sleep measures, namely Total Sleep Time (TST), SE, WASO and SOL.

In [88] the authors also support the use of ACT in Insomnia subjects, reporting good results in the discrimination between Insomnia and healthy subjects. Finally, in [89] and [90] the authors report a reasonable correspondence between ACT and PSG, stressing, however, the limited wakefulness detection capability of ACT.

The use of ACT for the diagnosis of **Periodic Limb Movement Disorder** seems natural, due to the nature of this disorder. In [91, 92] the authors report that, after some adaptations, ACT has a high validity in the documentation of Periodic Limb Movement Disorder, closely compared with PSG.

Other considered disorders include **Sleep-disordered breathing**[93], sleep **Apnea**[94] and **Narcolepsy**[95]. Although different degrees of agreement with PSG are reported, even within the same disorder, the common conclusion supports ACT as a supplementary tool in the assessment of sleep disorders.

Despite the inconsistent reports regarding the validity of ACT in the assessment of several disorders, it is consensual that for **Sleep-schedule disorders** ACT is a reliable tool. It has been used to characterize circadian rhythms in adults, children, infants and the elderly, helping to identify disturbances and trends. It has also been used to correlate the light-dark cycle with the naturally occurring rhythm and helped monitoring rhythm abnormalities accompanying dementia and psychiatric disturbances.

### 4.1.2 Sleep diaries and Actigraphy

Sleep diaries can provide valuable information, particularly in the diagnosis and treatment of circadian rhythm sleep disorders. The level of commitment of the subjects in the maintenance of the diary, is often a limitation to its reliability. On the other hand, it promotes self-awareness to the problems affecting sleep, thus promoting self-diagnosis.

The performance of Sleep Diaries in the assessment of sleep is often compared with ACT. The conclusions are not consensual, showing a high dependency on the specific disorder and on the population. Werner et al. [96] suggest that, in children, ACT and sleep diaries have similar performances in the assessment of SOL, but the estimated values of TST and WASO are not

## **Chapter 4. Behavioural data**

---

comparable.

On the other hand, Lichstein et al. [86] found significant differences in the estimated SOL but high correlations on TST, in Insomnia subjects.

Contradicting these results, Chambers [97] found that when total sleep time estimates from actigraphs and sleep logs were compared to polysomnography, on a group of insomnia patients, there was no significant difference.

Nevertheless, while comparisons between the two methods are valid, they should be considered complementary methods and not concurrent. The conjugation of ACT with sleep and dream diaries has been reported by several authors and is a common practice in sleep medicine. The combination of the data given by the ACT with the subjective information introduced in the diaries has been shown to greatly improve the characterization of sleep and circadian rhythm [66, 98].

### **4.1.3 General Actigraphy guidelines**

Despite the lack of consensus regarding its reliability, Actigraphy is a well established method in sleep medicine. It relies on cheap sensors and its non-cumbersome nature allows clinicians to monitor the patients activity for long periods. It is a valuable tool in the assessment of sleep as long as its limitations are taken into account. The following guidelines, adapted from [5], should be kept in mind when using ACT:

- When compared to PSG, ACT has reasonable validity and reliability in assessing sleep-wakefulness patterns in normal individuals with average or good sleep quality.
- Its validity is limited in special populations, such as elderly people and individuals with major health problems or severe sleep limitations.
- It is particularly useful assessing circadian rhythm disorders, such as compromised or altered sleep patterns, and in the detection of changes in sleep patterns associated with pharmacologic and non-pharmacologic interventions.
- Algorithms specially adapted for the assessment of periodic limb movements have shown promising results in validation studies and can be used for screening purposes in large populations.
- The main methodological problem associated with the validity of actigraphic sleep-wake scoring is the relatively low ability to detect wakefulness during sleep periods. This is the focus of the next section.

## **4.2 Sleep/Wakefulness estimation from Nocturnal Actigraphy**

Since the first publication of the guidelines for its application in clinical environment [65], wrist ACT has received great attention from clinicians and researchers. In the reviews [4, 5]

## 4.2. Sleep/Wakefulness estimation from Nocturnal Actigraphy

---

it is shown that the number of publications including ACT is rapidly increasing despite its performance still being far from the PSG.

As explained in the previous section, the highly-portable and non-cumbersome nature of ACT sensors makes them ideal for long term monitoring applications. They are a valuable tool to gather behavioural information and to characterize the circadian cycle [6, 7]. However, while certain disorders, such as circadian phase shifts, are accurately characterized from ACT data [8], sleep staging and accurate SW state discrimination are still open issues and active fields of research.

The different levels of agreement between PSG and ACT reported in the literature have raised some issues regarding the validity of ACT for SW estimation [99, 100, 90, 101] and the metrics used to evaluate the suggested algorithms [102].

For instance, Sitnick et al. [103] compared minute-by-minute SW scorings based on ACT and videosomnography in young children, they reported 94% overall accuracy, 97% sensitivity, and 24% specificity.

Similarly, Meltzer et al. [104] compared SW scorings based on ACT and PSG in infants and found low specificity because of poor wake identification.

De Souza et al. [105] reported relatively low specificity (34% and 44%) in their comparison of PSG and two actigraphic scoring algorithms in healthy volunteers. Paquet et al. [101] compared two actigraphic sleep scoring algorithms in a study of 15 healthy participants studied for 3 nights with concomitant PSG and ACT. They found that increasing wakefulness during the sleep period compromises the minute-by-minute ACT-PSG correspondence because of the relatively low specificity of the scoring algorithms. The authors concluded that “*the very low ability of actigraphy to detect wakefulness casts doubt on its validity to measure sleep quality in clinical populations with fragmented sleep*”.

These examples demonstrate a crucial issue, the high accuracies and sensitivities reported in SW estimation using nocturnal ACT data, often mask the low specificity associated to the poor wake detection ability, as reported in [99].

The validation of the ACT prediction rates is typically made from the hypnogram obtained from PSG data. Although this information is accurate, it is also unbalanced from a state distribution point of view. In fact, in a healthy subject hypnogram, at least 85% of the epochs correspond to *Sleep* state [105, 106, 107].

Table 4.1 shows some of the most relevant results obtained in SW state estimation in adults<sup>1</sup>. It illustrates how diverse is the performance of the methods and mainly, how different are the sensitivity and specificity in most of them.

In the assessment of the performance of new algorithms and comparison with existing methods, common datasets and figures of merit must be used. In [105], for instance, the authors implemented and compared the algorithms described in [6] and [7] obtaining results signifi-

---

<sup>1</sup>The methods from Sadeh et al. and Hedner et al. were implemented to compare the performance of the proposed algorithm.

Author	Sens (%)	Spec (%)	Acc (%)	G-mean (%)
Cole et al. [6]	95	<b>64</b>	88	<b>78</b>
Sadeh et al. [7]	96	<b>75</b>	92	<b>84<sup>1</sup></b>
Kushida et al. [108]	90	<b>45</b>	80	<b>64</b>
Ancoli-Israel et al. [84]	--	--	93	--
Hedner et al. [109]	89	<b>69</b>	86	<b>78<sup>1</sup></b>
Sivertsen et al. [90]	95	<b>36</b>	83	<b>59</b>
Paquet et al. [?]	95	<b>54</b>	90	<b>72</b>

Table 4.1: Performances reported in the literature for Sleep/Wakefulness estimation using Actigraphy data in adult populations.

cantly different than the originally reported.

In order to overcome the intrinsic limitations of ACT, new approaches are being explored. In [110] cardio-respiratory signals are combined with ACT data yielding promising results and in [111] the authors show that it is possible to accurately characterize human activity from accelerometer data in a non sleep scope. In [102] the authors employ artificial neural networks and decision trees to score infant ACT data obtaining relevant results and stressing the importance of using common metrics.

#### 4.2.1 Proposed method

The SW estimation method described in this chapter presents several novelties, not commonly discussed in the state of the art algorithms. The method is based on a Movement Detector (MD) designed to discriminate and detect movement and quietness periods from the nocturnal ACT data.

Movement detection is a central piece in the algorithm, it is shown that movements during *wakefulness* and *sleep* states are intrinsically different. The difference is not only in terms of magnitude but also from a spectral and statistical distribution perspective. While movements during *sleep* state are typically random and without purpose, i.e. *purposeless*, movements during *wakefulness* state are more coherent and correlated, usually with a defined purpose.

The features used are the coefficients and weights of a mixture distribution, describing the first order statistics of the ACT data, the residues of an Autoregressive model (AR) [112] fitted to the data, describing its high order statistics and finally, the signal energy that takes into account the intensity of the signal, the most important feature used in the traditional approaches for ACT data processing.

The classification/testing procedure is performed in three stages. After feature extraction, an estimation of the SW state is obtained for each epoch with a LDC, with parameters  $\theta^*$  and  $\theta_M^*$ , optimized for quietness and movement epochs respectively.

## 4.2. Sleep/Wakefulness estimation from Nocturnal Actigraphy

---

The previous result is then refined with a HMM that incorporates statistical information computed from the training data.

ACT based SW estimation algorithms typically combine several features extracted from the intensity and frequency counts of the recorded signal. In these algorithms, periods of strong activity are normally scored as *wakefulness* and long periods quietness as *sleep*.

This strategy leads to acceptable and relevant accuracies but also to the well documented limitations of ACT such as the poor ability to detect wakening episodes during quietness periods, very typical in insomnia, and the generalized tendency to overestimate *sleep* [8, 102].

Since sleeping is the natural state during the night, when estimating SW states for sleep disorders diagnosis purposes, it is generally more important to accurately estimate *wakefulness* than *sleep*.

The traditional state estimation algorithms usually maximize the overall accuracy that does not take into account this unbalanced state distribution, which leads to poor wakefulness state detection rate.

The proposed method is designed to achieve a similar performance during movement and quietness periods and it is tuned, using the *Geometric mean* (G-mean) [113] as the optimization criteria, for a balance between *sleep* and *wakefulness* detection ability. Thus, minimizing the tendency of ACT to underestimate the *wakefulness* periods [8, 102].

The complete state estimation method, displayed in Fig. 4.2, is composed by: pre-processing, feature extraction, training, state estimation and a final classification refinement.

### 4.2.2 Pre-processing and movement detection

Two pre-processing operations are performed on the data, 1) magnitude normalization and DC component removal, and 2) movement segmentation. Magnitude normalization and DC component removal is required to minimize the inter-patient and inter-device variability. This procedure, performed in a sliding window basis, is done according to

$$\tilde{a}(n) = \frac{a(n) - \mu(\mathbf{n})}{\sigma(\mathbf{n})} \quad (4.1)$$

where  $a(n)$  is the  $n^{th}$  actigraphy sample,  $\mu(\mathbf{n})$  and  $\sigma(\mathbf{n})$  are the mean and standard deviation of the data within the 5 minute window centred at the  $n^{th}$  sample and  $\tilde{a}(n)$  is the normalized sample.

In a second pre-processing step, movement events are identified on the normalized data with the MD displayed in Fig. 4.3.

This detector is composed by i) a non-causal low-pass stretching filter and a ii) threshold based binarization block. The smoothing filter computes the movement envelope, its width is

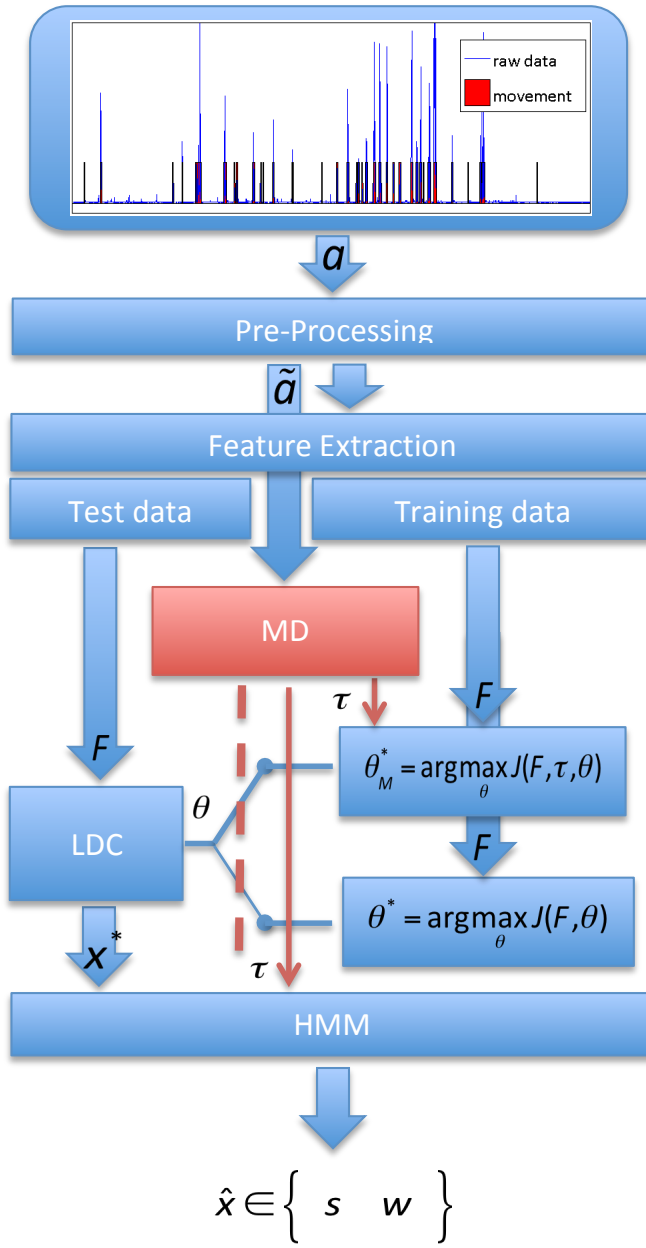


Figure 4.2: Fluxogram of the proposed *Movement based State Detection* (MSD) algorithm. After pre-processing and feature (F) extraction, an initial estimation ( $x^*$ ) is made using a LDC with parameters  $\theta^*$  and  $\theta_M^*$ . The final estimate,  $\hat{x}$ , is obtained with a HMM based regularization algorithm.

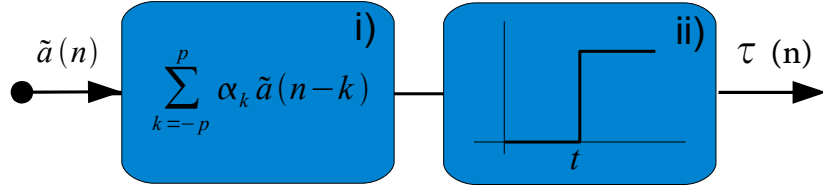


Figure 4.3: Structure of the movement detector.

controlled by the parameter  $p$ , defined as  $p = 5$  for a sampling frequency of  $1\text{Hz}$ . Let

$$S(t) = \left| \frac{dF(t)}{dt} \right| \quad (4.2)$$

denote the sensibility of the MD and  $F(t)$  the percentage of movement detected as a function of the threshold,  $t$ . The optimal value,  $t^*$ , is obtained for each dataset computing  $S$  and finding

$$t^* = \arg \min_x \frac{d^2 S(t)}{dt^2}. \quad (4.3)$$

The selected threshold corresponds to the point where the sensibility is more stable.

Figure 4.4 illustrates the determination of  $t^*$  for one dataset. The sensibility curve is evaluated for the range  $t \in [0.5 \dots 1]$ , this range was chosen by direct observation of the data. The average optimal threshold, computed from all datasets, is  $\hat{t}^* = 0.68 \pm 0.22$ .

The output of the detector is a binary function  $\tau(n) \in \{m, q\}$ , where  $m$  corresponds to movement and  $q$  to quietness.

Figure 4.5 displays an example of pre-processed data. Figure 4.5.a) shows the normalized ACT signal and the movement indicator and Fig. 4.5.b) the corresponding hypnogram segment. The hypnogram discriminates 5 different states, namely *wakefulness*, *Rem sleep*, and 3 *non-Rem* sleep states. All epochs marked as *Rem* and *non-Rem* were translated into a single *sleep* label.

### 4.2.3 Nocturnal Movement Characterization

The proposed SW estimation method relies on a set of features chosen to properly discriminate the states of interest. The features extracted from nocturnal ACT are typically limited to event counts and acceleration magnitude, or energy.

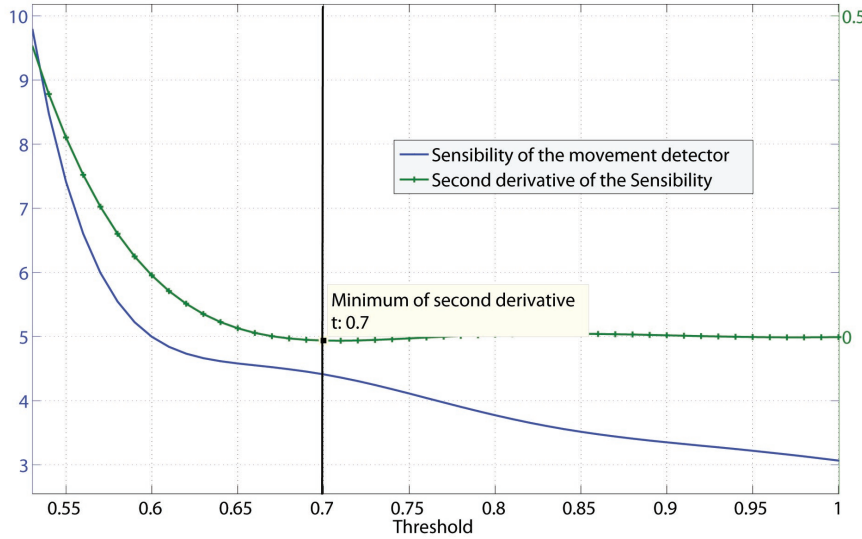


Figure 4.4: Sensibility of the MD and the respective second derivative for a given dataset. The minimum of the second derivative is selected as the optimal value for this dataset, corresponding to  $t^* \approx 0.7$ .

Here, three new sources of information are proposed. One is related with the time intervals between movement and quietness periods, which is included in the HMM to model temporal correlation between states, the other are related with the intrinsic nature of the recorded movements.

In the works by the same author [114, 115] it is hypothesized that movements during *wakefulness* and *sleep* states are intrinsically different, not only in terms of magnitude but from a spectral and statistical distribution perspective. While movements during *sleep* state are typically random and without purpose, i.e. *purposeless*, movements during *wakefulness* state are more coherent and correlated, usually with a defined purpose.

### Length of quietness and movement periods

The duration of the recorded movements is typically used by clinicians as a discriminative feature for SW assessment. The international standards define wakefulness when movements occur for periods longer than 30 seconds [65]. Here, this empirical rule is extended, by quantifying the duration of movements in sleep and wakefulness states but also the duration of quietness periods in the two states.

Figure 4.6 - A) shows the histograms of the duration of quietness periods during *sleep* and *wakefulness* states. As expected the mean value is larger during sleep and the periods tend to be longer, i.e. the subjects tend to stay still while sleeping. During wakefulness the quietness periods tend to be shorter, almost never exceeding 60 seconds.

Figure 4.6 - B) shows the histogram of the length of the recorded movements. During wakeful-

## 4.2. Sleep/Wakefulness estimation from Nocturnal Actigraphy

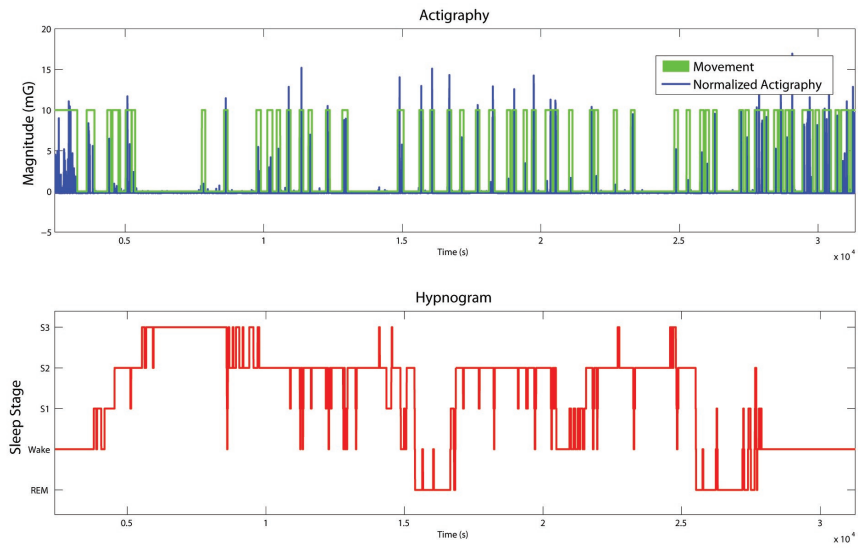


Figure 4.5: a) Actigraphy data and detected movements (top) b) Hypnogram (bottom). The binary movement function was rescaled for visualization purposes.

ness, movement duration is typically longer with a large standard deviation around the mean. Sleep movements are typically quick, with the large majority being shorter than 5 seconds.

The data from Figure 4.6 A) and B) suggest an Exponential and Gaussian distribution for quietness and movement periods, respectively, characterized by different parameters on sleep and wakefulness states.

The data from Figure 4.6 A) can thus be described as  $\mathcal{E}(\lambda_x)$ , an exponential probability distribution,  $P(t|\lambda_{s,w})$ , giving the probability of a *quietness* period of length  $t$  being observed during *sleep* and *wakefulness*. This distribution arises naturally if movement events are assumed to be a stochastic Poisson process. The parameters  $\lambda_s$  and  $\lambda_w$  are computed as

$$\hat{\lambda}_x = \frac{1}{\bar{t}_x} \quad (4.4)$$

where  $\bar{t}_x$  is the mean duration of the vector containing all *quietness* intervals for *sleep* ( $x = s$ ) and *wakefulness* ( $x = w$ ) states.

The data from Figure 4.6 B) can be described as  $\mathcal{N}(\sigma_x)$ , a zero mean Gaussian probability distribution,  $P(t|\sigma_{s,w})$ , giving the probability of a movement of length  $t$  being observed during *sleep* and *wakefulness* states. The parameter  $\sigma_s$  and  $\sigma_w$  is the standard deviation of the duration of all movements recorded during *sleep* and *wakefulness* states, respectively.

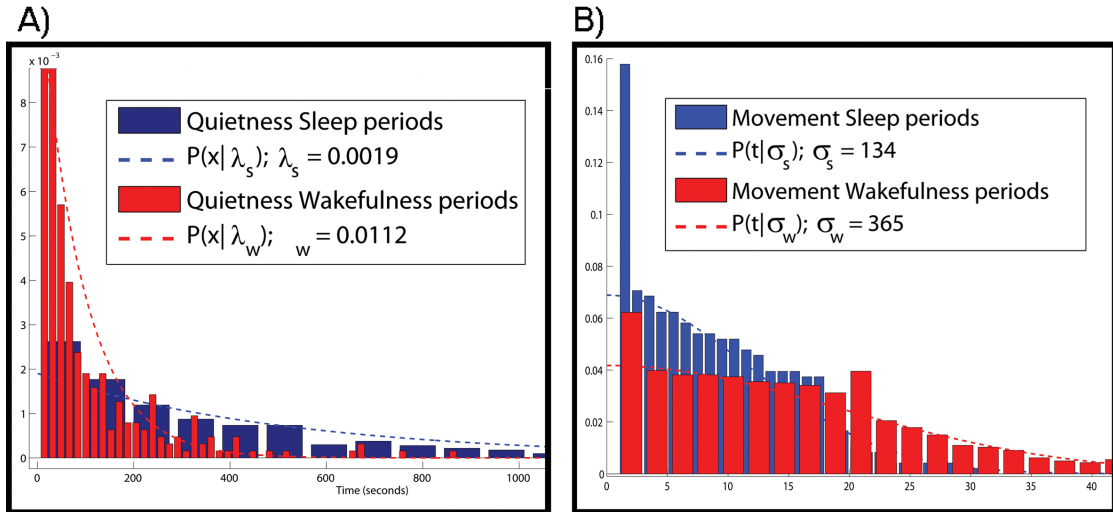


Figure 4.6: Normalized histograms of: A) the length of *quietness* periods and B) duration of the recorded movements, during *sleep* (blue) and *wakefulness* (red) states.

### Mixture distributions

The different pattern of movements observed during the circadian cycle, shown on Figure 2.8, can be easily used to roughly distinguish wakefulness and sleep states [116]. During the day, when wakefulness state is dominant, the movements are usually very heterogeneous and dense. On the other hand, during the night, sleep state is dominant and the movements are more impulsive and sparse [98].

This difference resides not only in the intensity of the actigraphy signal but also in its statistical characterization. The differences on the actigraphy data in these two different states is related with their different natures. During wakefulness there is usually a goal and the corresponding movements have specific coherent and consistent purposes. On the other hand, during sleep, movements are involuntary and usually purposeless which make them impulsive, non-coherent and sparse.

In [117] and [98] the authors propose a weighted mixture of two distributions to describe ACT data across the entire circadian cycle. One component of the mixture being mainly associated with the wakefulness state and the other associated with sleep state, the weight of each components is shown to evolve along the circadian cycle.

In [118] the ACT data is described as a function of the number of events, this analysis led to an exponential probability distribution to describe data during sleep state, and an activity dependent distribution for wakefulness state data. While activities such as running or walking can be described with a normal distribution, standing or laying is best described by Poisson or exponential distributions [119].

The previous methods can be extended to find statistical differences in nocturnal ACT movement, which is the focus of this method. The histogram of nocturnal movement data, displayed

## 4.2. Sleep/Wakefulness estimation from Nocturnal Actigraphy

---

in Figure 4.7, supports that the data can be described by a mixture of probability density functions.

Based on this information, four combinations of distributions were initially tested; i) Exponential, Rayleigh and Gaussian (ERG), ii) Exponential and Rayleigh (ER), iii) Exponential and Gaussian (EG) and iv) Rayleigh and Gaussian distribution (RG).

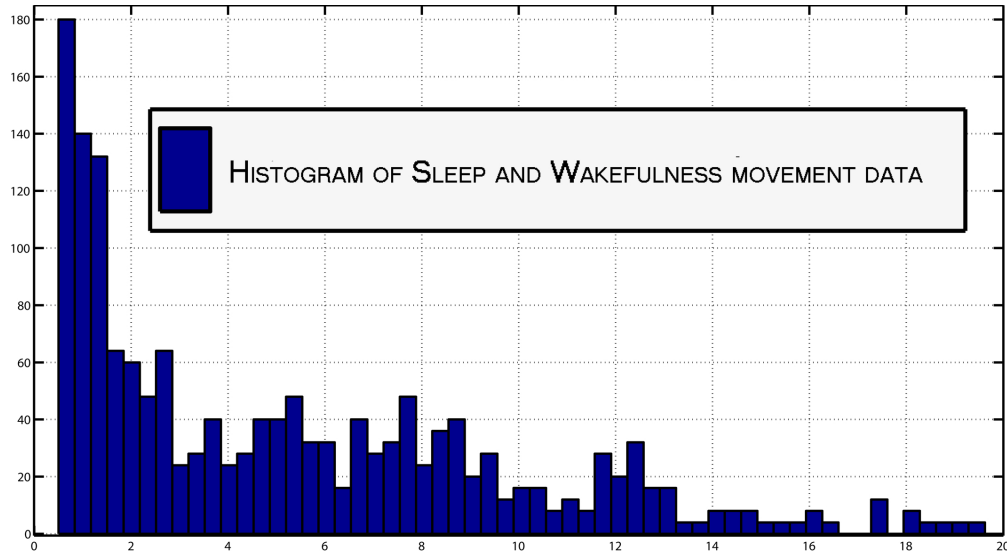


Figure 4.7: Histogram of movements, recorded on nocturnal Actigraphy.

Let  $\mathbf{y} = \{y_i\}, 1 \leq i \leq N$ , be a vector with the ACT samples for a particular state, sleep or wakefulness, acquired at a constant sampling rate. Each sample, corresponding to the magnitude of the ACT data at a given instant, is considered a random variable with the following PDF,

$$p(y_i|\mathbf{W}, \boldsymbol{\theta}) = w_e p(y_i|\lambda) + w_r p(y_i|f) + w_g p(y_i|\mu, \sigma) \quad (4.5)$$

where  $\theta = \{\lambda, f, \mu, \sigma\}$  are the parameters of the components and  $\mathbf{W} = \{w_e, w_r, w_g\}$  are the weights of the mixture satisfying the following normalization constraint:

$$w_e + w_r + w_g = 1. \quad (4.6)$$

The mixture in Eq. 4.5 is composed by three components,

$$p_e(y_i|\lambda) = \lambda e^{-\lambda y_i} \quad (4.7)$$

is an exponential distribution with parameter  $\lambda$ ,

$$p_r(y_i|f) = \frac{y_i}{f} e^{-\frac{y_i^2}{2f}} \quad (4.8)$$

is a Rayleigh distribution with parameter  $f$  and

$$p_g(y_i|\mu, \sigma) = \frac{1}{\sqrt{2\pi}\sigma} e^{-\frac{(y_i-\mu)^2}{2\sigma^2}} \quad (4.9)$$

is a Gaussian distribution with parameters  $\mu$  and  $\sigma$ .

The Maximum Likelihood (ML) estimation problem of weights,  $\mathbf{W} = \{w_e, w_r, w_g\}$  and parameters,  $\boldsymbol{\theta} = \{\lambda, f, \mu, \sigma\}$ , assuming statistical independence of the observations is formulated as:

$$\{\hat{\mathbf{W}}, \hat{\boldsymbol{\theta}}\}^{ML} = \arg \max_{\boldsymbol{\theta}, \mathbf{W}} L(\mathbf{y}|\mathbf{W}, \boldsymbol{\theta}) \quad (4.10)$$

where

$$L(\mathbf{y}|\mathbf{W}, \boldsymbol{\theta}) = \log(p(\mathbf{y}|\mathbf{W}, \boldsymbol{\theta})) = \log \prod_{i=1}^N p(y_i|\mathbf{W}, \boldsymbol{\theta}) \quad (4.11)$$

is the likelihood function and

$$p(y_i|\mathbf{W}, \boldsymbol{\theta}) = \sum_j [w_j p_j(y_i|\boldsymbol{\theta}(j))] \quad (4.12)$$

is the mixture.  $\boldsymbol{\theta}(j)$  is the set of parameters associated with the  $j^{th}$  component of the mixture. The maximization of Eq. 4.11 can be efficiently performed using the EM method [120], here a set of hidden variables,  $\mathbf{k} = \{k_i\}$ , are introduced with  $k_i \in \{1, \dots, L\}$  and  $L$  the number of elements of the mixture. Each integer  $k_i$  indicates what component of the mixture (4.5) has generated the  $i^{th}$  sample with probability  $p_{k_i}(y_i)$ , defined in (4.7), (4.8) and (4.9).

The estimation process becomes an iterative process, where new values of  $\{\mathbf{W}, \boldsymbol{\theta}\}$  are calculated, following two steps:

#### E step:

Computation of a new likelihood function that is the expectation of  $L(\mathbf{Y}, \mathbf{k}, \mathbf{W}, \boldsymbol{\theta})$  with respect

to  $\mathbf{k}$

$$\mathbf{Q}(\mathbf{y}, \mathbf{W}, \boldsymbol{\theta}) = E_{\mathbf{k}} [L(\mathbf{y}, \mathbf{k}, \mathbf{W}, \boldsymbol{\theta})] \quad (4.13)$$

**M step:**

Maximization of  $\mathbf{Q}(\mathbf{y}, \mathbf{W}, \boldsymbol{\theta})$

$$\{\hat{\mathbf{W}}, \hat{\boldsymbol{\theta}}\} = \arg \max_{\mathbf{W}, \boldsymbol{\theta}} \mathbf{Q}(\mathbf{y}, \mathbf{W}, \boldsymbol{\theta}) \quad (4.14)$$

The likelihood function is given by

$$\begin{aligned} L(\mathbf{y}, \mathbf{k}, \mathbf{W}, \boldsymbol{\theta}) &= \log p(\mathbf{y}, \mathbf{k} | \mathbf{W}, \boldsymbol{\theta}) \\ &= \sum_{i=1}^N \log p(y_i, k_i | \mathbf{W}, \boldsymbol{\theta}) \\ &= \sum_{i=1}^N \log \underbrace{[p(y_i | k_i) p(k_i | \mathbf{W}, \boldsymbol{\theta})]}_{w_{k_i} p_{k_i}(y_i | \boldsymbol{\theta}(k_i))} \\ &= \sum_{i=1}^N [\log p_{k_i}(y_i | \boldsymbol{\theta}(k_i)) + \log w_{k_i}] \end{aligned} \quad (4.15)$$

The maximization of (4.15) is not possible because the hidden variables  $k_i$  are not known. The expected value of  $L(\mathbf{y}, \mathbf{k}, \mathbf{W}, \boldsymbol{\theta})$  with respect to  $\mathbf{k}$  is thus used instead,

$$\begin{aligned} \mathbf{Q}(\mathbf{W}, \boldsymbol{\theta}) &= E_{\mathbf{k}} [L(\mathbf{y}, \mathbf{k}, \mathbf{W}, \boldsymbol{\theta})] \\ &= \sum_{i=1}^N E_{\mathbf{k}} [\log p_{k_i}(y_i | \boldsymbol{\theta}(k_i)) + \log w_{k_i}] \\ &= \sum_{i=1}^N \sum_j \phi_{i,j} [\log p_j(y_i | \boldsymbol{\theta}(j)) + \log w_j] \end{aligned} \quad (4.16)$$

where  $\phi_{i,j}$  is the distribution of the unobserved variable,  $\mathbf{k}$ , given by

$$\begin{aligned} \phi_{i,j} &= p(k_i = j | y_i, \mathbf{W}^{n-1}, \boldsymbol{\theta}^{n-1}) \\ &= \frac{p(y_i | \boldsymbol{\theta}^{n-1}(k_i)) p(k_i = j)}{p(y_i | \mathbf{W}^{n-1}, \boldsymbol{\theta}^{n-1})} \\ &= \frac{w_j^{n-1} p(y_i | \boldsymbol{\theta}^{n-1}(k_j))}{\sum_j w_j^{n-1} p_j(y_i | \boldsymbol{\theta}^{n-1}(j))} \end{aligned} \quad (4.17)$$

with the condition

$$\sum_j \phi_{i,j} = 1 \quad (4.18)$$

The expression in (4.16) can now be separated in two terms dependent on  $w_j$  and  $\theta_j$ , becoming:

$$Q(\mathbf{W}, \boldsymbol{\theta}) = \sum_{i=1}^N \sum_j \phi_{i,j} \log p(y_i | \boldsymbol{\theta}(j)) + \sum_{i=1}^N \sum_j \phi_{i,j} \log w_j \quad (4.19)$$

which can be maximized separately for  $\mathbf{W}$  and  $\boldsymbol{\theta}$ .

The minimization of (4.19) with respect to  $\mathbf{W}$  is done using the method of *Lagrange multipliers* [78]. This method provides a strategy for finding the maxima and minima of a function subject to constraints, which in this case is given (4.6).

Let  $\epsilon$  be the Lagrange multiplier and solving the partial derivative of (4.19) with respect to  $w$  leads to

$$\frac{\partial}{\partial w_j} \left[ \sum_{i=1}^N \sum_j \phi_{i,j} \log w_j + \epsilon \left( \sum_j w_j - 1 \right) \right] = 0 \quad (4.20)$$

which results in

$$\begin{aligned} \sum_{i=1}^N \phi_{i,j} &= -\epsilon w_j \\ \sum_{i=1}^N \underbrace{\sum_j \phi_{i,j}}_{\text{Constraint (4.18)}} &= -\epsilon \underbrace{\sum_j w_j}_{\text{Constraint (4.6)}} \\ \epsilon &= -N \end{aligned} \quad (4.21) \quad (4.22)$$

Replacing the value of  $\epsilon$  in (4.21) and rearranging, the expression for  $w_j$  becomes

$$w_j = \frac{1}{N} \sum_{i=1}^N \phi_{i,j} \quad (4.23)$$

The minimization of Eq. 4.19 with respect to  $\boldsymbol{\theta}$  is performed computing the corresponding

## 4.2. Sleep/Wakefulness estimation from Nocturnal Actigraphy

---

stationary point, leading to:

$$\hat{\lambda} = \frac{\sum_{i=1}^N \phi_{i,0}}{\sum_{i=1}^N \phi_{i,0} y_i} \quad (4.24)$$

$$\hat{f} = \frac{1}{2} \frac{\sum_{i=1}^N y_i^2 \phi_{i,1}}{\sum_{i=1}^N \phi_{i,1}} \quad (4.25)$$

and

$$\begin{aligned} \hat{\mu} &= \frac{\sum_{i=1}^N y_i \phi_{i,2}}{\sum_{i=1}^N \phi_{i,2}} \\ \hat{\sigma} &= \sqrt{\frac{\sum_{i=1}^N \phi_{i,2} (y_i - \hat{\mu})^2}{\sum_{i=1}^N \phi_{i,2}}} \end{aligned} \quad (4.26)$$

where

$$\phi_{i,j} = \frac{w_j^{n-1} p(y_i | \boldsymbol{\theta}^{n-1}(k_j))}{\sum_j w_j^{n-1} p_j(y_i | \boldsymbol{\theta}^{n-1}(j))} \quad (4.27)$$

On each iteration, the Kullback-Leibler divergence (KL) [121] is computed and the iterative process stops when i) the difference between successive values is smaller than  $10^{-3}$  or ii) the number of iterations reaches 1000.

Figure 4.8 shows the normalized histograms of sleep and wakefulness nocturnal movement data, fitted with the 4 considered distributions. None of different mixture distributions is able to perfectly fit the data. The curves corresponding to ERG, ER and EG show that the exponential distribution appears to have a reduced influence on the mixture distribution. This is due to the fact that most zero valued samples were removed by the movement detector.

The convergence of the EM algorithm is also a problem since it is extremely sensitive to the initialization of the parameters. The problems inherent to the proposed mixtures led to a simplification of the mixture, which was restricted to Rayleigh components.

The physical reasoning to use a Rayleigh Mixture Model (RMM) is related with the model adopted for the actigraph sensor, as described in [98]. If the acceleration along each axis is described by a zero mean Gaussian distribution, the acceleration magnitude follows a Rayleigh

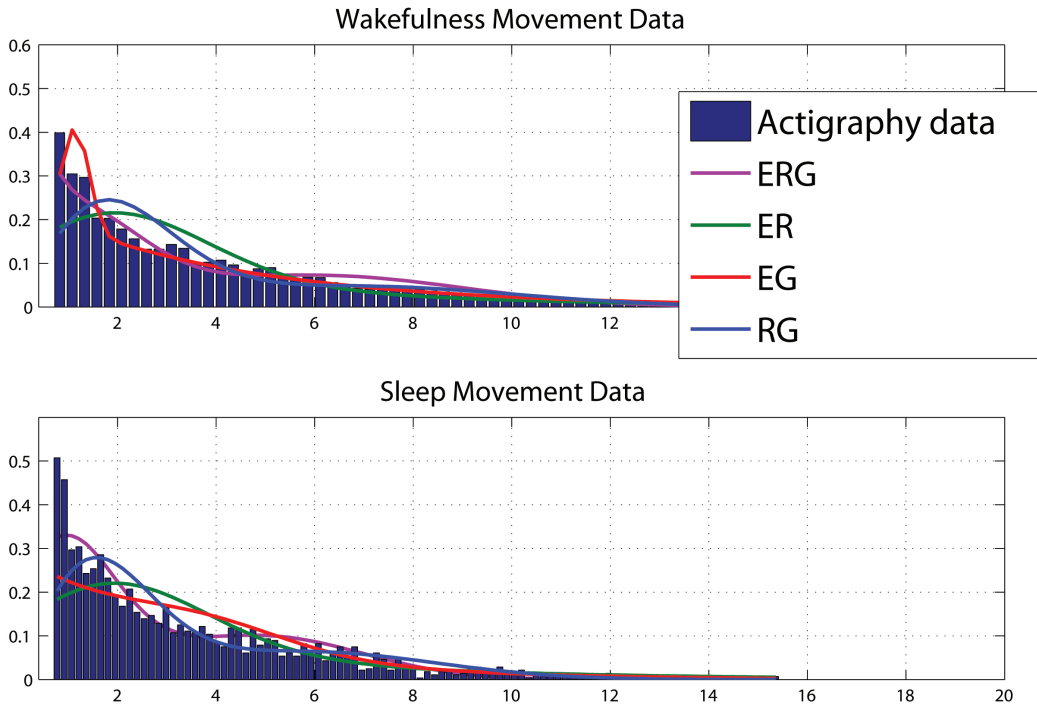


Figure 4.8: The four different mixture distributions fitted to the ACT movement data. None of the mixtures is able to accurately fit the data.

<b>L</b>	1	2	3	4	5
<b>KL</b>	0.230	0.042	<b>0.036</b>	0.036	0.035

Table 4.2: Kullback-Leibler divergence using different number of components for the Rayleigh mixture distribution.

and a Maxwell distribution in 2D and 3D respectively.

The estimation of the parameters of the RMM is similar to the previously described except that Eqs. 4.24 and 4.26 are replaced by the expression in Eq. 4.25.

The number of Rayleigh components,  $L$ , was selected by fitting the complete set of movement data with different values of  $L$  and selecting the one yielding the lower KL value. The result of this process is shown in Table 4.2, the number of Rayleigh components was thus set to 3.

Figure 4.9 shows the normalized histograms of sleep and wakefulness nocturnal movement data, the RMM and the individual components of the mixture. The mixture model is able to fit both Sleep and Wakefulness movement data, largely improving the results shown in Figure 4.8.

## 4.2. Sleep/Wakefulness estimation from Nocturnal Actigraphy

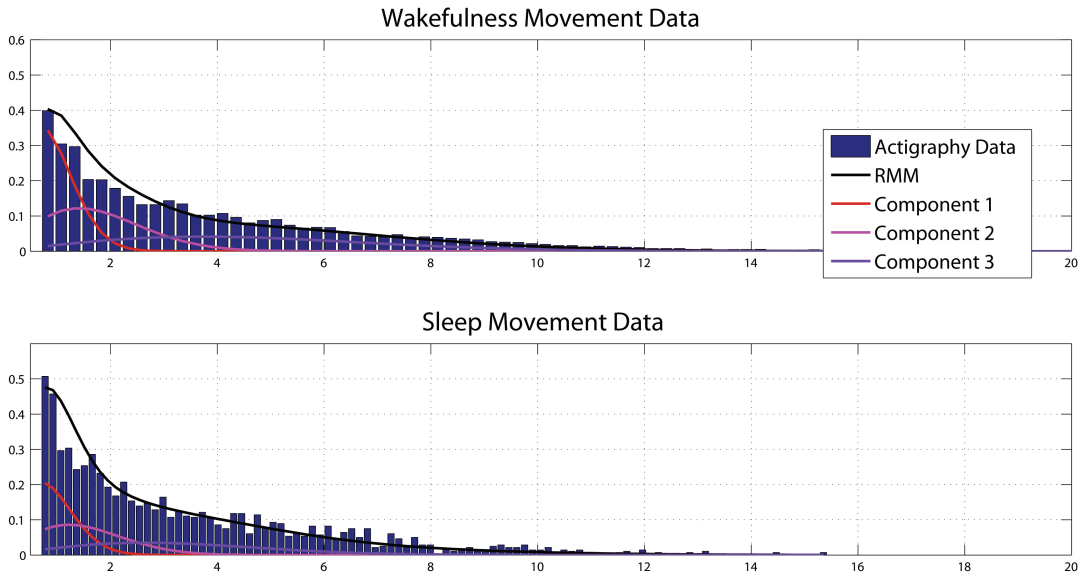


Figure 4.9: 3 component Rayleigh Mixture Model fitted to the histograms of sleep and wakefulness nocturnal movement data.

Table 4.3 summarizes the results obtained, showing the i) kullback-leibler divergence, ii) weights ( $\{\mathbf{w}_0, \mathbf{w}_1, \mathbf{w}_2\}$ ) and iii) parameters for the different mixture distributions, for the two different states. As expected, the RMM yields the lowest KL followed by the RG mixture distribution.

### Autoregressive model coefficients

The coefficients of an Autoregressive model constitute another source of information used for SW state characterization and discrimination. By modelling the temporal correlation between adjacent samples, the coefficients allow the characterization of high order statistical properties of the data.

Similarly to the mixture distributions described in the previous section, the characterization of the ACT data using AR coefficients is restricted to movement periods, as obtained from the MD. On an initial approach, the coefficients estimation is performed on a per sample basis where previous estimates of the coefficients are used to guide the estimation algorithm in the present time, thus increasing time resolution.

The overall idea is to estimate the vector of coefficients,  $\mathbf{a}(n) = \{a_1(n), a_2(n), \dots, a_p(n)\}^T$ , of a  $p$ -order AR model based on the current sample,  $n$ , on the  $p - 1$  previous samples and on the previous estimated set of coefficients,  $\mathbf{a}(n - 1)$ , obtained in the previous sample  $n - 1$ . By doing this, the estimation of the coefficients is strongly guided by the previously estimated coefficients, incrementally updated with the information provided by the new sample.

Wakefulness						
	ERG	ER	EG	RG	RMM	
k.l.	0.22	0.31	0.15	0.32	k.l.	0.04
$w_0$	0.06	0.6	0.80	–	$w_0$	0.38
$w_1$	0.58	0.4	–	0.61	$w_1$	0.41
$w_2$	0.36	–	0.20	0.39	$w_2$	0.21
$\lambda$	0.2	0.32	0.31	–	$f_1$	1.56
$f$	2.52	13.58	–	2.62	$f_2$	11.7
$\mu$	6.14	–	5.50	6.27	$f_3$	34.1
$\sigma$	2.46	–	2.46	2.71	–	–

Sleep						
	ERG	ER	EG	RG	RMM	
k.l.	0.74	0.77	0.57	0.64	k.l.	0.05
$w_0$	0.22	0.83	0.92	–	$w_0$	0.4
$w_1$	0.40	0.172	–	0.48	$w_1$	0.3
$w_2$	0.38	–	0.08	0.52	$w_2$	0.3
$\lambda$	0.18	0.24	0.28	–	$f_1$	1.4
$f$	1.25	1.072	–	1.48	$f_2$	8.4
$\mu$	5.23	–	6.18	5.85	$f_3$	20.1
$\sigma$	2.079	–	0.62	2.94	–	–

Table 4.3: Weights and Parameters obtained for the different mixture distributions, for Sleep and Wakefulness movement data.

## 4.2. Sleep/Wakefulness estimation from Nocturnal Actigraphy

---

Let us consider  $y(n)$ , the  $n^{th}$  actigraph sample, generated according to the following  $p$ -order AR model

$$\begin{aligned} y(n) &= \sum_{k=1}^p a_k(n)x(n-k) + \epsilon(n) \\ &= \mathbf{x}_p^T(n)\mathbf{a}(n) + \epsilon(n) \end{aligned} \quad (4.28)$$

where  $\mathbf{x}_p(n) = \{x(n-1), x(n-2), \dots, x(n-p)\}^T$  is a column vector containing the  $p$  previous samples and  $\epsilon(n)$  is the residue. The vector of coefficients is obtained by minimizing the energy of the residue

$$\epsilon^2(n) = [y(n) - \mathbf{x}_p^T(n)\mathbf{a}(n)]^2 \quad (4.29)$$

which is an ill-posed problem [122], thus a regularization term is needed.

Let us consider the following energy function with regularization

$$\begin{aligned} E(n) &= [y(n) - \mathbf{x}_p^T(n)\mathbf{a}(n)]^2 + \\ &\quad \alpha \|\mathbf{a}(n) - \mathbf{a}(n-1)\|_2^2 \end{aligned} \quad (4.30)$$

where  $\|\cdot\|$  is the Euclidean distance. The quadratic term,  $\|\mathbf{a}(n) - \mathbf{a}(n-1)\|_2^2$ , is a prior function that forces similarity between consecutive model parameters. The constant  $\alpha$  tunes the strength of that similarity and was selected to be 150 on a trial and error basis.

The stationary point of (4.30) with respect to  $\mathbf{a}(n)$  is computed as

$$\begin{aligned} \nabla_{\mathbf{a}(n)} E &= \mathbf{x}_p(n) \left( \mathbf{x}_p^T(n)\mathbf{a}(n) - y(n) \right) + \\ &\quad \alpha [\mathbf{a}(n) - \mathbf{a}(n-1)] = 0 \end{aligned} \quad (4.31)$$

leading to

$$\hat{\mathbf{a}}(n) = \left( \mathbf{x}_p(n)\mathbf{x}_p^T(n) + \alpha I_p \right)^{-1} (\mathbf{x}_p(n)y(n) + \alpha \mathbf{a}(n-1)) \quad (4.32)$$

where  $I_p$  is the  $p \times p$  identity matrix.

By stacking the  $N^\tau$  vectors  $\hat{\mathbf{a}}(n)$ , obtained for each sample, from Eq. 4.32, and for each state, wakefulness and sleep, two  $N^\tau \times p$  matrices are obtained,  $\mathbf{A}^\tau$ ,  $\tau = \{w, s\}$ . Each line  $\mathbf{a}_l^\tau(n)$ ,

$0 \leq n \leq N^T$ , corresponds to the vector of  $p$  coefficients computed for the  $n^{th}$  sample and each column  $\mathbf{a}_c^\tau(i)$ ,  $0 \leq i \leq p$ , corresponds to the  $i^{th}$  coefficient computed for the  $N^T$  samples. Here,  $N^s \neq N^w$  since the number of samples for each state is different.

The order of the model,  $p = 50$ , was obtained using the Akaike criterion [123], allowing a good fit of the model to the data and an acceptable computation time. While this order is optimal for data description, state discrimination can be optimized by selecting a subset of coefficients (columns of  $\mathbf{A}^\tau$ ) that leads to the maximization of the discriminative power.

The coefficient selection procedure is performed using a *forward selection* based algorithm [124], where the following measure

$$D(c) = \frac{\|\mu_s - \mu_w\|}{\|\Sigma_s\|_F + \|\Sigma_w\|_F} \quad (4.33)$$

is used to quantify the cluster separability given a subset of coefficients. Here,  $\|\cdot\|$  and  $\|\cdot\|_F$  are the euclidean and Frobenius norms, respectively, and  $\mu_\tau$  and  $\Sigma_\tau$  are the mean vectors and covariance matrices, computed with data from state  $\tau$ , of the given subset of coefficients.

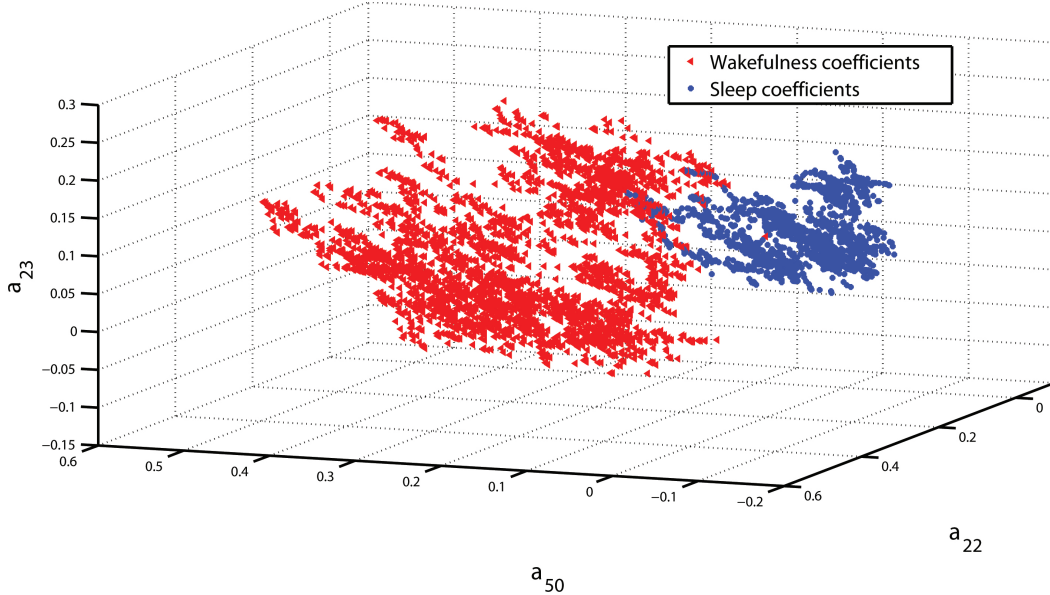


Figure 4.10: The three most significant coefficients of the AR model yield almost separate clusters for Sleep (blue) and Wakefulness (red).

Figure 4.10 shows the 3D plot of the three most discriminative coefficients. The samples are organized into two separable regions, showing that the characteristics of the movements are intrinsically different during sleep and wakefulness and suggesting that AR coefficients can be used as valid discriminative features for SW estimation from nocturnal ACT data.

The results obtained using RMM and AR coefficients are limited to movement data. Using these two approaches it has been shown that movements during distinct states are intrinsically

## 4.2. Sleep/Wakefulness estimation from Nocturnal Actigraphy

---

different. However, these results can not be generalized to complete datasets (movement + quietness periods). The two methods require small adaptations, which will be discussed in the feature extraction section.

The next three sections describe 1) the feature extraction, 2) the Main Classification Stage (MCS) and 3) the refinement algorithm, which compose the proposed method, here called Movement based State Detection (MSD).

### 4.2.4 Feature extraction

The feature set includes the features describing first and higher order statistics and one intensity related feature. After pre-processing, each ACT time course is divided in contiguous epochs of  $T = 30$  seconds.

Let  $\mathbf{w}_j$  represent a  $L$  dimensional window, 210 seconds long (3.5 minutes), centred on the  $j^{th}$  epoch, where  $j \in \{1, \dots, M\}$  with  $M$  the total number of epochs. Features are extracted from each window,  $\mathbf{w}_j$ , as follows

- Energy,  $E_j$ . The energy of the epoch given by  $E_j = \sum_k^M h(k) w_j^2(k)$  where  $\mathbf{h} = \{h(k)\}$  is Hanning window with length  $L$ .
- Coefficients  $\alpha_j(k)$  - Coefficients of the three component RMM, fitted to each  $\mathbf{w}_j$  according to the method described in the previous section. The statistical significance of the obtained parameters and coefficients was assessed performing a one-way ANOVA test (for a significance level of 0.05), it was found that only the coefficients,  $\alpha_j(k)$  are discriminative for SW state estimation and not the parameters of the Rayleigh components.
- Residue,  $r_j$  - Residue and coefficients of the 8-order AR, estimated using the Yule-Walker equations, for each  $\mathbf{w}_j$  based on a  $L$  dimension window, centred on it. The coefficients and residue are estimated in batch, contrary to the *per sample* estimation described in the previous section. By using a forward search feature selection algorithm, it was concluded that the residue is more discriminative than the coefficients of the AR in the estimation of the SW state. Figure 4.11-B) shows the normalized histograms of the residues obtained for *sleep* and *wakefulness*. The residues roughly follow a Gaussian distribution with different means and standard deviations for the two states.

### 4.2.5 Main classification stage

The Main Classification Stage performs the initial estimation of the SW state, denoted as  $x^* \in \{s^*, w^*\}$ .

The MCS is composed by the following three steps.

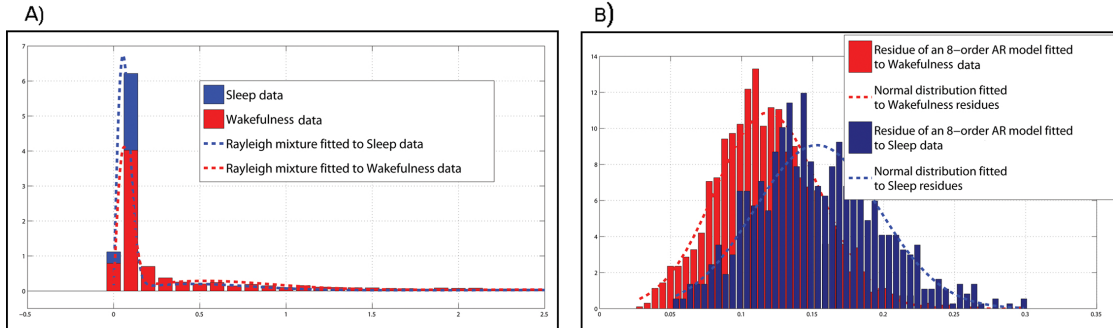


Figure 4.11: Normalized histograms of A) Sleep (blue) and Wakefulness (red) data and the respective Rayleigh distributions and B) Sleep (blue) and Wakefulness (red) residues, obtained using a order 8 AR model fitted to the data.

1. Classification of the test data with  $LDC(\theta^*)$ . The parameters  $\theta^*$  were obtained through the maximization of the G-mean, described in Chapter 3.3, taking into account the complete training data set.
2. Classification of the test data with  $LDC(\theta_M^*)$ .  $LDC(\theta_M^*)$  is trained using the whole data but the cost function (G-mean) is optimized taking into account only the movement data ( $\tau(n) = m$ ).
3. Combination of the previous results, where quietness epochs are scored from  $LDC(\theta^*)$  and movement epochs are scored using  $LDC(\theta_M^*)$ .

#### 4.2.6 HMM regularization algorithm

This final procedure refines the results obtained in the MCS leading to the final estimation,  $\hat{x} \in \{\hat{s}, \hat{w}\}$ .

A HMM was chosen for this task since it models processes which have a temporal relation between states, which is the case in the sleep/wake cycle.

Two hidden states are considered,  $x \in \{s, w\}$ , where  $s$  and  $w$  refer to *sleep* and *wakefulness* states, respectively.

Let us consider  $x^* \in \{s^*, w^*\}$ , the output, of the MCS,  $\tau \in \{m, q\}$  the output of the MD and  $t \in \mathbb{N}$  the time, in seconds, since the last movement (quietness periods) or since the patient started to move (movement periods).

The observation model takes into account the following information, extracted in the training step:

- The accuracy rate of the MCS, given by  $P(x^*|x)$ .

- The conditional distribution of the activity given the state, expressed as  $P(\tau|x)$  and shown in Table 4.4.
- The duration of the quietness and movement periods during *sleep* and *wakefulness* (see section 4.2.3). Expressed as

$$P(t|x, \tau) = \begin{cases} \mathcal{N}(\sigma_x) & \text{if } \tau = m \\ \mathcal{E}(\lambda_x) & \text{if } \tau = q \end{cases} \quad (4.34)$$

The probability of any observation  $y = \{x^*, \tau, t\}$  given the state  $x \in \{s, w\}$  is expressed as

$$\begin{aligned} P(x^*, \tau, t|x) &= P(x^*|x)P(t, \tau|x) \\ &= P(x^*|x)P(\tau|x)P(t|x, \tau) \end{aligned} \quad (4.35)$$

The transition matrix is computed from the training data as

$$P = \begin{bmatrix} \frac{N(ss)}{N(ss)+N(sw)} & \frac{N(sw)}{N(ss)+N(sw)} \\ \frac{N(ws)}{N(ws)+N(ww)} & \frac{N(ww)}{N(ws)+N(ww)} \end{bmatrix} \quad (4.36)$$

where  $N(\cdot)$  is a counting operator for *ss*, *sw*, *ws* and *ww*, corresponding to *sleep-sleep*, *sleep-wakefulness*, *wakefulness-sleep* and *wakefulness-wakefulness* transitions, respectively.

The hidden state,  $x(t)$ , is estimated along the time from the observations,  $y(t)$ , and the model parameters. The initial probabilities are set to 0.0 and 1.0 for *Sleep* and *Wakefulness* states respectively, because all patients were awake in the beginning of the exam, and the optimal solution, the most probable state sequence, is computed using the *Viterbi Algorithm*.

## 4.3 Experimental Results

In this section the data used to test the algorithm is described and the experimental results, obtained with the MSD are presented. The results are compared with the two methods by Sadeh [7] and Hedner [109] described in Appendix A. The performance is assessed with several *Figures of Merit* (FOM). These FOMs are computed in a *leave-one-patient-out* cross validation basis, where each patient dataset is tested after training the classifier with the remaining data.

### 4.3.1 Data

The nocturnal ACT data was acquired with a *Somnowatch™* device, from Somnomedics, placed in the non-dominant wrist of the subjects, acquiring with a sampling rate of 1Hz.

The output format of these devices is configurable, here, the output of the actigraph is the acceleration magnitude. Some authors suggest that this configuration, also known as digital integration, is the most reliable to measure activity levels [8, 125].

The nocturnal ACT data was jointly acquired with PSG data for validation purposes, the hypnogram, obtained by trained technicians, is used as a ground truth to accurately identify *sleep* and *wakefulness* states in epochs of 30 seconds. Twenty nine adult subjects (age  $48 \pm 13$  years, 13 Males, 16 Females), with no particular pre-diagnosed sleep disorder, participated in this study.

The SE, computed as the ratio between total *sleep time* and total *bed time* was obtained for each patient. All the values of SE fell within the range 75% – 85%. These values are below the typical values found in healthy subjects, usually above 85% [126], which indicated sleep disturbances, although not necessarily pathological.

The normalization step applied to the data reduces the variability observed in the datasets recorded with distinct devices. This step also contributes to the generalization of the described algorithm to data acquired with different models/brands of actigraph devices.

#### 4.3.2 ACT data characterization

Nocturnal ACT data is highly unbalanced from a state distribution point of view. This can be confirmed in Table 4.4 where experimental conditional distribution means and standard deviation values, computed from the relative frequencies observed in the real hypnograms are displayed. Here,  $s$  and  $w$  denote *sleep* and *wakefulness* and  $m$  and  $q$  denote *movement* and *quietness* respectively, e.g.  $P(w|m)$  is the probability of observing *Wakefulness* given that the patient is moving.

$P(\mathbf{x} \boldsymbol{\tau})$			
$P(w m)$	$0.58 \pm 0.19$	$P(s m)$	$0.42 \pm 0.18$
$P(w q)$	$0.15 \pm 0.1$	$P(s q)$	$0.85 \pm 0.09$
$P(\boldsymbol{\tau} \mathbf{x})$			
$P(m w)$	$0.18 \pm 0.07$	$P(q w)$	$0.82 \pm 0.07$
$P(m s)$	$0.06 \pm 0.03$	$P(q s)$	$0.94 \pm 0.04$

Table 4.4: Conditional probabilities obtained from the relative frequency observed in the real hypnograms.  $x \in \{s, w\}$  denotes *sleep* and *wakefulness* states and  $\tau \in \{m, q\}$  denotes *movement* and *quietness*.

During movement periods, the most frequent state is *wakefulness*,  $P(w|m) = 0.58$ , although

closely followed by *sleep*,  $P(s|m) = 0.42$ . During quietness periods the gap between the two states is larger,  $P(s|q) = 0.85$  against  $P(w|q) = 0.15$ .

This observation suggests a correlation between movement and *wakefulness* state and quietness and *sleep* state respectively, but in fact, the probability of a patient moving during wakefulness is much smaller than the probability of not moving, as can be seen from  $P(m|w) = 0.18$  and  $P(q|w) = 0.82$ .

This illustrates the main limitation of nocturnal ACT for SW state estimation: although most methods rely on direct measures of recorded movements, these movements only occur during  $6 \pm 3\%$  of the time in the whole register.

The information from Table 4.4 clarifies why simple empirical classification rules can actually lead to apparently impressive performances. The traditional FOMs, accuracy, sensitivity and specificity, are not able to cope with the type of unbalanced data present on nocturnal ACT. The classification results displayed in Table 4.5, obtained with two naive methods, are used to illustrate this point.

	<i>Sens</i> (%)	<i>Spec</i> (%)	<i>Acc</i> (%)	G-mean(%)
M1	100	0	$80.4 \pm 5.9$	0
M2	$97.2 \pm 2.5$	$22.9 \pm 7$	$84.8 \pm 5.4$	47.2

Table 4.5: Performance of two naive classification methods: M1) All data is scored as *sleep* and M2) movement is scored as *wakefulness* and quietness is scored as *sleep*.

Method M1 classifies all data as *sleep* resulting in a surprising global accuracy of 80.4%. This result is relevant because it shows that a good accuracy is not a good indicator of the performance of the method since it has no ability to detect *wakefulness* state. The second method, M2, classifies all the quietness periods as *sleep* and all the movement periods as *wakefulness*. Even by misclassifying all the *sleep* epochs during movement periods, the method is able to achieve a sensitivity of 97.2% and global accuracy of 84.8%, this is actually not far from previously published results, as can be seen on Table 4.1. The limitation of both M1 and M2 methods is revealed by the low specificity and G-mean, thus reinforcing the need for adequate metrics when dealing with such classification problems.

#### **Movement and Posture**

Another interesting approach in the analysis of ACT data is the correlation of posture, as given by the chest accelerometer from the PSG set-up, and the sleep or wakefulness state. A simple set of heuristic rules was defined to separate each detected movement into one of 8 pre-defined types. The separation rule, together with the percentage of movements found in each group are shown in Figure 4.12. Here, *State Change* was assumed whenever a state transition was observed in the previous or following epoch of the observed movement.

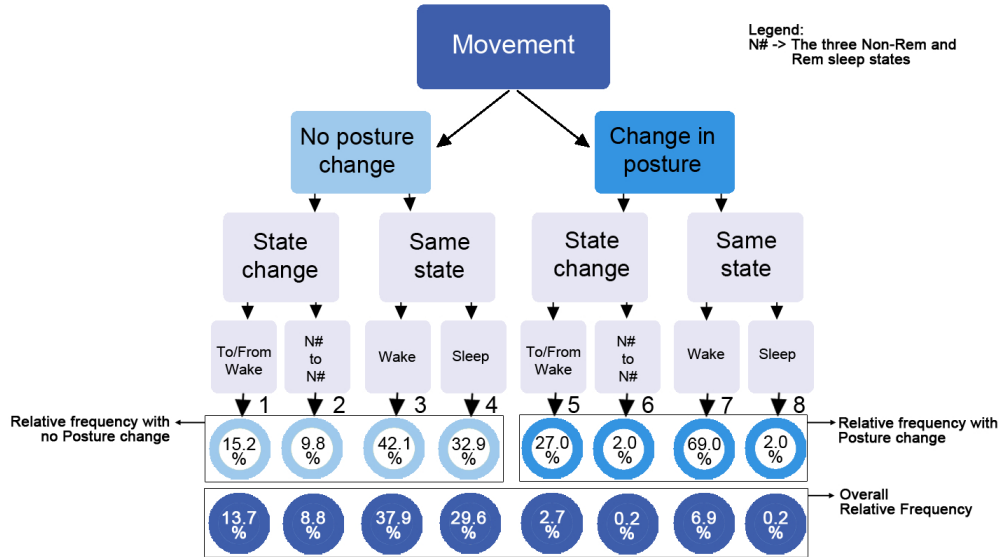


Figure 4.12: Posture and Movement - Each detected movement was labelled according to a simple set of heuristic rules. The subject Posture is given by the chest accelerometer, from the standard PSG and a state transition is assumed when the sleep or wakefulness state changes in the previous or following epoch of the considered movement. N# is used to indicate NREM 1 – 3 and REM sleep states.

As expected, movements not corresponding to a posture change are the majority,  $\approx 90\%$ , when a movement is not related to a posture change, (types 1 – 4) they are mostly observed during wakefulness, closely followed by the movements observed during sleep, supporting the data from Table 4.4. However, approximately 25% of these movements are related to state changes, from which 15% occur when waking up or falling asleep.

When a movement is accompanied by a change in posture (types 5 – 8) the subject is in wakefulness state in approximately 69% of the times, however, in 27% of the cases, the change in posture marks a transition to sleep or wakefulness.

Although the information from Figure 4.12 is not incorporated in the state detection algorithm, it suggests that movement analysis might be used not only to identify sleep states but also to mark state transitions.

### 4.3.3 Sleep / Wakefulness discrimination

Table 4.6 summarizes the results obtained in the individual steps of the method outlined in Figure 4.2. The results include the performance of the individual LDC classifiers,  $LDC(\theta^*)$  and  $LDC(\theta_M^*)$ , the intermediate MCS (which is the combination of both LDC's) and the final MSD. Some results are presented for two distinct scenarios; i) when all the data is considered in the classification and ii) when only movement data is considered,  $\tau_n = m$ .

The  $LDC(\theta^*)$  classifier achieves a global accuracy of 75.9% with sensitivity, specificity and

		<i>Sens</i> (%)	<i>Spec</i> (%)	<i>Acc</i> (%)	G-mean (%)
LDC( $\theta^*$ )	<i>i)</i>	$75.9 \pm 9.8$	$74.8 \pm 9.6$	$75.9 \pm 8.7$	75.3
	<i>ii)</i>	$15.8 \pm 11.6$	$96.6 \pm 2.9$	$65.7 \pm 12.2$	39.1
LDC( $\theta_M^*$ )	<i>ii)</i>	$74.5 \pm 16.8$	$63.4 \pm 11.6$	$66.5 \pm 11.3$	68.7
MCS	<i>i)</i>	$72.1 \pm 3.2$	$73.6 \pm 11.1$	$71.3 \pm 8.2$	72.8
MSD	<i>i)</i>	$75.6 \pm 8.3$	$81.6 \pm 7.5$	$77.8 \pm 8.1$	78.5
	<i>ii)</i>	$73.8 \pm 14.2$	$73.5 \pm 9.5$	$75.5 \pm 9.2$	73.7

Table 4.6: Mean and Standard deviation of the *Sens*, *Spec* and *Acc* and G-mean obtained for the different components of the MSD. The performance was assessed considering i) all the data and ii) only movement data.

G-mean in the same range. The limitation of this classifier arises when only movement data is considered, with the sensitivity falling to 15.8%. This means that during movement periods the classifier tends to classify all epochs as *wakefulness*.

The  $LDC(\theta_M^*)$  is only evaluated for movement segments. It achieves a G-mean of 68.7%, approximately 30% higher than the  $LDC(\theta^*)$  during the same periods. On the other hand, the specificity drops to 63.4% due to the *wakefulness* periods misclassified as *sleep*.

The MCS combines the scores from the two LDC's. It achieves a G-mean of 72.8% when the complete data is considered (the decrease in specificity is due to reason explained before) and the performance during movements is similar to the  $LDC(\theta_M^*)$ .

Finally, the performance of the MSD clearly reflects the improvement obtained with the HMM. It achieves a G-mean of 78.5% when all the data is considered and 73.7% when limited to movement data.

It is important to stress the balance of *Sens* and *Spec* achieved with the proposed method in global terms but specially during movement periods. This results can be very useful when ACT is used together with other physiological data, e.g. ECG, whose sensors are typically sensitive to movement artefacts.

### Algorithm generalization

In order to assess the generalization capability of the algorithm the following procedure was performed:

1. Ten datasets were randomly selected from the pool of 29 available datasets.
2. From these 10 datasets, 5 were randomly selected to train the algorithm.
3. The remaining 5 datasets were used to test the algorithm and the average G-mean was computed.

This procedure was repeated 15 times resulting in an average G-mean of  $76.3 \pm 2\%$ . This value is only 2% smaller than the G-mean reported in Table 4.6 and, together with the low standard deviation, suggests that the reported results should be extensible to other datasets.

### Sensibility to movement detector threshold

The sensibility of the method, to small variations on the MD threshold, was assessed by forcing random variations of  $\pm 20\%$  on each dataset threshold. The variation in the G-mean's for i) All the data and for ii) Movement data (see Table 4.6) was less than 1% in average.

### Performance comparison

		<i>Sens</i> (%)	<i>Spec</i> (%)	<i>Acc</i> (%)	G-mean(%)
MSD	i)	<b><math>75.6 \pm 8.3</math></b>	<b><math>81.6 \pm 7.5</math></b>	<b><math>77.8 \pm 8.1</math></b>	<b>78.5</b>
	ii)	<b><math>73.8 \pm 14.2</math></b>	$73.5 \pm 9.5$	<b><math>75.5 \pm 9.2</math></b>	73.7
Sadeh	i)	$75.1 \pm 6.5$	$61.6 \pm 15.2$	$73.9 \pm 3.7$	68.0
	ii)	$47.3 \pm 12.8$	$75.8 \pm 9.2$	$62.4 \pm 12.8$	59.9
Hedner	i)	$73.6 \pm 10.7$	$68.6 \pm 11$	$74.1 \pm 9.3$	71.1
	ii)	$14.5 \pm 14.1$	<b><math>88.7 \pm 26.1</math></b>	$64.2 \pm 16.3$	35.9

Table 4.7: Mean and Standard deviation of the *Ssb*, *Spec* and *Acc* obtained for the 3 considered methods in two conditions, i) complete data set and ii) only movement data.

In Table 4.7 the results obtained with the MSD are compared with the two comparative methods by Sadeh [7] and Hedner [109]. Using the complete datasets MSD achieves higher sensitivity, specificity, global accuracy and G-mean than the considered methods. While the difference in global *Acc* is relatively small ( $\approx 3\%$ ), the increase in the G-mean is 10.5% and 7.4%. This result clearly illustrates the limitation of using the global accuracy as the only performance metric. When only movement periods are considered the MSD clearly outperforms the comparative methods, which present a bias to classify the movement periods as *wakefulness* thus achieving a low *Sens*.

#### 4.3.4 Final remarks

Nocturnal ACT can be roughly clustered in two classes of 1) quietness periods, when only background activity and noise are recorded and 2) movement periods.

During the periods of quietness the relevant information for SW state estimation lies on the inter-movement durations, whose statistics are shown in Fig. 4.6-A), and on the *a priori* correlation knowledge about activity and state, shown in Table 4.4. The ACT signal magnitude itself does not provide useful information during these periods.

On the contrary, during movement periods the magnitude of the ACT signal is relevant for state estimation but the *a priori* information ( $P(s|m) = 0.42$  and  $P(w|m) = 0.58$ ) is not so important for estimation process as in the quietness periods ( $P(s|q) = 0.85$  and  $P(w|q) = 0.15$ ).

The magnitude characterization in these periods can be performed in a spectral and statistical basis, namely, with first and second order statistics, as shown in Figure 4.11.

The presented algorithm is optimized for proper SW estimation in the scope of sleep disorders diagnosis. Other applications may have different requirements not fulfilled by this method. For example, the detection of rest and activity periods for ambulatory blood pressure monitoring, such as the work described in [127], requires an algorithm less sensitive to micro-wakening episodes.

## 4.4 Conclusions

This chapter explored the use of behavioural data in the context of sleep monitoring and sleep disorders diagnosis. A new sleep/wakefulness state estimation algorithm was described, that uses an extended set of features related with signal magnitude and time events. Two LDCs, trained with the magnitude related features, provide a first state estimation that is refined with a HMM based algorithm taking into account time events and a priori information about movements and states correlation.

Relevant novelties are related with the optimization strategy in the training process based on the G-mean metrics. The goal is to improve simultaneously the performance in movement and quietness periods as well as the balance between specificity and sensitivity which improves the wakefulness detection rate.

A new database of ACT data was built specifically for this project. With these data, the MSD yields a global accuracy of 77.8%, a sensitivity of 75.6% and a specificity of 81.6%, revealing a balance in the detection of both *sleep* and *wakefulness* states, a key issue of this work. Additionally, under the G-mean metrics the proposed method clearly outperforms the other tested methods.

During movement periods the method achieves an accuracy of 75.5%, sensitivity of 73.8%, specificity of 73.5% and G-mean 73.7%.



## 5 Physiological data

The sleep cycle is controlled by a highly complex system with numerous variables. Some of the changes that characterize this cycle can be easily observed from the subjects behaviour, with deviations to the accepted pattern being generally a good indicator of some kind of disorder. However, as described in Chapter 2, the majority of changes occur on a physiological level. The array of easily observable physiological variables is diverse and has been increasing with the development of new technologies. They include hormonal levels, the electrical activity of the muscles and the brain, mechanical changes induced by the beating heart and the respiratory effort, blood flow and arterial oxygen concentration, among others.

In the design of a portable sleep monitor it is important to maintain the array of acquired variables to a minimum and, at the same time, including variables with known relevance in sleep assessment.

The EEG is a obvious choice for sleep monitoring, since it reflects, almost directly, the brain activity and, consequently, sleep. However, the use of EEG is impractical over long periods and non-controlled environments. The same reasoning can be used to discard physiological signals implying any kind of discomfort for the subject, such as an oral/nasal cannula and the finger oximeter.

The ECG, Galvanic Skin Response (GSR) and breathing waveform, in the form of RIP, can be obtained without any significant disturbance to the subject, often across several days. Although none of these physiological signals give a direct insight regarding sleep, they are all highly connected to the activity of the ANS. Which, in its turn, is an important system in sleep and sleep regulation.

In this chapter, the Autonomous Nervous System is briefly presented, with emphasis given to the HRV and its main control system, the baroreflex. A mathematical model for the Baroreflex is presented and used to support a physiology based theory for the frequency bands of the HRV activity. Finally, the relevance of the ANS in the context of sleep is discussed with focus on the changes observed in breathing and heart rate.

## 5.1 Autonomic Nervous System

The CNS is responsible for the regulation of two distinct motor systems. The voluntary motor system allows conscious muscular control of the limbs, body and head, and the involuntary motor system, or Autonomic Nervous System, controls most visceral functions of the body. The ANS helps to control arterial pressure, gastrointestinal mobility, gastrointestinal secretion,

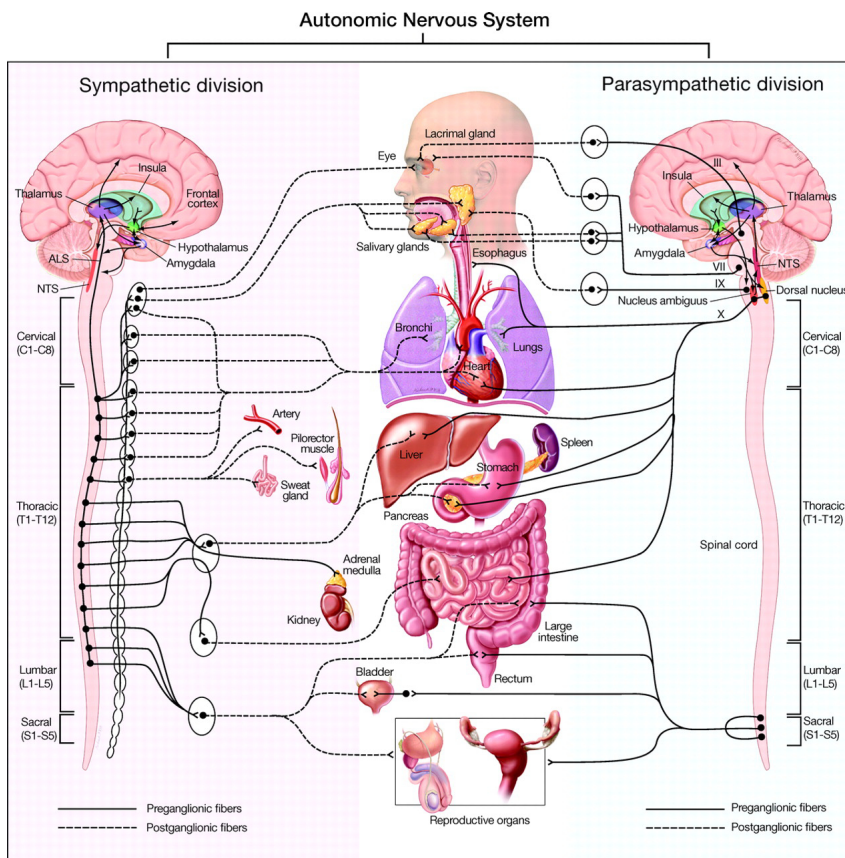


Figure 5.1: The **Sympathetic** and **Parasympathetic** branches of the ANS are shown on the left and right sides, respectively, together with the targets of the innervations (center). The Sympathetic (left side) brain pathways include those to the thalamus from the Anterolateral System (ALS) of the spinal cord, output from the thalamus to the neocortex, insula, and amygdala, bidirectional pathways between the hypothalamus and both the amygdala and frontal cortex, output from the hypothalamus to the Nucleus Tractus Solitarius (NTS), and output from the amygdala to the ALS and brainstem. On the Parasympathetic side (right), the pathways include those to the thalamus from the NTS, output from the thalamus to the neocortex, insula, and amygdala, and bidirectional pathways between the hypothalamus and amygdala. Roman numbers III, VII, IX, and X (vagus) designate cranial nerves. (Reused from [128] with permission)

urinary bladder emptying, sweating, body temperature, among other [129]. These regulatory mechanisms are constantly adapting the body to the environmental conditions and can occur extremely fast. For example, the heart can double its normal heart rate within 3 to 5 seconds after a stimuli from the ANS; in 10 to 15 seconds the BP can be lowered enough to cause

fainting; and sweating can occur within a few seconds.

### 5.1.1 Structure

ANS activation is mediated mainly by centres located in the *spinal cord*, *brain stem* and *hypothalamus*. Portions of the *cerebral cortex* can also transmit signals to the lower centres thus influencing autonomic control. The ANS also operates through *visceral reflexes*, i.e. afferent sensory signals from visceral organs can enter the autonomic ganglia, the *brain stem*, or the *hypothalamus* and then return subconscious reflex responses directly back to the visceral organ to control its activities[129].

The efferent autonomic signals are divided into two opposing pathways, depicted in Figure 5.1, composing the **sympathetic** and **parasympathetic** nervous systems, which induce opposing responses on the affected organs.

The sympathetic nervous system, activated in physically or mentally stressful situations is often referred as the "*fight or flight*" response. It causes an increase in the heart rate, BP, Cardiac Output (CO), blood flow to the muscles, pupil dilation and a decrease in the digestive system activity. The sympathetic nerve fibers, shown on the left side of Figure 5.1, originate in the spinal cord along with spinal nerves between cord segments T1 and L2 and pass first into the sympathetic chain and then to the tissues and organs that are stimulated by these nerves. Each sympathetic pathway from the cord to the stimulated tissue is thus composed by two neurons, a preganglionic neuron and a postganglionic neuron, these nerves contrast with skeletal motor nerves which are composed by a single neuron in the skeletal motor pathway.

The parasympathetic nervous system is often referred as the "*rest and digest*" mechanism, causing the heart rate and BP to decrease and the digestive system activity to increase. The parasympathetic nerve fibres, shown on the right side of Figure 5.1, leave the central nervous system through cranial nerves III, VII, IX, and X; additional parasympathetic fibers leave the lowermost part of the spinal cord through the second and third sacral spinal nerves and occasionally the first and fourth sacral nerves. About 75 percent of all parasympathetic nerve fibers are in the vagus nerves (cranial nerve X) [129], passing to the entire thoracic and abdominal regions of the body. It is thus common for the vagus nerves to be referred as the parasympathetic nervous system. These nerves supply parasympathetic nerves to the heart, lungs, esophagus, stomach, entire small intestine, proximal half of the colon, liver, gallbladder, pancreas, kidneys, and upper portions of the ureters.

### 5.1.2 Neurotransmitters

Two main synaptic transmitter substances are involved in the propagation of the sympathetic and parasympathetic impulses, **acetylcholine** and **norepinephrine**. Fibres secreting acetylcholine are said to be cholinergic and those secreting norepinephrine (commonly known as adrenalin) are said to be adrenergic.

## **Chapter 5. Physiological data**

---

All preganglionic neurons are cholinergic in both the sympathetic and the parasympathetic nervous systems. Acetylcholine or acetylcholine-like substances, when applied to the ganglia, will excite both sympathetic and parasympathetic postganglionic neurons.

Either all or almost all of the postganglionic neurons of the parasympathetic system are also cholinergic. Conversely, most of the postganglionic sympathetic neurons are adrenergic. However, the postganglionic sympathetic nerve fibers to the sweat glands, to the piloerector muscles of the hairs, and to a very few blood vessels are cholinergic.

Thus, the majority of terminal nerve endings of the parasympathetic system secrete acetylcholine. Almost all of the sympathetic nerve endings secrete norepinephrine, but a few secrete acetylcholine. These neurotransmitters in turn act on the different organs to cause respective parasympathetic or sympathetic effects. Therefore, acetylcholine is called a parasympathetic transmitter and norepinephrine is called a sympathetic transmitter

### **5.1.3 Sympathovagal balance**

On a healthy subject the sympathetic and parasympathetic systems are permanently active, the basal rates of activity are known as sympathetic tone and parasympathetic tone, respectively.

A delicate balance between the two activities allow a single branch of the ANS to decrease or increase the activity of a stimulated organ. For instance an increase in the heart rate can be achieved by a slight increase in the sympathetic stimulation or, inversely, by a decrease on the parasympathetic activity.

This complicated interaction between the sympathetic and parasympathetic branches and the overall effect that they have on the autoregulation of the cardiovascular system and the autonomic tone, is commonly known as the **sympathovagal balance**.

## **5.2 The Baroreflex**

Autonomic reflexes regulate several important visceral functions of the body. For example, the smell of food or the presence of food in the mouth transmits information to the brain stem which will then stimulate the secretory glands of the mouth and stomach via parasympathetic nerves, thus initiating digestion even before any food intake.

Other examples of autonomic reflexes include the control of the urinary bladder and colon, activating the gastrointestinal function, and several different reflexes involved in the control of the cardiac function and BP homeostasis.

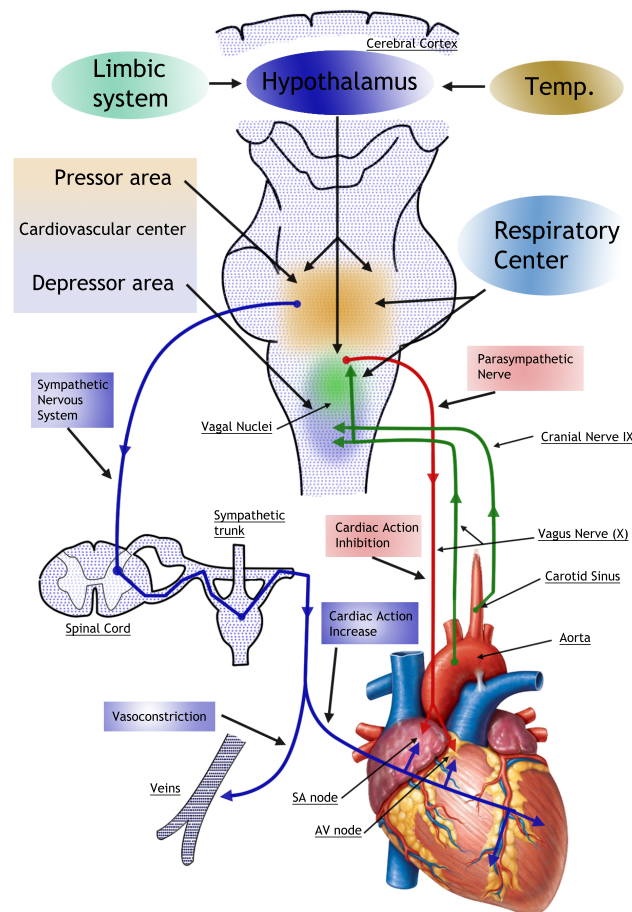


Figure 5.2: Central regulation of blood flow: The cardiovascular center, situated in midbrain and medulla oblongata receive information from a network of sensors that measure i) arterial blood pressure, ii) pulse rate and iii) filling pressure. If the measured values differ from the set-point, the CNS transmits regulatory impulses through nerve fibers to the heart and blood vessels. The pressor's efferent fibers continuously transmit sympathetic impulses to the heart, increasing its activity, and to the vasculature, setting its resting tone. The pressor and depressor areas of the cardiovascular center are connected to the dorsal nuclei of the vagus nerve, the stimulation of which reduces the heart rate and cardiac conduction rate. (Adapted from [19]).

Proper blood flow regulation is critical to ensure adequate blood supply and must be guaranteed even under abnormal environmental and psychological conditions.

BP is influenced by various factors, the heart rate and stroke volume have a profound effect on the pressure by acting on the CO. Other major influence in the BP is the vascular resistance and blood viscosity. The regulation of cardiac activity and BP is guaranteed by different mechanisms, on which the ANS plays a fundamental role.

The most studied nervous mechanism for arterial pressure control is the baroreceptors reflex, or **baroreflex**. This reflex has its origin on stretch receptors, called *baroreceptors*, located at

## Chapter 5. Physiological data

---

specific points in the walls of several large systemic arteries. The main sensors are located in high pressure locations, such as the aorta and carotid artery, in low pressure locations, such as the vena cava and atria and in the left ventricle of the heart [19, 130]. Depending on the location, each sensor can measure one or various variables, including arterial BP, pulse rate, and filling pressure (an indirect measure of blood volume)[131].

The stimulated *baroreceptors* fire trains of action potentials, (*spikes*), with a firing rate depending on its mechanical deformation changes which are then relayed to the NTS, where the cardiovascular center and the *medullary rhythmicity* center, also known as respiratory center, are located [132].

The frequency of the action potential impulse train determines the response and actions triggered in the NTS, if the measured values differ from the set-point value, the control centres will induce a feedback response.

Under normal conditions, a pressor area, situated in the cardiovascular center continuously transmit sympathetic nerve impulses to the heart to increase its activity (heart rate, conduction and contractility). Sympathetic impulses are also responsible for the vasoconstriction, setting the resting tone. Both the pressor and depressor areas are connected to the dorsal nuclei of the vagus nerve, which acts as effector and affecter. Sympathetic stimuli are conducted by two cranial nerves, the *glossopharyngeal* (IX) and the *vagus* (X) leading to a reduction of heart rate and cardiac impulse conduction rate.

The main purpose of homeostatic control via the Baroreflex, is to maintain the arterial BP at a stable level. Sudden increases in the BP increase the firing rate of the baroreceptors and the rate of afferent impulses to the cardiovascular center. The depressor area elicits the depressor reflex through the parasympathetic neurons of the vagus nerve, leading to a decrease of the CO. In addition, inhibition of the sympathetic pathways causes the vessels to dilate thus reducing the peripheral resistance. On the other hand, a sudden decrease in the BP will induce the opposite response.

### 5.3 Heart Rate Variability

The rhythmical contraction of the heart is controlled by a group of specialized cells, the Sinoatrial Node (SAN), positioned on the wall of the heart's right atrium (see Figure 5.2). Although all of the heart's cells have the ability to rhythmically generate action potentials, it is the SAN that initiates each cardiac contraction.

In the absence of any neurohumoral influence (nervous or hormonal) the SAN generates approximately 100 – 120 action potentials per minute, resulting on an equivalent HR. However, a resting healthy human is likely to have a slower HR of around 70 – 80 bpm due to the modulation of the SAN firing rate by the innervations of both sympathetic and parasympathetic branches of the ANS.

Acetylcholine, released by the postganglionic parasympathetic terminals at the SAN slows

### 5.3. Heart Rate Variability

the rate of the node's depolarization and discharge by binding to muscarinic cholinergic receptors and increasing the cell membrane  $K^+$  conductance [133, 129]. On the other hand, norepinephrine, released by the sympathetic terminals, increase the node's rhythm via the activation of  $\beta$ -adrenergic receptors, resulting in cAMP-mediated phosphorylation of membrane proteins and increases in  $I_{Cal}$  and  $I_f$  [129, 134, 135].

In addition to the direct neural innervation of the heart, other processes responsible to influence the heart rate include the indirect effect of the sympathetic system through the release of adrenomedullary catecholamines and the fluctuations induced by the respiratory-related mechanical stretch of the SAN.

Although not exclusively responsible, it is commonly accepted that the chronotropic control of the heart is performed by the ANS. The instantaneous HR is thus considered a manifestation of both the (antagonistic) effects of the parasympathetic and the sympathetic nerves through permanent changes in neurotransmitters levels. During rest, both autonomic divisions are thought to be tonically active with the parasympathetic effects achieving dominance, thus lowering the natural frequency of the pacemaker.



Figure 5.3: Approximately one minute of RR (blue line) and Breathing data (green line), acquired on a relaxed subject. The RR interval has a natural variation, due to regulatory mechanisms mediated by the ANS. During rest, this variation is highly correlated with the breathing waveform.

Figure 5.3 shows approximately one minute of RR (see Appendix ??) and RIP data, acquired from a healthy subject under resting conditions. It is clear that the RR (blue line) varies around a mean, representing the fine tuning of the beat-to-beat control mechanisms, this oscillation is partially correlated with the breathing waveform.

The natural oscillation in the interval between consecutive heartbeats has received many names, including RR variability, RR tachogram and cycle length variability, but the most commonly accepted term to this phenomenon is Heart Rate Variability.

The natural variability of heart rate has been noted as early as the 17<sup>th</sup> century but it wasn't until 1963 that its physiological relevance was appreciated. Hon and Lee [136] noted that fetal distress was preceded by changes in the pattern of beat-to beat intervals before any significant change in the baseline heart rate. Since then, HRV has received the attention of researcher and medical communities from several areas and changes on HRV have been related to a large range of pathologies and medical conditions including Myocardial Infarction, Diabetes, Cardiac Transplantation, Myocardial Dysfunction, Tetraplegia, Hypertension, Stress,

Depression, Epilepsy, among others [10, 137].

Several methods for the analysis of HRV are described in the literature, they are commonly divided in *Time Domain Methods*, including statistical and geometric measures and *Frequency Domain Methods*. The algorithm described in Chapter 6 involves the computation of measures from both domain, however, only Frequency Domain Methods will be discussed in this chapter, particularly due to their close relation with physiology and the nature of HRV.

For a complete insight on the Time and Frequency domain methods, please refer to the review by the *Task Force of the European Society of Cardiology and the North American Society of Pacing and Electrophysiology* [10].

The periodic components of heart variability tend to aggregate around well known frequency bands, three major components are typically recognized [138]. The Very Low Frequencies (VLF) in the interval 0.0 – 0.015Hz, the Low Frequencies (LF), in the interval 0.015 – 0.15Hz and the High Frequencies, 0.15 – 0.4Hz. The spectrum of the arterial BP variability also exhibits two main frequency bands, highly correlated with the LF and HF components of the HRV. It is believed that in the closed-loop circulatory system, these components correspond to vasomotor activity (LF band) and to the respiratory activity oscillation (HF band).

The two LF and HF HRV frequency bands are thus intimately connected with the activity of the two branches of the ANS. It has long been established that the HF component is a reliable marker of vagal (parasympathetic) activity. Exercises of controlled respiration, cold stimulation of the face, and rotational stimuli have been shown to increase the HF components, conditions that are known to increase vagal activity [138].

The interpretation of the LF component, on the other hand, is more controversial. Some authors [139] have defended that LF reflects vagal activity when the subject is in supine position, and both sympathetic and parasympathetic activities when the subject is in upright position. The alternative, yet related, interpretation is that LF is in fact a marker of sympathetic activity although resulting from the interaction of the two branches [140]. Under controlled test conditions, exercises characterised by a shift of sympatho-vagal balance towards sympathetic predominance, have resulted in the increase of the LF component and simultaneously a decrease in the HF component. Commonly used frequency-domain measures now include the LF/HF ratio, interpreted as the balance between sympathetic and parasympathetic tones [10, 138, 141].

Although this metric remains a topic of much debate amongst researchers [142], there is a general consensus that it is a useful model for clinical applications [143].

### 5.3.1 Origin of the frequency components

The frequency components of the HRV described in the previous section, are mainly attributed to the activity of the two branches of the ANS. The LF band is believed to roughly translate the activity of the sympathetic nervous system and HF the activity of the parasympathetic

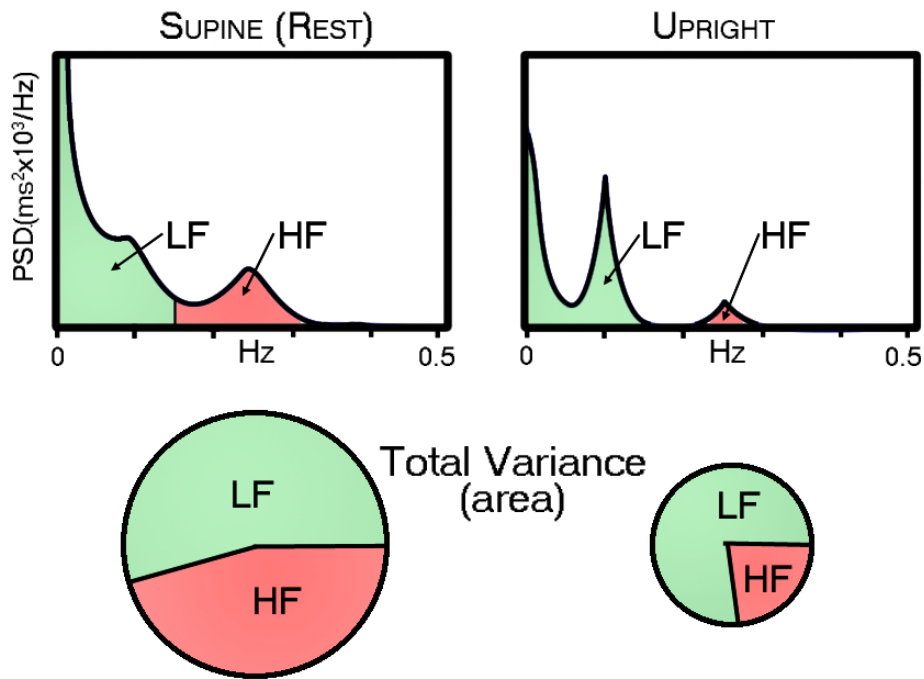


Figure 5.4: Spectral analysis of the HRV on a healthy subject performing an active orthostatic test. Top) The normalized power spectrum density ( $ms^2 \times 10^3 / Hz$ ) shows that in supine position the two components, LF and HF, have approximately similar powers. In the upright position the LF component predominates, appearing to have a power similar to the supine position. Bottom) The pie charts areas reflect the total variance on the HRV. This reveals a strong reduction of the HRV power in the upright position. Both LF and HF components are strongly reduced, something not easily perceived in normalized units.

branch. Although these frequency bands are widely accepted and used in the literature, its physiological origin is seldom discussed.

Vagus nerve activity can change heart rate substantially within one cardiac cycle, and the chronotropic effects decay almost completely within one cardiac cycle after cessation of vagal activity. In 1979 Spear and colleagues [144] studied the effect of vagal stimulation on the SAN of rabbits, they found that a vagal burst has its maximum effect after approximately 0.5 seconds, with a return to baseline within  $\approx 1$  second.

A sympathetic burst caused no effect for at least 1 second and its maximum expression was only verified 4 seconds later, followed by a 20 seconds relaxation time. These results were later confirmed by Berger and colleagues [145] in 1989 using dogs. Both groups suggested that vagal and sympathetic responses could be characterized by low-pass filters, with an additional delay in the case of the sympathetic system. Vagal filter response was characterized as fast with little delay, with a corner frequency of  $\approx 0.15Hz$  and the sympathetic response as slow, with 1 – 2 seconds delay and a corner frequency of  $\approx 0.015Hz$ .

These filter responses are consistent with the observations in humans, where the sympathetic

## Chapter 5. Physiological data

---

system modulates the HR in frequencies under  $\approx 0.15$  Hz and parasympathetic system in frequencies between  $0 - 0.5$  Hz.

A possible explanation to the difference in the responses of the two systems is related to receptor processes and postsynaptic responses. Hill-Smith and Purves [146] suggested that the delay in the cardiac response to acetylcholine and norepinephrine probably arises from processes subsequent to the binding of the agonist to the receptor. This interpretation is consistent with the demonstration by Hille [147] that the linkage between muscarinic receptor activation and changes in ionic currents is mediated by signalling molecules located largely within the cell membrane, opposed to adrenergic stimulation, which is initiated in the membrane and requires a second-messenger activation (a protein kinase in the cytosol) which eventually sends a signal back to the membrane to change the ionic currents.

The emphasis for the physiological explanation of the different responses is usually placed on the speed of the process that initiates the responses, however, the processes that terminate the responses to the ANS stimuli might provide further answers, in particular the processes responsible for the removal of the released neurotransmitters.

The norepinephrine released by the sympathetic nerve endings is removed from the cardiac tissues much more slowly than the acetylcholine, released from the vagal terminals [148]. As a consequence of the potential harmful effects associated with the slow removal of norepinephrine, the cardiac neural control system might have evolved such that the sympathetic nerves ordinarily release the norepinephrine at a slow rate. Hence, changes in sympathetic neural activity can alter cardiac behaviour only slightly from beat to beat. Beatwise control of cardiac function would thus be negligible, regardless of how swiftly the sympathetic nerve impulse is transduced to a change in cardiac performance.

### 5.3.2 Respiratory Sinus Arrhythmia and Mayer Waves

Underlying the complexity of heart rate variability, two distinct rhythms can be typically isolated.

In healthy resting individuals, the respiratory cycle induces a marked beat-to-beat fluctuation in the entire arterial pressure waveform and on the HR. Figure 5.3 illustrates the modulation of HR by the respiration, increasing during inspiration and decreasing during expiration.

Frequency analysis of the RR often reveals a marked peak in the respiratory frequency, this modulation of the HR by the respiration is known as **Respiratory Sinus Arrhythmia**. It has been proposed that the synchronization between the respiratory rhythm and the heart beat optimizes the pulmonary gas exchange by matching alveolar ventilation and capillary perfusion [15, 149], thus justifying RSA as an evolutionary adaptation.

The physiological process behind RSA is still not entirely clear. The fluctuations in BP in synchrony with respiration are unlikely to be mediated by sympathetic activity, since the time constant of the vaso-motor response is too long to follow neural signals oscillating at breathing frequencies. It has been suggested that this phenomenon is mainly mediated by fluctuations

of vagal-activity [137] and that the variability induced by controlled breathing can be used as a direct measure of the cardiovagal function [150].

However, variations on the RSA have been shown to occur independently of vagal tone. In [151, 152] the authors suggest that the RSA is regulated centrally, with its magnitude being proportional to the respiratory drive and attributing chemoreceptors a role in RSA.

In [153] the authors reported that heart transplanted patients, with no autonomic HR control, still exhibited RSA, suggesting a mechanical action on the SAN by the changes in lung volume and intrathoracic pressure, this idea was corroborated in [154] after complete autonomic blockade.

Some authors defend that RSA results from "spillover" of signals from the medullary respiratory center into the adjacent vasomotor center during inspiratory and expiratory cycles of respiration. The spillover signals cause alternate increase and decrease in the number of impulses transmitted through the sympathetic and vagus nerves to the heart [129].

In summary, the RSA is likely to be caused by both respiratory and circulatory centers in the brainstem. Two major mechanisms are probably in its genesis: direct modulation of the cardiac vagal preganglionic neurons by central respiratory drive; and inhibition of cardiac vagal efferent activity by lung inflation.

The second rhythm occurs over approximately 10 seconds cycles, affecting both HR and arterial pressure. This natural oscillation was first described by Siegmund Mayer and his colleagues, and is commonly referred as **Mayer waves**.

Mayer waves rhythm has been attributed to various sources, but most recently has been presumed to reflect reflex mediated fluctuations in sympathetic outflow to the vasculature and in parasympathetic and sympathetic outflows to the heart. Cardiac interval oscillations at the Mayer wave frequency are mediated primarily by cardiac vagal but also cardiac sympathetic outflows and are thought to represent arterial baroreflex responses to pressure oscillations. One popular theoretical and practical explanation is a resonant response in the baroreflex due to feedback delays [155].

## 5.4 The ANS and sleep

As explained throughout this chapter, HR is modulated by the combined effects of the sympathetic and parasympathetic nervous systems. HRV monitoring is thus a simple way to gain insight regarding autonomic functions.

Since ECG is a standard signal acquired in the PSG, the assessment of HRV during sleep is straightforward and has been the focus of many researchers in the last years.

The list of possible applications for HRV is extensive, it has been applied to understand the effect of sleep disordered breathing, periodic limb movements, insomnia, sleep deprivation and epilepsy, among others [12, 156, 157]. Due to the large range of devices able to monitor

## Chapter 5. Physiological data

---

ECG, it has a large potential in the screening of subjects for possible referral to a Sleep Lab and it is one of the main sources of data being explored in portable monitors.

The process of falling asleep, briefly addressed in Chapter 2, is accompanied by an increase in the activity of the parasympathetic system of the ANS, which slowly dominates the decreasing sympathetic system. After sleep onset, NREM sleep stages are characterized by a gradual general relaxation of the cardiovascular system, stable and deep respiratory patterns and a decrease in the metabolic rate, leading to a drop in BP, HR, stroke volume, cardiac output and vascular resistance [158]. When compared to Wakefulness and REM, NREM stages 1 and 2 have a progressive power increase in the HF band, accompanied by a decrease in the  $\frac{LF}{HF}$  ratio and SWS presents diminished power in all frequency bands [159, 160, 161, 162, 163].

The overall reduction of autonomic activity and stability of the cardiovascular system during NREM states are occasionally interrupted by arousals, which are characterized by abrupt increases in chemosensitivity, momentary restoration of the irregular/fast breathing characteristic of Wakefulness. HR and BP also increases from NREM to relaxed wakefulness involving an increase in sympathetic activity, although with no parasympathetic withdrawal [141].

The transition to REM sleep is marked by an increase on LF components and a shift in the respiratory/cardiovascular systems, which present behaviours similar to Wakefulness [164, 162, 163]. This HRV variation is consistent with sympathetic nervous system activation during REM sleep and wake periods.

Some authors have reported that this shift begins several minutes prior to the actual transition from NREM to REM, as scored from EEG. The opposite effect was also verified, with high levels of sympathetic activation often continued beyond the end of REM sleep [165]. The same authors also reported early activations of the sympathetic system in the case of arousals from stage 2 NREM and REM, with heart rate acceleration being verified at least 10 beats prior to the EEG arousal. This data supports the theory that increases in ANS sympathetic activity precede and possibly play a role in the initiation of REM sleep and arousals during sleep.

A brief retrospective of the study of HRV in the scope of sleep studies is presented in [161], where the authors show detailed data on the variation of the HRV across the different sleep stages. Recent studies focus on nocturnal HRV under confinement conditions [166] and in [12] an in depth review of the relationship between HRV and several sleep disorders is presented.

The respiration pattern during sleep is another source of useful information regarding the activity of the ANS. Breathing is controlled by a cyclic stimulation of the diaphragm mediated by the phrenic nerve, which contains motor, sensory, and sympathetic nerve fibers. The involuntary breathing process is thus a direct reflection of the activity of the ANS which can be included in the characterization of sleep.

In [167] the authors show that respiration is more irregular during REM states when compared to Non-REM and in [16] the authors show that different sleep stages lead to distinct autonomic regulation of breathing.

## 5.5 Baroreflex Model

In this section, the Baroreflex model described in [168] is extended to include the dynamics of acetylcholine and norepinephrine in the Sinoatrial Node. The model is used to simulate an Active Orthostatic Test and the predicted dynamics are compared with real data, acquired from healthy volunteers.

### 5.5.1 Existing models

In 1987 DeBoer and colleagues proposed a beat-to-beat model for the hemodynamic fluctuations and baroreflex sensitivity in humans [155]. This model includes the control of interbeat interval and of peripheral resistance by the baroreflex; the Windkessel properties of the systemic arterial tree; the contractile properties of the myocardium, modelled using Starling's law [169] and restitution properties; and the mechanical effects of respiration on BP.

Since the original publication, some of the physiological claims supporting this model have been reformulated and several new models for the baroreflex and for the individual components of this complex system have been proposed [170, 171, 172, 173, 174, 175, 176, 177]. However, the work by DeBoer *et al.* is still cited by many authors in state of the art studies.

The model adopted in this study, first described in [168], is a closed loop system where most of the operations are linear. Although other models are able to better simulate processes such as the non-linear behaviour of baroreceptors, the used model is a good approximation in the considered regions of operation.

In the next section, the main blocks of the model are briefly presented together with the newly introduced changes. A detailed description of each block is outside the scope of this chapter and can be found in the original publication.

### 5.5.2 Model description

In the scope of control theory, the baroreflex mechanism is a regulator, as it maintains the Mean Arterial Pressure (MAP) constant, independently of the external or internal disturbances.

Figure 5.5 shows the structure of the proposed model, which is composed by four main blocks: the i) heart and ii) the vasculature (CVS), are the systems to be controlled, iii) the ANS is the controller block and iv) the baroreceptors are the sensory inputs.

The baroreceptors sense the instantaneous blood pressure and provide their information to the ANS which in its turn acts on the heart and blood vessels, thus closing the controlling loop.

The **ANS block** represents the baroreflex control centers in the brainstem nuclei. This block is the main controller of the baroreflex loop, a *Proportional, Integral and Derivative* (PID) controller is responsible for the minimization of the "error", given by the spike density generated on the Baroreceptors. This minimization guarantees low fluctuations on the MAP.

The design of this control block ensures that the sympathetic system is inhibited by an in-

## Chapter 5. Physiological data

---

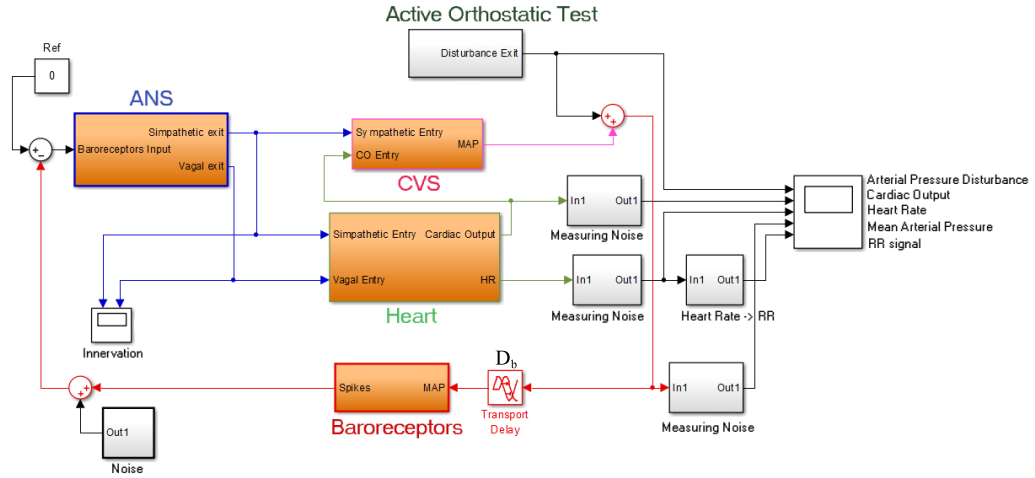


Figure 5.5: Structure of the proposed model. The model contains four major blocks, modelling the Autonomic Nervous System (ANS), the Cardiovascular System (CVS), the Heart and the Baroreceptors. The Active Orthostatic Test is modelled by a disturbance in the Mean Arterial Pressure (MAP).

crease of the baroreceptors activity and the vagal activity increases with the baroreceptors stimulation.

The **Heart block**, here adapted from the original model and shown in Figure 5.6, receives the sympathovagal stimuli, originated in the ANS block and outputs a HR and a CO.

The dynamics of the influence of each system, sympathetic and vagal, on the SAN pacemaker activity is modelled with a time delay and a low-pass filter, following the *in vitro* study by Spear *et al.* [144].

Due to the different metabolic pathways of the parasympathetic and sympathetic systems, discussed earlier in this chapter, these stimuli suffer different time delays. Therefore, the release of Acetylcholine and Norepinephrine in the SAN are affected by a *transport delay*, modelled by  $D_P$  and  $D_S$ , respectively.

The neurotransmitters' dynamics are modelled by two low pass filters with unitary gain and coefficients  $\tau_P$  and  $\tau_S$ , whose values were taken from the literature and optimized experimentally.

Parasympathetic activation increases the SAN depolarization period, rising the RR interval (decreasing the HR). On the other hand, sympathetic stimulation decreases the RR interval (increasing HR).

The CO is computed from

$$CO = SV \times HR \quad (5.1)$$

where the systolic volume (SV) depends on the effect of sympathetic system over the myocardium and the HR is a function of both systems.

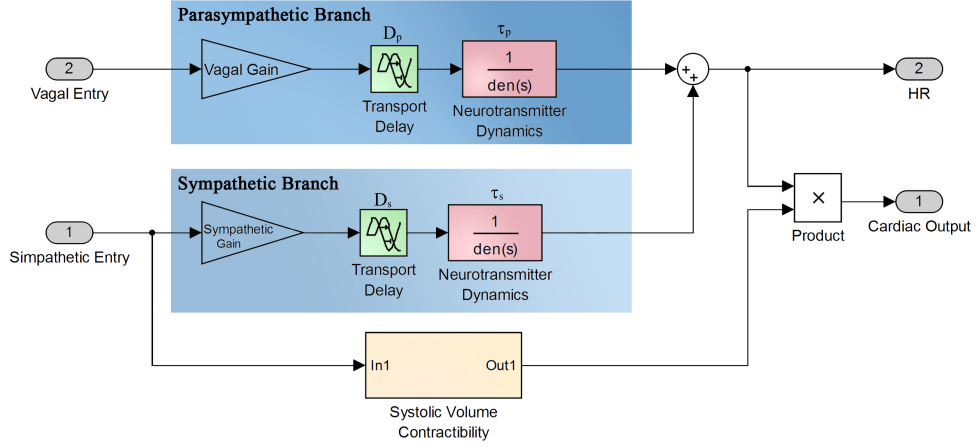


Figure 5.6: The efferent stimuli of the ANS suffer different time delays, due to distinct sympathetic and parasympathetic pathways. The dynamics of the neurotransmitters in the SAN are modelled by two low pass filters, with different time constants. The SAN depolarization rate gives rise to an instantaneous HR, which, combined with the hearts varying contractility, results in the CO.

The **cardiovascular system**'s inputs are the sympathetic system and the CO. This system can be characterised by an elastic component and a viscous component of the blood vessels' walls. The sympathetic innervation modulates primarily the total peripheral resistance by changing the vascular tonus and the vessels' radius.

The **baroreceptors block** receives the MAP as input. This block is a first order system proceeded by a gain, representing the rate of spike generation, by the baroreceptors, as a function of the MAP. The physiological characteristics of the MAP signal in the aortic arch and carotid sinus imply the existence of a time delay, expressed as  $D_B$  (see Figure 5.5).

### 5.5.3 Active Orthostatic Test

The dynamics of the neurotransmitters released by the two branches of the ANS on the SAN are modulated in the Heart block of the Baroreflex model, the parameters for these dynamics were based on the work by Spear [144] on Rabbits. In order to understand if the dynamics in humans are similar, the dynamics predicted by the model were compared with real data, acquired from subjects performing an AOT.

The AOT causes a sympathetic activation triggered by the baroreflex response to a sudden blood pressure reduction, resulting in an increment on the heart rate and blood pressure [178, 179]. This test was chosen due to its simplicity and easy observation of the time constants on the responses of the HR.

## Materials and Methods

Real RR data was acquired from 7 healthy young subjects (4 women and 3 men; age range: 23 – 31 years) who performed the AOT twice. The AOT was chosen due to its easy implementation and for providing a clear evidence of baroreflex and ANS activation [178, 179]. The experimental protocol was adapted from Cybulski *et al.* [180].

The test begins with a 5 minute resting period in supine position. After the indication, the subject stands up in 2 – 4 seconds, and remains in the orthostatic position for 5 minutes. Active postural change from supine to standing position causes a BP decrease and activation of the negative feedback baroreflex arc.

In the baroreflex model, the AOT was simulated by adding a ramp shaped disturbance to the MAP, as shown in Figure 5.7. This perturbation mimics the variation of BP associated to the change of body position.

## Experimental Results

The analysis of the model's response provides a physiological based explanation for the HRV frequency bands discussed before. The physiological limits of the sympathetic and parasympathetic frequency are supported by the intrinsic properties of the SAN autonomic regulation, i.e., the dynamics of the neurotransmitters. The ANS modulation of the heart rate can be simulated by the response of LP filters, with the cut-off frequencies determined by Acetylcholine and Norepinephrine kinetics.

While the original Baroreflex model contains several adjustable parameters, these were kept

Variable	Value	Variable	Value
$D_s$	1.0 s	$\tau_s$	1
$D_p$	0.2 s	$\tau_p$	0.5
$D_b$	0.5 s	–	–

Table 5.1: Model gain factors and time delay parameters used in the simulation.

constant, following the reported optimal values. Only the parameters of the Heart block were changed, their initial values were taken from the literature and manually fine tuned. Table 5.1 shows the values used for each parameter.

The time constants from Table 5.1 lead to an estimated cut-off frequency of approximately 0,173Hz for the sympathetic system and a cut-off frequency of 1,263Hz for the parasympathetic. These values are well within the generally accepted values [10] for the frequency bands present on HRV.

The simulation results, shown in Fig. 5.8, support the existence of a time delay, due to the sympathetic activation of smooth arterial muscles, included in the model in the CVS block.

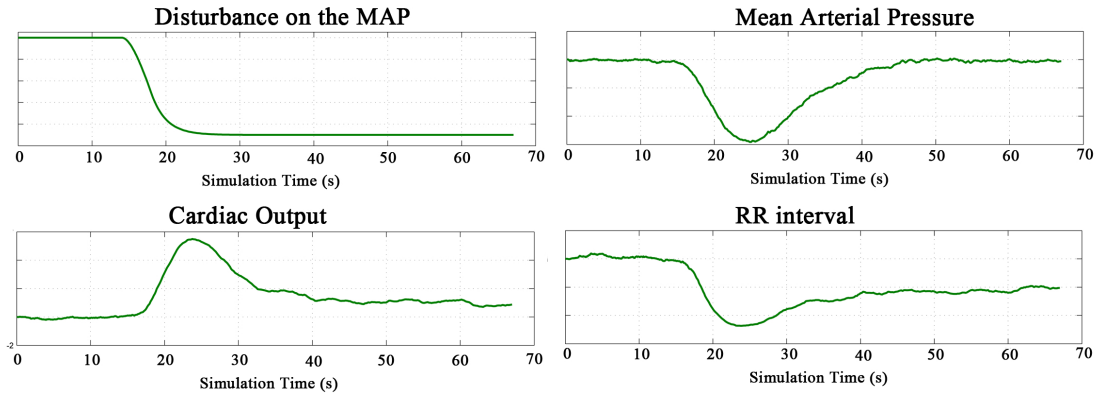


Figure 5.7: Results of the Active Orthostatic Test simulation, obtained with the proposed model.

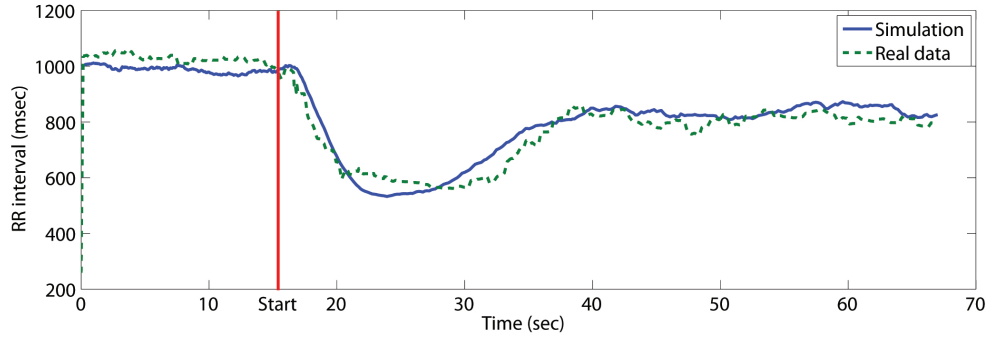


Figure 5.8: Variation on the RR interval, during an AOT, as predicted by the model (solid line) and the average curve, obtained experimentally, from 7 subjects performing an AOT (dashed line).

Fig 5.8 compares the real data, acquired from the volunteers performing the AOT, and the RR interval variation predicted by the model. The model's response is very similar to the real data and the results are in agreement with the reports by Spear *et al.* [144]. The main difference between the real and predicted curves lies in the recovery time after the maximum sympathetic activation. This difference is expected since the baroreceptors response is not linear to the decreasing and rising BP. The cardiorespiratory coupling was also not considered in the model which would introduce some variability in the baroreflex response. Nevertheless, the level of agreement between the real and simulated data suggests that the human short-term blood pressure regulation dynamics, consequence of the baroreflex, can be approximated by a simple incremental model.

## 5.6 Conclusions

Our current capability of precisely measuring short-term cardiovascular fluctuations provides an observation window for the regulatory functions of the ANS. However the full understanding of this system is still far from complete, with several problems still left unsolved.

The control of the HR by the two ANS branches, with opposing effects, might suggest that

## **Chapter 5. Physiological data**

---

autonomic regulation is a simple one-dimensional problem, i.e. when the parasympathetic increases the sympathetic decreases and vice-versa. However this simple reciprocal control is just one of the possible modes, co-activation and uncoupled activation are also possible, thus highly increasing the complexity of the estimation of each branch's activity.

Several signal-processing methods have been proposed to decouple the sympathetic and parasympathetic influences on HRV. For example, Vetter et al. [181] proposed a blind-source-separation technique assuming that the two branches exert independent influences on the HRV, extracting their relative contribution by means of independent components analysis. However, this independence assumption is known to be invalid due to frequent reciprocal activation of the two branches. More recently, Choi et al. [182] proposed a method to estimate the individual activation of the two branches based on a non-linear system-identification technique known as principal dynamic mode.

Although this method presented promising results, further advances are limited by another characteristic of the system. The validation of any proposed method is always limited by the inability to directly measure the true activity of each branch of the ANS system.

Several methods can be used to mitigate this problem, for example, performing tests such as the AOT and the tilt test or the use of pharmacological blockades, however, none of these methods fully solve the unobservable nature of the variables.

The arterial baroreflex has been cited as the mechanism for both respiratory and Mayer wave frequency fluctuations. However, data suggest that both cardiac vagal and vascular sympathetic fluctuations at these frequencies are independent of baroreflex mechanisms and, in fact, contribute to pressure fluctuations.

Results from cardiovascular modelling can suggest possible sources for these rhythms as well as for the standard frequency bands commonly accepted for parasympathetic and sympathetic activities.

In this chapter, a model taking into account the physiological background for HRV frequency bands was used to corroborate the theory that their origin lies in the dynamics of the neurotransmitters in the SAN and in the different propagation speeds of the two branches. However, the complex stochastic relations between all the variables in these intrinsic rhythms indicate that a multitude of mechanisms lie in their origin.

# 6 Automatic Sleep Staging

## 6.1 Introduction

The PSG, described in detail in Chapter 2, is by far the most reliable and accurate method for sleep assessment. The hypnogram allows an easy and quick insight into the sleep pattern, and the computation of several important parameters, used to quantify and characterize sleep. These parameters include the SE, SOL, REM sleep percentage ( $\text{REM}_p$ ), Non-REM sleep percentage ( $\text{NREM}_p$ ) and *REM latency*.

However, the PSG involves complex acquisition devices and long set-up procedures. It is uncomfortable to the subject and is usually done in clinical facilities. These highly constrained conditions prevent its use in a non intrusive way in normal daily life and limits the duration of the typical exam, which is usually performed over 1 or 2 nights.

Due to these constraints, simpler alternatives are desirable to perform the initial screening for sleep disorders and to support the follow-up after diagnosis. The main goal is not to replace PSG but to complement it and reduce the number of unnecessary exams, releasing the load from sleep labs.

The advent of small portable devices with high storage and processing capabilities have allowed physiological and behavioural data to be acquired, outside clinical environments, in a reliable way, often across several days. As explored in the previous chapter, sleep patterns are intimately connected with the activity of the ANS [183]. This activity can be indirectly estimated from several physiological signals, easily acquired from portable recorders, such as the ECG, RIP, the Peripheral Arterial Tone (PAT) and the GSR.

The automatic extraction of useful indicators for sleep disorders diagnosis, using data acquired in mobile environments, is still an open issue that poses many challenges.

The problems to solve have different degrees of complexity and include the accurate estimation of *Sleep* and *Wakefulness* periods, detection of REM and NREM sleep and the automatic computation of *Sleep Parameters*.

Several approaches have been proposed to address these issues. Spectral analysis of the HRV

## Chapter 6. Automatic Sleep Staging

---

plays a major role in many publications, where the frequency bands discussed in Chapter 5 are a central key to sleep assessment.

Some authors have proposed variations to these standards with relevant results. In [184] the authors propose an algorithm that adaptively extracts features from HRV for sleep and wakefulness classification. They show that the adaptive frequency bands improve the discriminative power of the frequency based features. In [185, 186] the authors propose the use of Time-Variant Autoregressive Model (TVAM) to extract the spectral features, they show that using TVAM the algorithm becomes more sensitive to fast variations in the sleep state.

An accurate detection of sleep stages across the entire night has been presented by some authors. In [187] the authors present an algorithm, optimized for sleep-disordered breathing patients, which discriminates sleep stages based on a set of heuristic rules and a threshold based discriminative function. In [14] and [188] a HMM classifier based on features extracted from TVAM is presented to discriminate Wake-REM-NREM and REM-NREM, respectively. A recent study by Willemen et al. [189] evaluates the discriminative capacity of a large set of cardio-respiratory and movement features in three classification tasks: Sleep-Wake, REM-NREM and light-deep sleep achieving high agreement rates.

In [13] the authors present an interesting approach, also adopted in this chapter, where parts of the data, ambiguous from a classification point of view, are discarded in order to improve the final estimation of *Sleep* and *Wakefulness* periods.

The estimation of sleep parameters and stages from multi-modal data is presented in some papers with promising results. In [190] the authors combine ACT and Cardio-Respiratory signals achieving high accuracies in *Sleep* and *Wakefulness* detection, although no proper validation data, (i.e. the hypnogram from the PSG), is used. In [191] and [167] the authors present a sleep staging algorithm that combines HRV and RIP, and explore the influence of Obstructive Sleep Apnea (OSA) in the performance of the algorithm.

In [69] the authors combine ACT, Respiratory effort and HRV obtaining a high accuracy but relatively low sensitivity in the discrimination between *Sleep* and *Wakefulness*.

This chapter deals with the problem of automatically estimating a simplified Hypnogram (*Wakefulness*, REM and NREM) and computing three standard sleep parameters; i) SE, ii) REM<sub>p</sub> and iii) NREM<sub>p</sub> from data easily acquired with portable sensors.

The sleep parameters are estimated using two different methods; first, the Hypnogram is estimated from the data and the sleep parameters computed. Then an alternative method is described that eliminates the need for an Hypnogram by combining the rejection of ambiguous samples and a regularization operation.

The two methods rely on an extended set of features, extracted from HRV, RIP and ACT, an ensemble of classifiers and a HMM based algorithm used in the estimation of the simplified hypnogram.

## 6.2 Method overview

The structure of the proposed method is shown in Figure 6.1.

Before feature extraction, the raw data is pre-processed: the RR tachogram is built from the

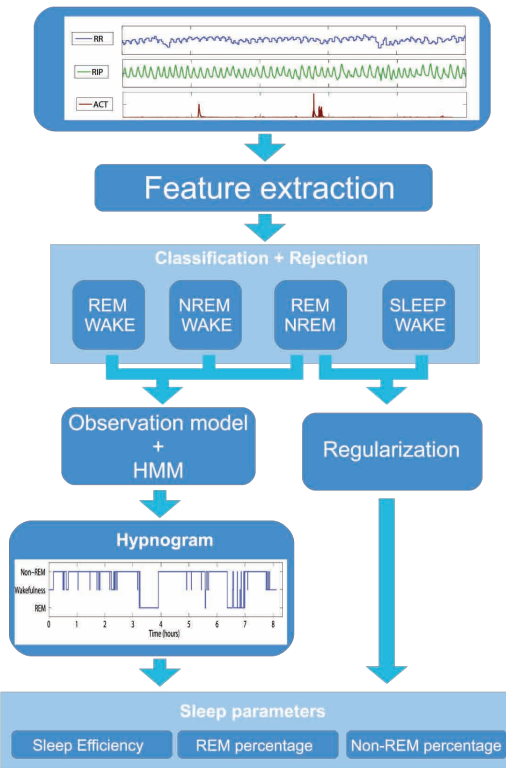


Figure 6.1: Fluxogram of the proposed method. The hypnogram and sleep parameters are initially estimated from the output of 3 binary classifiers, fed to a HMM based algorithm (left). An alternative method for the estimation of the sleep parameters is also described based on the output of 2 binary classifiers and a regularization operation (right).

pre-filtered ECG and the ACT and RIP data is normalized.

After feature extraction a classification stage, designed to reject ambiguous features, performs an initial discrimination of SW and REM/NREM states. The output of this classification stage is used as the input for a HMM based algorithm that estimates the optimal state sequence, i.e. the most probable Hypnogram. The estimated Hypnogram is then used to compute the sleep parameters.

An alternative method to compute the sleep parameters is also described that relies on the output of the classifiers and a regularization operation.

## 6.3 Pre-processing

The algorithm is designed to support multi-modal datasets that include ECG, RIP and ACT data. Figure 6.2 shows a 5 minute segment of pre-processed data (RR, RIP and ACT signals) together with the ground truth hypnogram of one subject.

The pre-processing operations are required to compensate the movement artefacts present on ECG, normalize the data across different subjects and prepare it for feature extraction.

### 6.3.1 Detection of QRS complexes and RR tachogram formation

ECG filtering, QRS complex detection and RR signal construction is performed according to the method described in detail in [141]. This method is based on the QRS complex detection method described by Hamilton and Tompkins in 1986 [215] and includes a filtering step for abnormal beat detection and removal. The filtering step, also described in [216], works by removing any beat corresponding to instantaneous heartbeat variations larger than 20%.

Before feature extraction, the RR signal is downsampled to 2 Hz. This operation consists in an anti-aliasing filtering, using a 8<sup>th</sup> order Chebyshev low pass filter, with 0.8Hz cutoff frequency, followed by decimation. The 2 Hz sampling frequency is within the accepted range, as shown in [141] and [10], being above the Nyquist frequency for the frequency ranges of interest.

### 6.3.2 Actigraphy and RIP pre-processing

Magnitude normalization and DC component removal are applied to both RIP and ACT signals in a sliding window basis as follows

$$\tilde{a}(n) = \frac{a(n) - \mu(n)}{\sigma(n)} \quad (6.1)$$

where  $a(n)$  is the original sample,  $\mu(n)$  and  $\sigma(n)$  are the mean and standard deviation of the data within the 5 minute window centred at the  $n^{th}$  sample and  $\tilde{a}(n)$  is the normalized sample.

## 6.4 Feature extraction

The developed algorithm combines features extracted from the RR, RIP and ACT signals and one synchronization measure between RR and RIP.

After pre-processing, each dataset is divided in contiguous epochs of  $T = 30$  seconds. For validation purposes the data was synchronized with the ground-truth hypnogram provided by the medical staff. All the epochs corresponding to any of the 3 distinct NREM sleep stages were grouped into one single label.

Let  $w_j = \{RR_j \text{ RIP}_j \text{ ACT}_j\}$  represent a  $T$  dimensional window, containing the multi-modal

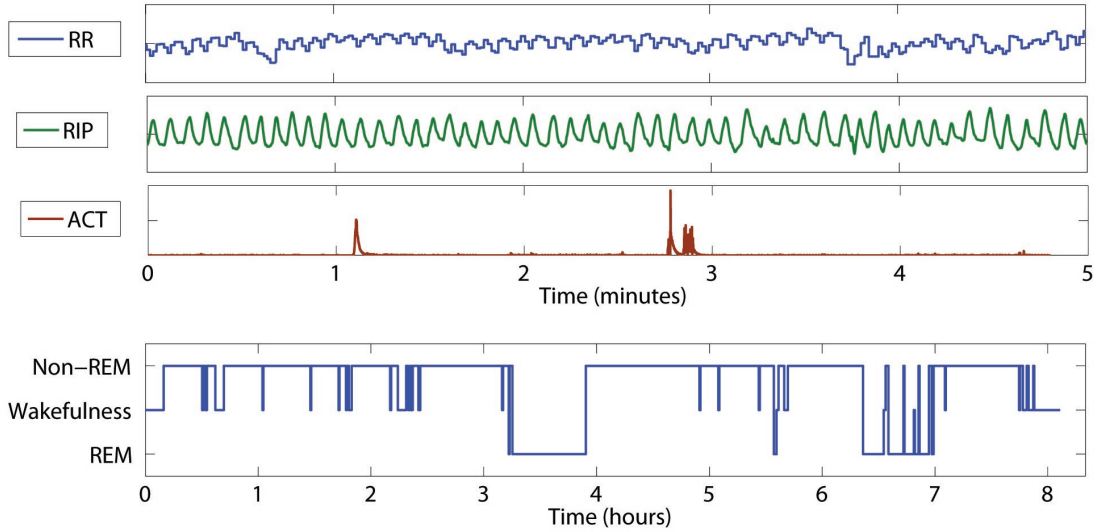


Figure 6.2: Five minute segment of pre-processed data (top) and the full night simplified hypnogram (bottom).

data from the  $j^{th}$  epoch, where  $j \in [1, \dots, M]$  and  $M$  the total number of epochs.

The feature extraction procedures are performed as described in the following subsections.

#### 6.4.1 RR features

The RR frequency domain features are computed, according to the guidelines from [10], in the LF and HF bands. The rational behind these bands is discussed in detail in Chapter 5.

In order to extract the spectral features from each epoch,  $\text{RR}_j$ , an 8-order AR is fitted to the extended window  $\text{RR}_j^* = [\text{RR}_{j-3} \dots \text{RR}_j]$ , using the Yule-Walker equations, a set of optimal coefficients  $\hat{\alpha}_{RR}$  and a residual,  $E_{RR}$ , are obtained.

The length of  $\text{RR}_j^*$ , 2 minutes, follows the standards set by [10], allowing to capture the low frequency components of the RR signal. The power spectrum is computed from the estimated AR coefficients and the following features are extracted:

- $\text{PM}_j$ : Magnitude of the high frequency pole of the filter *impulsive response filter* (IIR) described by the coefficients  $\hat{\alpha}_{RR}$ .
- $\text{PP}_j$ : Phase of the high frequency pole.
- $E_{RRj}$ : Residual of the AR model fitted to  $\text{RR}_j^*$ .
- $\text{TP}_j$ : Total power (LF+HF).

- $\text{HF}_j$ : Power in the HF range.
- $\text{LF}_j$ : Power on the LF range.
- $\text{LF}/\text{HF}_j$ : Power ratio between the two frequency bands.
- $\text{MHR}_j$ : Mean heart rate on the considered  $\text{RR}_j$ .

### 6.4.2 RIP features

The RIP related features are extracted by estimating the optimal parameters  $\hat{\alpha}_{BR}$  of the 4-order AR model fitted to each  $\text{RIP}_j$ , and computing:

- $\text{BV}_j$ : Magnitude of the high frequency pole of the filter, describing the variance in the breathing rate.
- $\text{BPM}_j$ : Phase of the high frequency pole, reflecting the average breathing rate.

### 6.4.3 RR + RIP features

The temporal interplay between oscillations of heartbeat and respiration, reflect information related to the cardiovascular and autonomic nervous system [192].

Let  $\text{RR}_j^{\text{Br}}$  denote the breathing component of  $\text{RR}_j$ . The phase synchronization between  $\text{RIP}_j$  and  $\text{RR}_j^{\text{Br}}$  is quantified computing the *Phase-Locking Factor* (PLF) [193] given by

$$\theta_j = \left| \frac{1}{T} \sum_{n=1}^T e^{i(\phi_{\text{RIP}}[n] - \phi_{\text{RR}}[n])} \right| \quad (6.2)$$

where  $\phi_{\text{RIP}}$  and  $\phi_{\text{RR}}$  are the instantaneous phases of  $\text{RIP}_j$  and  $\text{RR}_j^{\text{Br}}$ , respectively, computed using the Hilbert transform. The value of  $\theta_j$  is a measurement of the synchronization between the two oscillators, with 1 corresponding to perfect synchronization and 0 to no correlation between the phases.

The breathing component  $\text{RR}_j^{\text{Br}}$  is obtained filtering  $\text{RR}_j$  with the bandpass IIR filter described by the set of optimal coefficients  $\hat{\alpha}_{BR}$ . To compensate the non linearity of the phase the signal is filtered in both forward and backward direction.

Figure 6.3 illustrates the steps in the computation of  $\theta_j$ .

### 6.4.4 ACT features

The features extracted from ACT are derived from the features described in Chapter 4. Each set of features is computed from a 3.5 minute window  $\text{ACT}_j^* = [\text{ACT}_{j-3} \dots \text{ACT}_{j+3}]$ , centred on

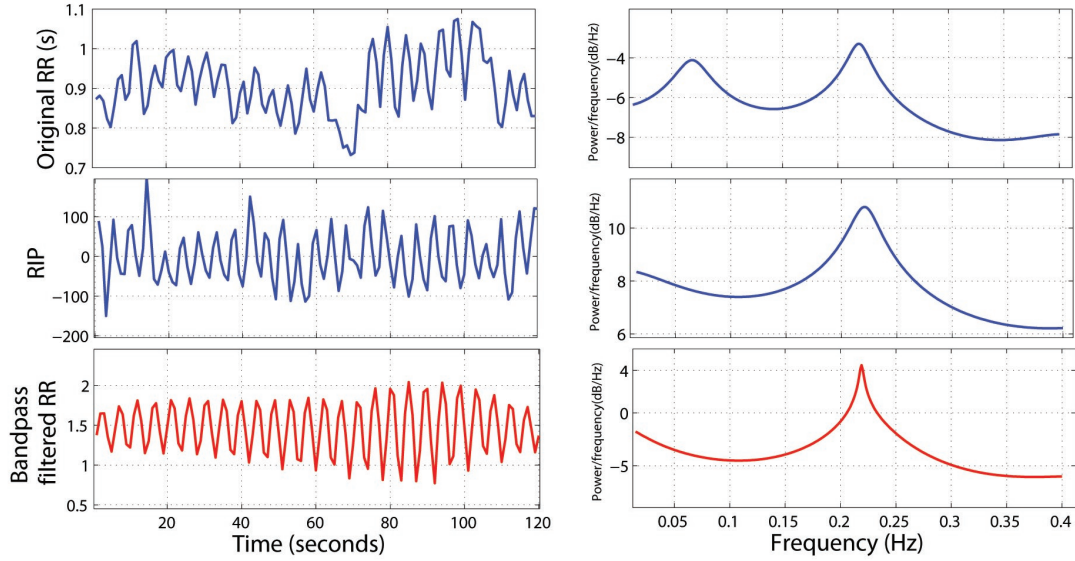


Figure 6.3: A two minute window of the RR signal (top left) and the respective Power spectrum (top right) showing two peaks centred in the LF and HF bands. The breathing signal (middle left) has its frequency response centred (middle right) in the breathing frequency. This response is used to bandpass filter the RR signal, resulting in the signal and Power spectrum displayed in the bottom left and right, respectively.

the  $j^{\text{th}}$  epoch. The following features are extracted:

- AR - Coefficients ( $a_{\{1,\dots,4\},j}$ ) and residue ( $E_{\text{AR}j}$ ) of a 4-order AR model fitted to  $\text{ACT}_j^*$ .
- RMM - Weights ( $w_{\{1,\dots,3\},j}$ ), parameters ( $r_{\{1,\dots,3\},j}$ ) and the KL divergence of the RMM distribution fitted to  $\text{ACT}_j^*$ .
- Mag $_j$  - The energy of  $x(k) = \text{ACT}_j^*$  given by  $\sum_k h(k)x(k)^2$  where  $\mathbf{h} = \{h(k)\}$  is a Hanning window.

In order to minimize the inter-patient variability, a normalization operation was applied to the feature matrix. Let  $\mathbf{f}_{ij}$  denote the vector containing all the samples from feature  $i$  and subject  $j$ , the normalization is performed according to,

$$\tilde{f}_{ij}(n) = \frac{1}{1 + e^{-\frac{f_{ij}(n) - \mu_{ij}}{\sigma_{ij}}}} \quad (6.3)$$

where  $\tilde{f}_{ij}(n)$  is the  $n^{\text{th}}$  normalized sample and  $\mu_{ij}$  and  $\sigma_{ij}$  the mean value and standard deviation of  $\mathbf{f}_{ij}$  respectively. This normalization step ensures that all features fall in the range  $[0, \dots, 1]$ .

## Chapter 6. Automatic Sleep Staging

---

The discriminative power of each feature was computed using the Mahalanobis Distance (MhD) and the statistical significance was assessed performing a one-way ANOVA test. Table 6.1 shows the MhD and the result of the  $p$ -value test (for a significance level of 0.05) obtained for each feature in four different tasks: i) *REM vs Wakefulness*, ii) *REM vs NREM*, iii) *NREM vs Wakefulness* and iv) *Sleep vs Wakefulness* discrimination.

Figures 6.4 and 6.5 show the histograms of the extracted features for all datasets. Figure 6.4 compares the histograms of the features extracted during REM and Non-REM sleep states and Fig. 6.5 the histograms of the features extracted for *Wakefulness* and *Sleep* states.

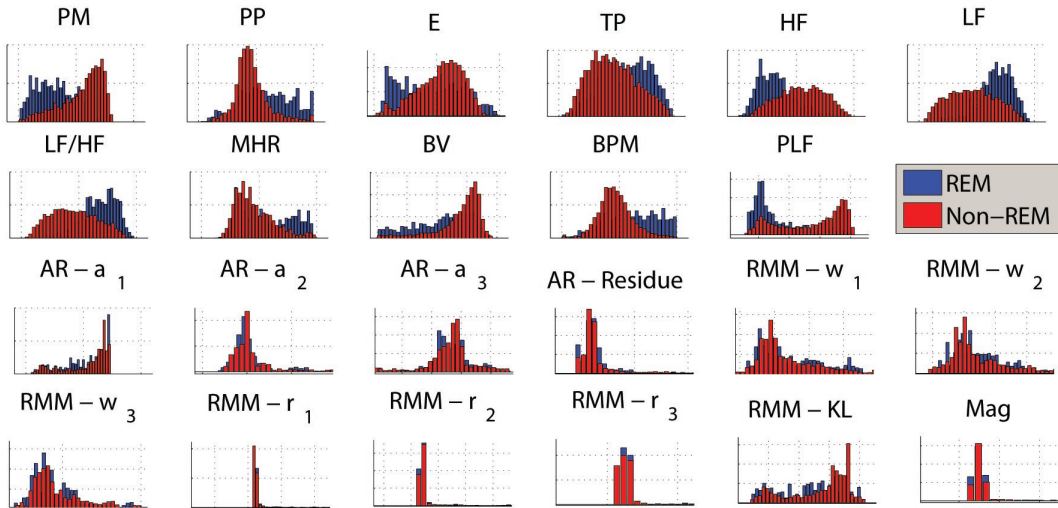


Figure 6.4: REM vs Non-REM features.

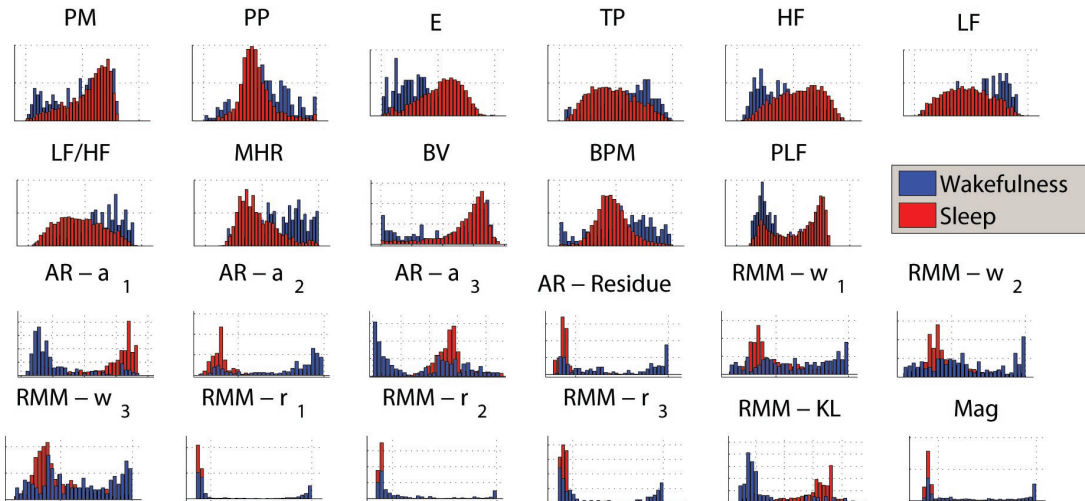


Figure 6.5: Sleep vs Wakefulness Features.

#### 6.4. Feature extraction

	MhD	p										
	PM		PP		E		TP		HF		LF	
RW	<b>0.53</b>	1	0.02	0	<b>0.37</b>	1	0.01	0	0.39	1	0.16	1
RN	<b>1.69</b>	1	<b>0.63</b>	1	<b>0.17</b>	1	<b>0.28</b>	1	<b>1.75</b>	1	<b>1.09</b>	1
NW	<b>0.51</b>	1	<b>0.43</b>	1	<b>1.48</b>	1	<b>0.21</b>	1	<b>0.67</b>	1	<b>0.47</b>	1
SW	0.24	1	0.21	1	<b>1.13</b>	1	0.14	1	<b>0.35</b>	1	0.26	1
	LF/HF		MHR		BV		BPM		PLF		<b>a</b> <sub>1</sub>	
RW	0.36	1	<b>0.38</b>	1	0.01	0	0.04	0	0.19	1	<b>2.6</b>	1
RN	<b>1.62</b>	1	<b>0.32</b>	1	<b>0.61</b>	1	<b>0.72</b>	1	<b>1.19</b>	1	<b>0.2</b>	1
NW	<b>0.65</b>	1	<b>1.9</b>	1	<b>0.42</b>	1	<b>0.32</b>	1	<b>0.47</b>	1	<b>2.7</b>	1
SW	<b>0.35</b>	1	<b>1.42</b>	1	0.23	1	<b>0.14</b>	1	<b>0.23</b>	1	<b>2.68</b>	1
	<b>a</b> <sub>2</sub>		<b>a</b> <sub>3</sub>		<b>a</b> <sub>4</sub>		E <sub>AR</sub>		<b>w</b> <sub>1</sub>		<b>w</b> <sub>2</sub>	
RW	<b>3.8</b>	1	<b>1.0</b>	1	0.62	1	<b>3.5</b>	1	<b>0.52</b>	1	0.28	1
RN	0.01	0	0.001	0	0.03	1	0.03	1	<b>0.02</b>	1	0.01	0
NW	<b>3.5</b>	1	<b>1.34</b>	1	0.4	1	<b>4.6</b>	1	0.9	1	0.4	1
SW	<b>3.7</b>	1	<b>1.41</b>	1	0.53	1	5.2	1	0.89	1	0.46	1
	<b>w</b> <sub>3</sub>		<b>r</b> <sub>1</sub>		<b>r</b> <sub>2</sub>		<b>r</b> <sub>3</sub>		<b>KL</b>		<b>Mag</b>	
RW	0.75	1	1.05	1	0.74	1	1.4	1	<b>1.1</b>	1	<b>2.5</b>	1
RN	0.02	1	0	0	0.03	1	0	0	0.08	1	0.01	0
NW	0.63	1	<b>2.1</b>	1	<b>0.5</b>	1	<b>3.4</b>	1	<b>1.89</b>	1	<b>4.60</b>	1
SW	0.69	1	2.27	1	0.58	1	3.5	1	<b>1.75</b>	1	<b>5.08</b>	1

Table 6.1: Mahalanobis Distance (MhD) and the result of the significance test, ( $p = 1$  means that the null hypothesis is rejected) for all the extracted features on 3 binary classification tasks: i) RW - [REM / Wakefulness], ii) RN - [REM / Non-REM] and iii) NW - [Non-REM / Wakefulness]. Bold MhD values mark features selected during the feature selection procedure.

## 6.5 Classification and Feature Selection

The discrimination between the considered classes, *Wakefulness*, REM and NREM, falls within a common multi-class classification problem. Several approaches are possible to solve this kind of problem, they include:

1. The design of a All-vs-All classifier, where each sample is classified into one of the 3 possible classes.
2. A Hierarchical classifier, with an initial classification separating *Wakefulness* and *Sleep* and a second classifier discriminating the former class into REM and NREM states.
3. A combiner classifier composed by 3 One-vs-All classifiers with the final score given by a specific combining rule.

The main limitation of approach 1. is that the same group of features is used to discriminate the three different classes. From Table 6.1 it is clear that distinct features are optimal to discriminate different classes thus motivating the use of binary classifiers.

The hierarchical classification approach, 2., enables the use of distinct features to discriminate between different classes, but the classification error in SW estimation propagates into the second stage, REM/NREM. The results using this approach are presented in the results for comparison purposes.

The solution adopted, is an extension of approach 3. The estimation of the Hypnogram, described in Section 6.6, is based on three binary classifiers that independently classify all the samples into i) REM/Wakefulness (RW), ii) REM/Non-REM (RN) and iii) Non-REM/Wakefulness (NW).

The estimation of the sleep parameters, described in Section 6.7, uses a fourth binary classifier that maps all samples into *Sleep* and *Wakefulness* classes.

Each classifier is designed to take into account a Rejection Factor (RF), rejecting a specified percentage of samples, whose classification is ambiguous. In large biomedical datasets, such as the one considered, the systematic rejection of unreliable segments and/or samples has been shown to increase the accuracy of the classification procedures without compromising the overall result [13]. The rejection works by computing the true or estimate posterior probability of the winning class for each sample and rejecting those which are below the specified percentage.

Therefore each classifier maps each sample into one of three labels:  $RW \in \{rs, wk, r\}$ ,  $RN \in \{rs, ns, r\}$ ,  $NW \in \{ns, wk, r\}$  and  $SW \in \{sl, wk, r\}$ , where  $rs$ ,  $ns$ ,  $wk$ ,  $sl$  and  $r$  refer to *REM*, *Non-REM*, *Wakefulness*, *Sleep* and *Rejected sample* respectively.

During the training step, the RW, RN and NW binary classifiers are trained only with data from the 2 considered classes, respectively. However, during the test, they map samples belonging to

3 classes. Any sample from a class not predicted by the classifier will either be miss-classified or rejected. Figure 6.6 illustrates the rejection of ambiguous samples on a Sleep/Wakefulness

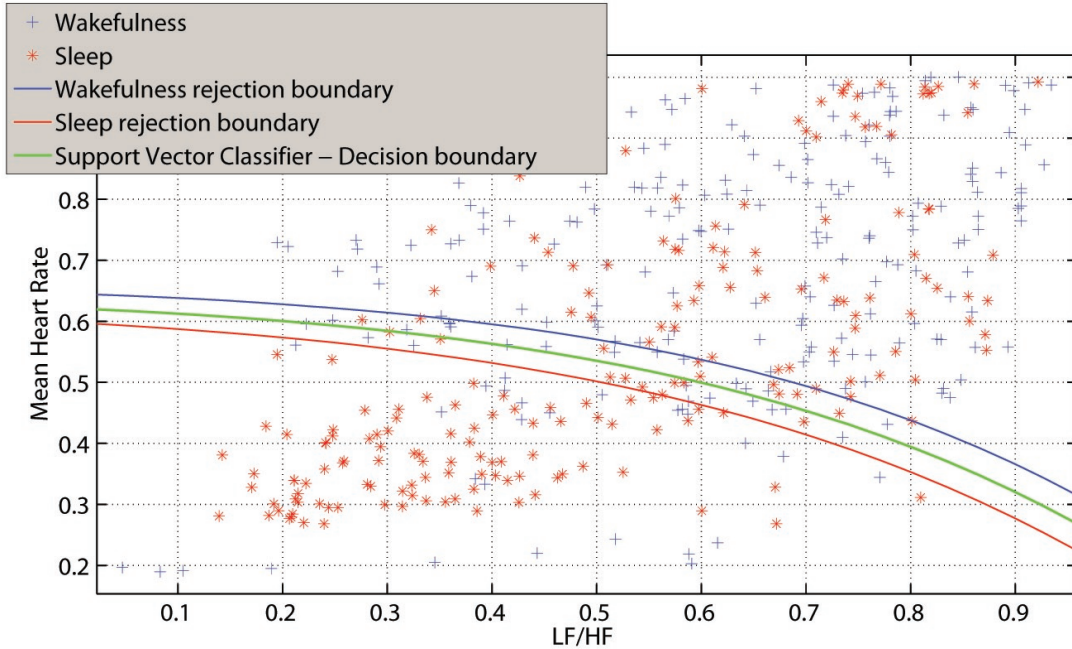


Figure 6.6: Rejection of ambiguous samples.

classification task, using two features (Mean Heart rate and LF/HF ratio) and a SVM with a quadratic polynomial kernel.

The four binary classification tasks were tested with several different classifiers, the Support Vector Classifier (SVC) with a 2<sup>nd</sup> degree polynomial kernel yielded the highest accuracy for all tasks with the exception of the REM vs Non-REM classification, where the Parzen classifier performed better.

Feature selection was performed for each classifier, considering only the statistically significant features and a floating feature selection algorithm without any constraint on the number of selected features. The evaluation criteria is the accuracy of the classifier, used on each classification task. The selected features are displayed in Table 6.1 with the respective MhD marked in bold.

## 6.6 Hypnogram and sleep parameter estimation

The Hypnogram estimation is based on a HMM, with 3 hidden states  $x \in \{\text{Wake}, \text{REM}, \text{Non-REM}\}$ . The HMM combines the output of the three binary classifiers (RW, NW, RN) producing a final estimate of the Hypnogram.

A HMM was chosen as the combiner of the 3 classifiers due to its ability to incorporate the

## Chapter 6. Automatic Sleep Staging

---

information regarding the rejected samples in the observation model. Furthermore, HMM's are particularly useful in this kind of problem since they able to model the temporal correlation between states which is the case on the sleep cycle dynamics.

Let us consider  $\mathbf{O}$  a  $N \times 3$  observation matrix, where each row/observation  $o_n = [RW_n, RN_n, NW_n]$  contains the output of the three binary classifiers for the  $n^{th}$  sample. The observation space is thus composed by  $3^3 = 27$  different possible observations.

The Emission Matrix (EM) is a  $3 \times 27$  matrix, representing the probabilities  $P(o_{1..27}|x_{1..3})$ , and is computed from the relative frequencies observed in the output of the binary classifiers using the training data.

The Transition Matrix (TM) is a  $3 \times 3$  matrix with the state transition probabilities, expressed as  $P(x_n|x_{n-1})$ . The TM is also computed from the relative frequencies observed in the training data true hypnograms.

The hidden state,  $x(n)$ , is estimated along the time from the observations,  $\mathbf{o}(n)$ , and the model parameters, EM and TM.

The initial probabilities of REM and NREM sleep are set to 0 and the initial probability of *Wakefulness* is set to 1 since all patients were awake in the beginning of the exam. The optimal solution, the most probable state sequence, is computed using the *Viterbi Algorithm*.

The three considered sleep parameters are computed from the estimated Hypnogram as

$$SE = \frac{N(s)}{N(s) + N(w)} \quad (6.4)$$

$$NREM_p = \frac{N(ns)}{N(ns) + N(rs)} \quad (6.5)$$

$$REM_p = \frac{N(rs)}{N(rs) + N(ns)} \quad (6.6)$$

where  $N(\cdot)$  is a counting operator for  $s$ ,  $w$ ,  $rs$  and  $ns$ , corresponding to *Sleep*, *Wakefulness*, *REM sleep* and *Non-REM sleep* epochs, respectively.

## 6.7 Alternative sleep parameter estimation

The estimation of the sleep parameters, as described in the previous section, follows the standard procedure, where the computation is performed directly from the Hypnogram. The error associated with the estimated Hypnogram will thus be directly reflected in the estimated parameters.

In this section an alternative method is proposed that computes the sleep parameters directly from the output of the SW and RN classifiers. This method improves the accuracy of the estimated sleep parameters by taking into account:

- The higher accuracy of the binary classifiers, compared to the full Hypnogram estimation.
- A correction factor, computed in the training step, that takes into account the percentage of miss-classified samples.
- An estimation of the number of samples that were rejected on each class.

Let us consider a binary classifier  $C$ , with a reject option, which maps each sample into one of three labels  $l \in \{p, n, r\}$  where  $p$ ,  $n$  and  $r$  denote Positive, Negative and Reject.

The confusion matrix is represented as

$$\mathbf{A} = \begin{bmatrix} \text{Tp} & \text{Fn} & \text{Rp} \\ \text{Fp} & \text{Tn} & \text{Rn} \end{bmatrix} \quad (6.7)$$

where  $\text{Tp}$ ,  $\text{Fn}$ ,  $\text{Fp}$ ,  $\text{Tn}$ ,  $\text{Rp}$  and  $\text{Rn}$  are the *True Positives*, *False Negatives*, *False Positives*, *True Negatives*, *Rejected Positives* and *Rejected Negatives* respectively.

The positive ( $\theta_{p,i}$ ) and negative ( $\theta_{n,i}$ ) correction factors and the fraction of rejected samples per class ( $\omega_{p,i}$  and  $\omega_{n,i}$ ) are computed for each training dataset as

$$\theta_{p,i} = \frac{\text{Tp}_i + \text{Fp}_i}{\text{Tp}_i + \text{Fn}_i} \quad (6.8)$$

$$\theta_{n,i} = \frac{\text{Fn}_i + \text{Tn}_i}{\text{Fp}_i + \text{Tn}_i} \quad (6.9)$$

$$\omega_{p,i} = \frac{\text{Rp}_i}{\text{Rp}_i + \text{Rn}_i} \quad (6.10)$$

$$\omega_{n,i} = \frac{\text{Rn}_i}{\text{Rp}_i + \text{Rn}_i} \quad (6.11)$$

with  $i \in [1, \dots, M]$ , and  $M$  the number of training datasets. The final values are obtained averaging over  $\boldsymbol{\theta}_{\{p,n\}}$  and  $\boldsymbol{\omega}_{\{p,n\}}$ .

The counting operation can thus be improved by correcting the number of predicted samples in each class as

$$N(\hat{p}) = \frac{N(p)}{\theta_p} \quad (6.12)$$

$$N(\hat{n}) = \frac{N(n)}{\theta_n} \quad (6.13)$$

and estimating the number of rejected samples from each class as

$$N(r_p) = \omega_p N(r) \quad (6.14)$$

$$N(r_n) = \omega_n N(r) \quad (6.15)$$

The expressions for the three sleep parameters can now be re-written as

$$SE = \frac{N(\hat{s}) + N(r_s)}{N(s) + N(w) + N(r)} \quad (6.16)$$

$$NREM_p = \frac{N(\hat{n}s) + N(r_{ns})}{(N(ns) + N(rs) + N(r)) \times SE} \quad (6.17)$$

$$REM_p = \frac{N(\hat{r}s) + N(r_{rs})}{(N(ns) + N(rs) + N(r)) \times SE} \quad (6.18)$$

where SE is computed from the output of the SW classifier and NREM<sub>p</sub> and REM<sub>p</sub> from the RN classifier.

## 6.8 Experimental Results

In this section the data used to test the algorithm is described and the obtained experimental results are presented.

The performance of all the described methods is assessed with several metrics which are computed in a *leave-one-patient-out* cross validation basis. This is, each patient dataset is tested after training the algorithm (i.e. the classifiers and the HMM model) with the remaining data.

Besides the Acc. and prediction rate for each class (Sens. and Spec. in the case of binary classifiers) the *Gmean* is also computed. This is motivated by the highly unbalanced nature of the classification tasks at hand, e.g. in the Sleep vs Wakefulness discrimination problem, up to 95% of the samples belong to the Sleep class, in Rem vs Non-Rem typically around 80% of the samples belong to Non-Rem class. The Gmean gives a global insight into the performance of the method, which is often masked in the Acc by the bias introduced by predominant classes. The Cohen's kappa index [80] is also computed, for performance comparison, when necessary.

### 6.8.1 Data Sets

The data used in this study was acquired from volunteers recruited along several months. No age or gender restrictions were imposed but only volunteers claiming to have a healthy perceived sleep and no pre-diagnosed sleep disorders were accepted.

Similarly to the study presented in Chapter 4, each subject performed one standard nocturnal PSG exam at a sleep laboratory together with an Actigraph, placed in the non-dominant wrist, acquiring with a sampling rate of 1Hz.

The hypnogram, obtained from the PSG by trained technicians, is used as a ground truth to identify *REM sleep*, *Non-REM sleep* and *wakefulness* in epochs of 30 seconds.

Twenty adult subjects, aged  $42.1 \pm 9$  years, 12 Males, 8 Females, participated in this study.

The SE was computed from the hypnogram for every subject, ranging from 75% to 95% with an average value of  $86.1 \pm 5.2\%$  suggesting the occurrence of sleep disturbances in some of the subjects, although not necessarily pathological.

### 6.8.2 Classifiers Performance

The four considered binary classifiers (see Figure 6.1) were initially tested to assess their performances. Table 6.2 shows the individual detection ratios of each classifier/class, the Acc., Gmean and the percentage of rejected samples on each class (under parenthesis). The displayed results were obtained using a RF of 10%.

	Wake. %	REM %	NREM %	Acc.	Gmean
RW	71.3 (12.2)	83.3 (11.6)	– ( <b>18.8</b> )	78.4	77.0
NW	75.9 (11.5)	– ( <b>20.2</b> )	84.4 (10.2)	83.4	80.0
RN	– ( <b>14.2</b> )	80.3 (11.8)	84.8 (9.9)	84.1	82.5
SW	83.3 (10.9)		85.1 (8.4)	84.9	84.3

Table 6.2: Detection ratios, Accuracy and Gmean for each of the individual classifiers, and the percentage of samples rejected (in parenthesis) on each class.

RW - REM / Wakefulness; NW - NREM / Wakefulness; RN - REM / NREM; SW = Sleep / Wakefulness.  
Rejection factor = 10%.

The three binary classifiers, RW, NW and RN have higher rejection percentages for the "unknown" class, i.e. the class not considered in the classifier, however the difference is not very significant.

All the classifiers yield acceptable detection ratios and Gmeans, but these results do not properly reflect the number of misclassified samples belonging to the "unknown" class.

Table 6.3 provides further information on the label given to the "unknown" classes by the three binary classifiers. Wakefulness samples tend to be classified mostly as REM which can be understood by the similarities in physiological processes during REM and wakefulness, the same applies to the classification of REM samples, which are mostly classified as Wakefulness. NREM samples are mostly classified as REM, although the difference is smaller than the

		Classified as:				Classifier
		Wake.	Rem	Nrem	Rejected	
Unknown Class	Wake.	–	51.0%	34.8%	14.2%	RN
	Rem	46.4%	–	33.4%	20.2%	NW
	Nrem	37.1%	44.1%	–	18.8%	RW

Table 6.3: Misclassification and rejection ratios of the binary classifiers

previous cases.

The ideal binary classifier should reject the large majority of the samples belonging to "unknown" class, something which wasn't verified in practice. A larger RF could be used to increase the rejected "unknown" samples, but this would also lead to an increased rejection percentage of the considered classes, as seen in Table 6.2.

### 6.8.3 Hypnogram estimation

The algorithm for Hypnogram estimation was tested with several RFs, the obtained results are listed in Table 6.4. The RF of 10% yields the highest values for almost all the metrics, achieving

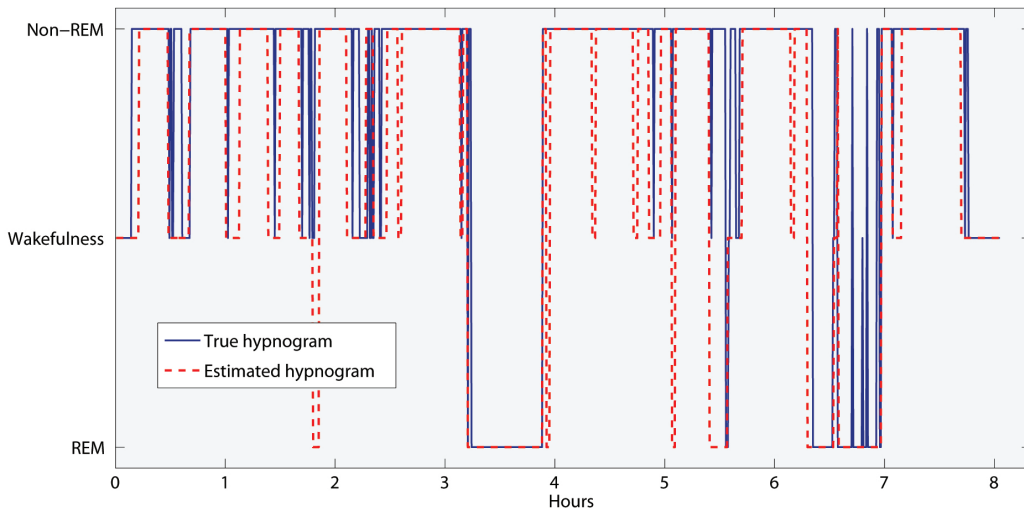


Figure 6.7: .

a detection ratio of 72.8%, 77.4% and 80.3% for Wakefulness, REM and NREM respectively and a global Acc. of 78.3%. This result (obtained with data previously unseen by the classifiers) corresponds to a G-mean of 76.8% and a kappa index of  $k = 0.58$ .

	Wake.(%)	REM(%)	Non-REM(%)	Acc.(%)	Gmean
0%	70.8	76.7	78.6	76.7	75.3
5%	70.0	<b>79.6</b>	76.0	75.4	75.0
10%	<b>72.8</b>	77.4	<b>80.3</b>	<b>78.3</b>	<b>76.8</b>
20%	68.5	73.4	78.7	76.0	73.4

Table 6.4: Performance of the Hypnogram estimation algorithm. Detection rates for the three considered states with different percentages of rejection.

Table 6.5 displays the average transition matrix, obtained in the training phase of the HMM. The emission matrix is not shown due to its large dimensions ( $3 \times 27$ ).

		Next State:		
		Wake.	REM	NREM
Current State:	Wake.	0.7473	0.0132	0.2395
	REM	0.0321	0.9059	0.0620
	NREM	0.0353	0.0176	0.9472

Table 6.5: Average transition matrix, computed from the training data.

For performance comparison purposes, the hierarchical classification method, with no data rejection, discussed in Section 6.5 was also implemented. Table 6.6 shows that the two classifiers Wake/Sleep and Rem/Non-Rem have relatively good performances ( $Acc \approx 80\%$ ) which are in concordance with the performances reported in [69] for SW discrimination using cardiovascular data and ACT and [188] for Rem/Non-Rem. However the hierarchical combination of the two classifiers (three class discrimination) leads to a poor Accuracy/Gmean, which are lower than the worst result from Table 6.4.

#### 6.8.4 Sleep parameters estimation

The three sleep parameters and the estimation error<sup>1</sup> were computed, for each dataset, using the estimated hypnogram and using the alternative method.

<sup>1</sup>Let  $\alpha$  represent a sleep parameter, the estimation error is given by  

$$E_\alpha = \frac{|\alpha_{true} - \alpha_{estimated}|}{\alpha_{true}}$$

	Wake. %	REM %	NREM %	Acc. %	Gmean
Wake/Sleep	71.1	81.5		80.2	76.1
REM/NREM	-	80.4	79.5	79.7	79.9
Wake/REM/NREM	71.1	58.2	67.9	66.4	65.5

Table 6.6: Hierarchical classification.

Table 6.7 shows the average value and error for each parameter, computed for several different RFs. As expected, by incorporating the rejection information, the alternative parameter estimation outperforms the hypnogram method in all the metrics.

Using a RF of 10% and the Alternative parameter estimation method, the average values are almost coincident with the real values. The estimation errors are 4.3% for the SE, 9.8% for the REM<sub>p</sub> and 5.5% for the NREM<sub>p</sub> respectively.

The optimal parameters  $\theta_{\{s, ns, rs\}}$  and  $\omega_{\{s, ns, rs\}}$ , computed from the training data according to Equations (6.8) – (6.11) are shown in Table 6.8.

### Method Generalization

In order to test the influence of the training and test sets and to assess the generalization capability of the algorithm the following steps were performed:

1. Ten datasets were randomly selected from the pool of 20 available datasets.
2. From these 10 datasets, 5 were randomly selected to train the algorithm.
3. The sleep parameters were estimated for the remaining 5 datasets and the average error computed.

This procedure was repeated 10 times resulting in average errors of  $5.9 \pm 1.4$ ,  $11.8 \pm 5.6$  and  $4.3 \pm 2.6$  for SE, REM<sub>p</sub> and NREM<sub>p</sub> respectively. These values are very similar to the ones reported in Table 6.7 suggesting that the reported results should be extensible to other datasets.

### 6.8.5 Final Remarks

The automatic estimation of a Hypnogram is often limited by noisy observations that need to be discarded. This is particularly relevant in real environments using data acquired from

## 6.8. Experimental Results

---

	SE		REM <sub>p</sub>		NREM <sub>p</sub>	
	T.V. - 86.1 ± 5.2%		T.V. - 17.4 ± 2.9%		T.V. - 82.5 ± 3.1%	
RF	Est.%	Err.%	Est.%	Err.%	Est.%	Err.%
Sleep Parameters from estimated Hypnogram						
0%	78.1 ± 7.2	10.9 ± 5.8	21.7 ± 4.7	27.3 ± 21.7	71.8 ± 5.6	17.3 ± 9.2
5%	78.4.4 ± 7.2	11.2 ± 5.3	22.8 ± 4.8	32.7 ± 22.4	71.1 ± 9.1	18.6 ± 9.9
10%	78.1 ± 7.5	10.6 ± 5.1	20.5 ± 5.3	27.3 ± 14.7	73.1 ± 8.4	15.5 ± 9.7
20%	78.3 ± 6.8	10.6 ± 5.5	20.6 ± 5.1	28.2 ± 15.5	73.2 ± 6.9	16.2 ± 10.4
Alternative parameter estimation						
0%	85.9 ± 5.0	4.9 ± 4.0	17.8 ± 2.5	12.3 ± 9.1	81.8 ± 6.1	5.7 ± 4.2
5%	86.8 ± 4.7	<b>3.7 ± 3.4</b>	17.9 ± 2.4	11.2 ± 8.8	82.2 ± 4.2	5.5 ± 3.6
10%	<b>86.2 ± 4.3</b>	4.3 ± 3.4	<b>17.7 ± 2.2</b>	<b>9.8 ± 7.7</b>	<b>82.3 ± 5.1</b>	<b>5.4 ± 3.9</b>
20%	86.7 ± 4.7	4.6 ± 4.0	18.2 ± 1.7	13.4 ± 8.3	82.3 ± 6.4	5.7 ± 2.3

Table 6.7: Mean of the estimated parameters (Est.) and estimation error (Err.) of the Sleep Parameters, computed from the estimated Hypnogram and using the Alternative method, for several values of the Rejection Factor (RF). The average of the True Values (TV) are displayed next to each parameter.

portable devices. In this chapter a HMM based algorithm is described to overcome this limitation and compute sleep parameters from a limited set of observations.

The Hypnogram estimation algorithm achieves an accuracy of 78.3% with similar detection rates for all considered states. The corresponding k-index,  $k = 0.58$ , is among the highest values reported in the literature for a 3 state discrimination task: [14] ( $k = 0.42$ ), [191] ( $k = 0.32$ ), [167] ( $k = 0.45$ ), [194] (Acc = 76%), [195] ( $k = 0.44$ ) and [189] ( $k = 0.62$ ). In addition, it is important to stress that many of the cited methods discard noisy observations, preventing the estimation of a continuous hypnogram, and do not take into account the inherent temporal correlation between sleep states.

A recent study by Rosenberg et al. [196] shows that the inter-scorer agreement in hypnogram estimation, from PSG data is approximately 83%. The accuracy reported in this work is already very close to this value.

	SE	NREM <sub>p</sub>	REM <sub>p</sub>
$\theta$	0.9126	0.9704	1.7318
$\omega$	0.8545	0.6638	0.2363

Table 6.8: Sleep Parameters - Regularization.

The sleep parameter estimation method, designed to reject ambiguous samples, led to estimation errors of  $\approx 5\%$  for SE and NREM<sub>p</sub> and  $\approx 10\%$  for REM<sub>p</sub>. These results are encouraging, suggesting that preliminary screenings for sleep disorders can be done using data acquired by non-cumbersome and portable devices.

The data used in this study was collected from a heterogeneous group of subjects, having no described pathological condition. The heterogeneity of the group promotes the generalization ability of the method. However, the absence of pathologies in the dataset might lead to poor performance of the method with subjects presenting aberrant sleep patterns, like in OSAs or Insomnia. A possible approach to overcome this limitation is the use of a multi-model approach.

## 6.9 Conclusion

In this chapter a new method to estimate the Hypnogram from RR, RIP and ACT data was presented. The method relies on an ensemble of classifiers, trained with a rejection option and a HMM based regularization algorithm, which takes into account statistical information regarding the sleep cycle.

The proposed method is able to estimate a 3 state Hypnogram with an acceptable accuracy, outperforming most of the state of the art algorithms. However it was shown that the computation of sleep parameters from this Hypnogram, particularly REM and NREM percentages, is strongly affected by an estimation error.

In order to solve this problem an alternative method was proposed that discards ambiguous samples and estimates the sleep parameters based on the informations regarding classifiers performance and rejection patterns. With this new method the estimation errors are  $\approx 5\%$  for SE and NREM<sub>p</sub> and  $\approx 10\%$  for REM<sub>p</sub>.

# 7 Portable sleep monitoring system

## 7.1 Introduction

The PSG, described in detail in Chapter 2, is the gold standard for sleep disorders diagnosis. The large range of physiological signals acquired, together with the supervised and controlled conditions in which it is performed, ensures reliable and reproducible results.

However, these controlled and restrictive conditions are also the source of its main limitations. Namely, the high costs associated, the long set-up procedures, the high technical difficulty on the data analysis and the impossibility of performing the exam across several days or weeks.

In this context, the recent widespread adoption of "smart" mobile devices, together with advances in sensor technologies, has created new opportunities regarding sleep monitoring. While it is unlikely that portable, unsupervised devices, will replace PSG in a near future, they can be a source of valuable data complementing the PSG and the information collected by the physician.

In this chapter the detailed structure and implementation of a smartphone based sleep monitoring system is presented. The overall idea is to design a system that allows relevant physiological signals to be acquired across several days or weeks, with minimum set-up procedures. The system is supported by a set of software and algorithms that extract relevant information and compute important parameters, storing them for later analysis. The acquired information will give support to the physician in the diagnosis process.

After the introduction, a brief overview of Body Sensor Networks (BSN) in the context of health assessment is performed followed by a description of the existing solutions in sleep context. Then, the structure of the proposed system, here called Smart Sleep Monitor (SSM), is presented. The hardware, responsible for data acquisition, is described, as well as the supporting software, which integrates data, controls the hardware and interacts with the user. The complete system is supported by the algorithms described throughout this thesis, particularly in Chapters 4 and 6.

## **7.2 Body Sensor Networks for health assessment**

Advances in sensor technology led to the creation of small, energy efficient and relatively cheap units. These units, small enough to be considered wearable and often with embedded computing power, together with recent communication protocols, led to the concept of BSN. In these networks various sensors are attached on clothing, on the body or even implanted under the skin acquiring data from physiological sources.

Another breakthrough supporting the generalization of BSN was the maturation and widespread adoption of wireless technologies, removing the need of any wires, thus giving a new level of freedom to the subjects. *Wireless body area networks*, first suggested by Van Dam *et al.* in 2001 [197], made pervasive health monitoring practically feasible.

Statistics show that the global population is growing but it is also aging. This is particularly relevant in western countries where the rapidly aging population is expected to lead to an increase in chronic age-related diseases such as diabetes, cancer, congestive heart failure, chronic obstructive pulmonary disease, arthritis, osteoporosis, dementia and sleep apnea [198]. The expected increase in the demand for medical assistance together with the increase of the associated costs, is thus slowly shifting the paradigm of healthcare. The tendency is now to adopt low cost monitoring solutions, bringing medicine to the patients home.

BSN can thus have a critical role in the future of healthcare. The domain of application spreads across several areas [199]. According to the World Health Organization the main cause of death in the world are cardiovascular diseases, every year 17.5 million people die of heart attacks or strokes. Many of these episodes are preceded by changes in physiological signals that can be detected with proper monitoring. Type II diabetes is another disease whose frequency is expected to increase in the near future, proper monitoring in early stages can prevent blindness, loss of circulation and other complications. The list of diseases that can benefit from continuous monitoring is extensive and includes hypertension, asthma, Alzheimer's disease, Parkinson's disease, renal failure, post-operative monitoring, stress-monitoring and, the focus of this thesis, Sleep Disorders.

Figure 7.1 depicts the basic structure of a BSN. The network of sensors connects to a master node which stores and process the data and/or acts as a gateway to the network. Depending on the nature of the acquired data and scope of application of the BSN, data can be stored for later analysis, processed immediately in the main node or relayed for an external server which will process and store the data. The main node can also generate reports for the physician and generate alarms in the case of pre-defined or disastrous events.

The scheme depicted in Figure 7.1 is a very general description of a BSN, that can be adapted depending on the intended application. The development of BSN for a large range of applications is currently the focus of many research groups and companies.

Regardless the scope of application, all BSN's share some common requirements.

Given the different nature of the acquired signals, the data **sampling rate** can range from one

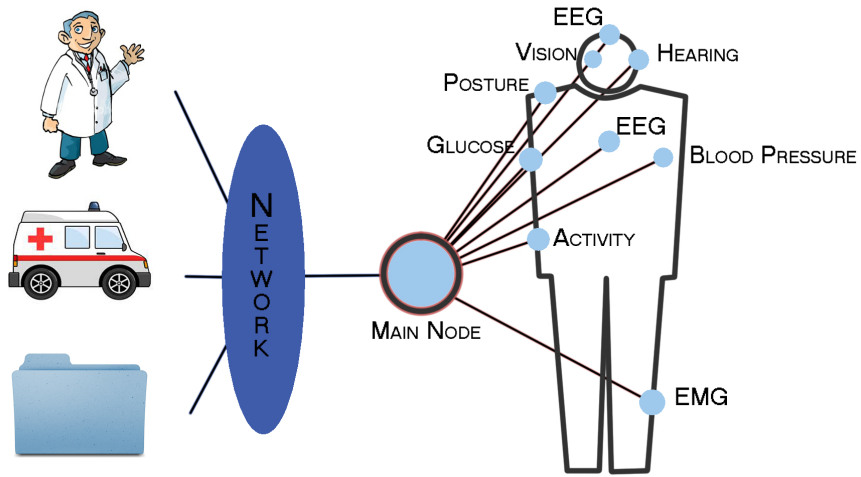


Figure 7.1: General architecture of a Body Sensor Network.

to several hundreds of hearts. For example, signals such as ECG should be sampled between 100-1000Hz, on the other hand, for light intensity a sample rate of 1Hz is sufficient. Table 7.1 shows the recommended sampling rate for several different physiological signals [199].

Signal Type	Sampling Rate
ECG	100 - 1000 Hz
EMG	1 - 10 kHz
Blood Saturation	1 - 1 Hz
Glucose	1 - 50 Hz
Temperature	0.1 - 1 Hz
Activity sensor	1 - 500 Hz

Table 7.1: Sampling rate for different physiological signals.

**Energy consumption** and autonomy is a critical issue. Depending on the application, the required autonomy of a BSN can range from some hours (e.g. sports monitoring) to several years (e.g. implantable devices such as pacemakers).

While the mobility inherent to BSN has several advantages, it raises **reliability** and quality-of-service issues. The network must be robust, allowing deviations around the optimal sensor locations.

Another requirement is concerned with **security** and **privacy of the data**. The system should provide protection against eventual losses (e.g. a subject that loses his smartphone should not have his data compromised) and intrusions.

## Chapter 7. Portable sleep monitoring system

---

Finally, since the final user of a BSN will often have no previous experience with this kind of technology. The whole system, in particular software, should be **user-friendly** and **easily configurable**.

In sum the system should be adaptable to use several heterogeneous devices, should be low-cost, low-power, non-invasive, unobtrusive and easy to use.

While the technology to implement a large range of BSN exists, with a wide range of options already available for developers, standards are yet to be defined. The IEEE Standards Association started, in 2007, the *IEEE 502.15 Task Group 6* whose objective is to *develop a communication standard optimized for low power devices and operation on, in or around the human body (but not limited to humans) to serve a variety of applications including medical, consumer electronics / personal entertainment and other.*

A complete review of BSN technologies and on going projects are presented in detail in [199].

### 7.3 Portable Sleep Monitoring

The increasing awareness of the general public and medical community to sleep disorders, and their strong impact on public health, together with many technological advances in the late 20th century, led to an increase in the use of portable recording devices intended to monitor and diagnose sleep disorders. OSA and other breathing related disorders received particular attention, in 1994 the American Sleep Disorders Association published the first practice parameters to guide the clinicians in the appropriate use of these devices [200].

In this guide, elaborated in the scope of OSA, the devices were grouped according to the nature of the acquired physiological signals, capacity to perform proper sleep staging and the requirement of a technician to be present during the exam. Four types of devices were defined:

**Type I** devices are restricted to the sleep laboratory. The exams are performed with the supervision of a trained technician and allow full sleep staging and proper detection of transitions through sleep stages. Type I devices rely on EEG to monitor brain activity and basically comprise the devices capable of performing a full PSG.

**Type II** monitoring devices can perform full PSG outside of the laboratory. The major difference from Type I devices is that a technologist is not present. These devices, also called *comprehensive portable devices*, must include a minimum of 7 channels.

**Type III** monitoring devices are characterized by not being able to determine sleep stages or sleep disruption. They typically include four physiologic variables, two respiratory, one cardiac variable, and arterial oxygen saturation. Some devices may have other signals including a monitor to record snoring, detect light, or a means to determine body movement and position. Type III devices do not require the presence of a technician.

**Type IV** devices are also unattended and have a minimum of 2 channels, typically arterial

### **7.3. Portable Sleep Monitoring**

---

oxygen saturation and airflow.

In 2007 the *Portable Monitoring Task Force* of the AASM published an updated review and guidelines for the usage of portable devices in sleep medicine [201]. The guidelines supported the use of portable devices, under very strict conditions, to monitor and diagnose OSA but discarded their usage in the case of co-morbidity with other sleep disorders (e.g. central sleep apnea, periodic limb movement disorder, insomnia, parasomnias, circadian rhythm disorders or narcolepsy) and co-morbidity with other medical conditions (e.g. moderate to severe pulmonary disease, neuromuscular disease, or congestive heart failure). The Task Force also concluded that portable monitoring should not be used to monitor asymptomatic populations, even if the case of high risk subjects.

Despite these conservative guidelines, the Task Force recognized the need to further address and research the potential of the emerging portable monitors. Recommendations for future research included tests in large sets of data and in patients with co-morbid conditions.

The release of the 2007 recommendations coincided with the announcement, by the United States *Centers for Medicare and Medicaid Services*, of the extension of the coverage of Continuous Positive Airway Pressure (CPAP) based on diagnoses using portable monitoring. Since then, more and more portable sleep monitoring solutions appeared in the market, with varying degrees of scientific support.

More recently, in 2011, the AASM considered that the ruling device classification methods were unsuitable since the classification scheme did not fit well with a large number of newly developed devices. The AASM board commissioned a task force to determine a more specific and inclusive method of classifying and evaluating sleep testing devices, other than PSG, used as aids in the diagnosis of OSA. The scope of the commission's work was limited to classification and evaluation of performance characteristics, and not the technology's use in practice guidelines, accreditation standards, or management principles [202]. This paper was coined by one of the authors as *the first step in a comprehensive process to evaluate and subsequently make recommendations on how to use home sleep testing devices in an outpatient population*.

The major companies providing Type I devices now offer several portable solutions. These devices are typically expensive and are limited to clinical environments, i.e. the exams are supervised by a clinician and are prescribed after a comprehensive sleep evaluation.

However, in recent years many sleep monitoring devices started being available to the general consumer market with affordable price tags. The available devices have different degrees of complexity and typically use combinations of questionnaires, activity from accelerometers and, not so frequently, analysis of the audio signals and one EEG channel.

While the availability of such devices is appealing to the general public, they might pose an hidden threat. The claimed features and accuracy of these devices are often misleading, they are not based on any published scientific evidence and lack systematic testing with large sets of data. While this is not a problem for the occasional curious user, it might mislead subjects suffering from actual sleep disorders with severe consequences for his health.

The widespread adoption of mobile devices, such as "smart" phones and tablets has also supported this new generation of sleep monitoring solutions. These devices are typically equipped with powerful processors, large storage capacity, internet access and multiple built-in sensors. They were soon applied to monitor all kinds of data, including health related information, such as food intake, exercise and sleep.

A quick search for sleep monitoring applications for smartphones currently returns hundreds of results. Once again, their reliability is, at least, questionable, as shown in the reviews [203] and [204].

On the other hand, several research groups are systematically applying modern signal processing techniques to the readily available data acquired from smartphones with interesting results [205]. Such an example is the prototype of an OSA screening application described in [206] which uses features derived from audio, actigraphy and pulse oximetry and a SVM to generate a probability that a subject has OSA.

The universe of solutions for portable sleep monitoring is thus quickly evolving, benefiting from easily available and cheap technologies and new signal processing algorithms. In the next section, a system is proposed that allows portable and long term sleep monitoring. The system is supported by the algorithms described throughout this thesis.

### 7.4 Smart Sleep Monitor

In Chapters 4, 5 and 6 the significance of 3 physiological and behavioural sources of information were discussed in the scope of sleep assessment, namely HRV, RIP and ACT. The presented algorithms describe a method to estimate a limited set of sleep parameters and sleep states from these signals. These sources of data were chosen in part due to relative simplicity in its acquisition.

In this section a Smartphone based Sleep Monitoring system, SSM, is presented with the goal of providing a physical platform to test these algorithms and describe a general structure for a simple sleep monitor. The proposed characteristics of the system are:

- Provide a simple solution for **long term** sleep monitoring.
- Based on **low-cost** and readily available hardware.
- Supported by scientific based, **published algorithms**.
- Provide a **user-friendly** interface, both in terms of hardware and software.
- Allow an easy extension to other sources of data.

The following subsections describe the structure of the SSM, hardware configuration and supporting software. At the moment of writing, the system is almost entirely implemented, although no proper testing has been performed. The following information can thus be regarded as a general structure/guideline for further development.

### 7.4.1 Structure

The structure of the SSM, shown in Figure 7.2, is composed by the portable sensors, worn by the subject and a central processing and controlling unit, here implemented using an Android smartphone.

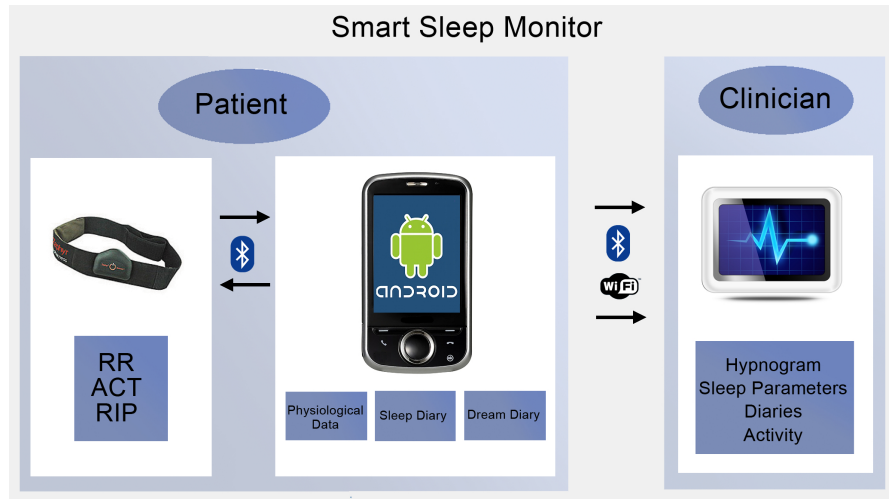


Figure 7.2: Structure of the proposed Smart Sleep Monitor

### 7.4.2 Data acquisition

The algorithms described in Chapter 6 require that the system is able to acquire ECG, RIP and ACT data. The current implementation of the SSM is supported by a the *Zephyr-Technology BioHarness* [207], shown in Figure 7.3. A smart-fabric (fabric with embedded sensors) chest-strap that monitors ECG, RIP, skin temperature, GSR and activity.

The ECG is captured by 2 capacitive sensors, covered by a conductive fabric, acquiring the signal with a sampling rate of 250Hz. Although the device is able to transmit the ECG in real-time, the automatically computed RR interval is used instead. This is due to the internal filtering performed on the ECG which may introduce delays and phase shifts, thus distorting the morphology of the QRS complex.

The ECG data is stored/transmitted in 10bits, resulting in a range of 0-1024. The *RR* interval, internally computed from the ECG is transmitted/stored every 56ms corresponding to a frequency of  $\approx 18$ Hz.

The chest skin temperature is obtained from an infrared sensor, a new value is obtained every second.

The RIP is acquired from a stretch sensitive sensor that converts the expansion and contraction



Figure 7.3: Zephyr BioHarness chest strap

of the rib cage, the sampling rate is  $\approx 18\text{Hz}$ .

Activity is obtained from a 3-axis accelerometer that monitors attitude (subject posture) and activity (acceleration), a new set of samples is obtained every 20ms.

The device implements a simple protocol that enables communications via Bluetooth, the data can be stored on the device's internal memory or transmitted in real time.

In a recent effort to reduce the costs associated to the Zephyr Bioharness, a new solution based on the locally developed BITalino [208] was created. This device is a highly customizable physiological signal acquisition platform that has been adapted for the considered application. The included sections of the device were the *Micro-Controller Unit*, *Bluetooth unit*, *Power unit*, *Accelerometry* and *Electrocardiography*. These 5 sections were packed together and connected to 3 pre-gelled electrodes that glue directly to the subject's chest resulting in the configuration shown in Figure 7.4. While this solution does not contemplate the acquisition of RIP, future work might extract this information directly from the breathing modulation on the ECG, as shown in [209, 210].

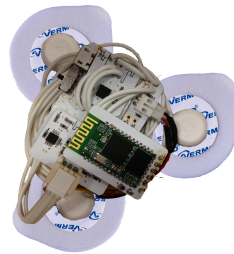


Figure 7.4: Sleep monitor based on the BITalino board

In the described solutions, the movement data is taken from the chest of the subject. However, most sleep related ACT algorithms, including the one described in Chapter 4 are developed for wrist ACT, in particular for the non-dominant [211] wrist. Alternative locations for accelerometer sensors have been explored by some authors. Some algorithms have been shown to be relatively insensitive to non-dominant vs dominant wrist placement [7, 212] although very different activity levels have been reported. Studies considering body areas other than the wrists have found significant differences in algorithms performance [213] and its use was recommended for specific applications, such as the precise assessment of body position given from waist and hip locations [214].

It is thus fundamental to properly test the performance of the algorithms from Chapters 4 and 6, using the PSG as ground-truth, with data acquired with the described hardware and in particular with accelerometer data acquired in the chest.

### 7.4.3 Supporting software

The software supporting the SSM was implemented for the Android operating system, a popular system among current smartphones. All the applications and already implemented algorithms were written in Java. The SSM software has three main components: Two diaries, sleep and dream, and one application responsible for the acquisition, storage and processing of real time data.

The Sleep electronic Diary (SeD) structure, depicted in Figure 7.5, allows the user to easily register a set of different events such as going to bed, waking up, meals, exercise, complaints, among others. Each event is associated with an hour/date and, depending on the type of event, the diary also registers the duration, location, intensity, etc.

The entries registered on the diary can easily be edited, deleted and displayed on a calendar.

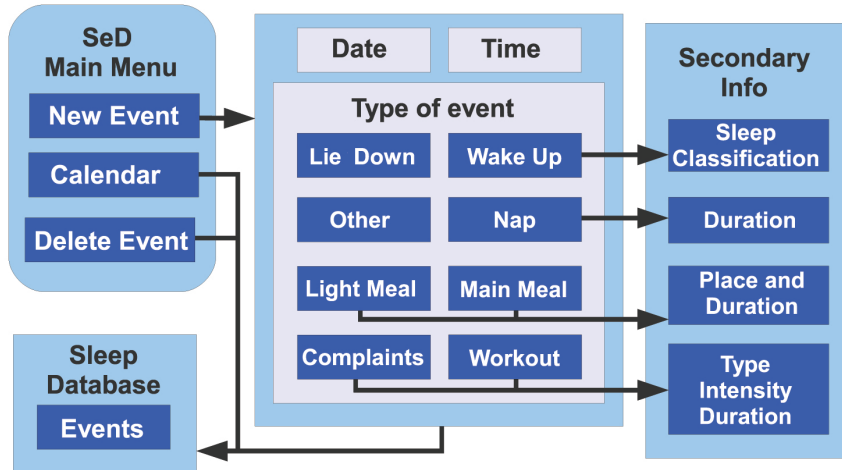


Figure 7.5: Sleep electronic Diary structure

All the data is kept on a dedicated *sql* database.

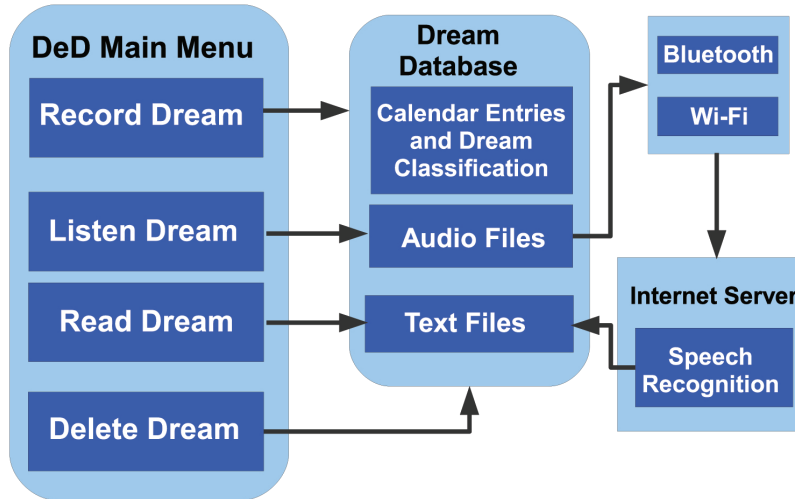


Figure 7.6: Dream electronic Diary structure

The structure of the Dream electronic Diary (DeD), shown in Figure 7.6, allows the user to register a new dream by simply recording its own voice. After the dream is recorded, the user has the option to submit the dream to a voice recognition service that translates the audio file to a text file. Although this feature is still being implemented, the goal is to develop a dedicated

## Chapter 7. Portable sleep monitoring system

---

pattern recognition algorithm that parses the text files and provides the clinician with a list of the most important and recurrent words in the dreams.

Dream diary entries are stored in a common database, with SeD entries.

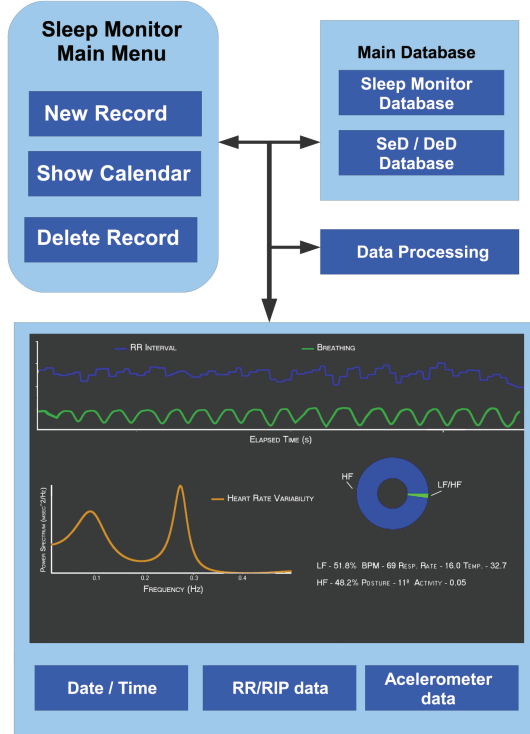


Figure 7.7: Structure of the main SSM application and aspect of the data acquisition panel.

The main application of the SSM has multiple functions:

- Manages the connection to the *Zephyr Bioharness/ BITalino* allowing the user to enable and disable the acquisition of certain signals.
- Provides an intuitive user interface that allows users to start/stop acquisitions.
- Manages all the data, including the entries from the diaries.
- Computes and displays in real-time the HRV and derived measures (such as the *LF/HF* ratio) and other physiological variables such as breathing waveform, RR signal, Heart Rate, Breathing rate, Activity, Posture and Skin Temperature.
- Allows users to generate events, synchronized with the data, for later analysis.
- After a nocturnal acquisition, processes the data in order to estimate the sleep/wakefulness periods, sleep states and sleep parameters discussed in Chapter 5.

#### 7.4.4 Other applications

The main application, shown in Figure 7.7 is very versatile, allowing users to acquire data in a non-sleep context. Namely, it is very useful to monitor events on which HRV and respiration play an important role, such as passive and active orthostatic tests, relaxation exercises and concentration tests.

Figure 7.8 illustrates the variation on the HRV, monitored using the SSM, on a subject consciously breathing using different inhale/exhale patterns.

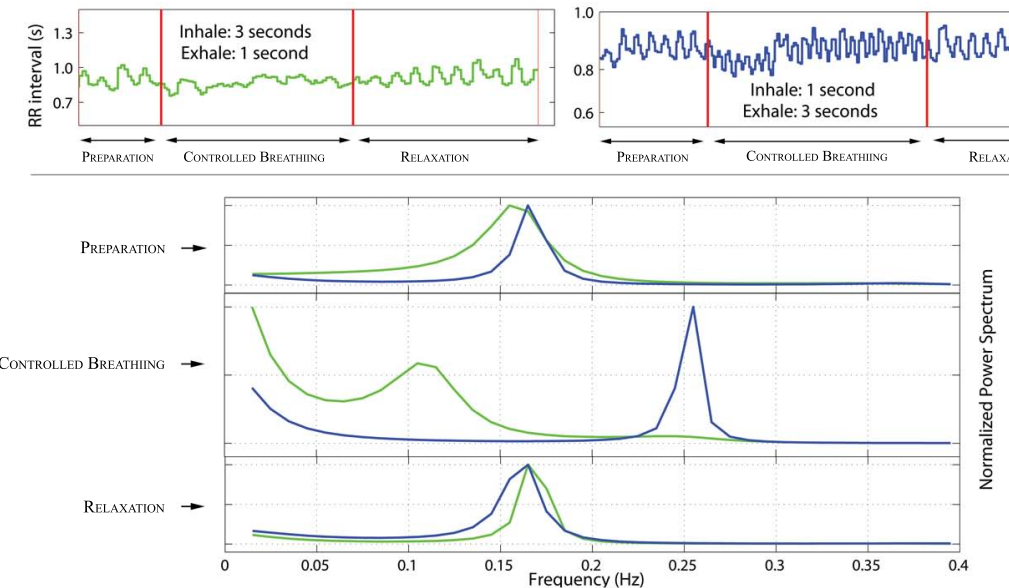


Figure 7.8: HRV variation induced by different breathing patterns. Top Left) After a resting phase, the subject starts inhaling for 3 seconds and exhaling during 1 second (1/3), this is repeated several times. Top Right) The subject changes his breathing pattern to 3 seconds inhale and 1 second exhale (3/1). Bottom) During the controlled breathing the 1/3 breathing pattern induces a strong sympathetic activation, on the other hand, the 3/1 induces a parasympathetic activation.

Other applications, currently being explored, include biofeedback for Insomnia and stress treatment, since it provides the users real-time information on the activity of their ANS. The system's architecture was designed to allow easy adaptation to new problems, thus providing a versatile platform for researchers and clinical applications.



## 8 Conclusions and Future Work

This thesis aims at exploring new methods for the assessment of sleep, supported by data acquired with portable devices and novel signal processing algorithms. The central idea is to automatically compute complementary information to support the gold standard PSG in the follow-up process and diagnosis of sleep disorders.

The presented methods suggest that modern signal processing techniques allied with the large processing capacity of portable devices, equipped with a wide range of sensors, might lead to a shift on the paradigm of sleep monitoring. The highly constrained PSG can already be complemented by portable devices that, if properly designed and tested, can provide important insights regarding sleep habits, patterns and sleep parameters.

### Sleep and Wakefulness estimation from Actigraphy data

Actigraphy data has been used with relative success in the last decades to characterize sleep and subjects habits. The simplicity and low costs associated to these devices makes them ideal for long term portable monitoring.

The characterization of ACT data is a central point in this thesis. Particular emphasis is given to the different types of information contained on a nocturnal ACT dataset. Typical algorithms for Sleep / Wakefulness discrimination are based on the intensity of the recorded movements, however, many fail to acknowledge that movement comprises only approximately 6% of the recorded data. The presented solution shows that the remaining 94% of the data contains useful information, described by the time intervals between successive movements. It was shown that the length of inactivity periods, during sleep and wakefulness states, are described by two different probability distributions.

Another novelty in the presented method is concerned with the features used to characterize the recorded movement data. Movements recorded in different states, here assumed to be intrinsically different, are described by the coefficients of an AR and by a RMM. The obtained results support the idea that movements during sleep and wakefulness states are different from a statistical point of view, and the parameters of the models are able to provide a rough discrimination between states.

## **Chapter 8. Conclusions and Future Work**

---

Under proper metrics, the proposed algorithm performs better than most of the state of the art algorithms described in the literature and better than the tested algorithms. The use of a HMM to model the sleep/wakefulness process plays an important role, since it incorporates the temporal relation between the two states.

Although there is still room for improvement on ACT based algorithms, in the authors opinion, the current state of sensor technology will make devices, based simply on accelerometer sensors, obsolete in a near future. Standard devices, such as the one shown in Figure 2.7, can currently incorporate other sensors, such as plethysmographs, able to monitor heart rate, without any particular increase in volume and/or price. This supports that the future of portable monitoring is based on multi-modal datasets instead of single sources of data.

### **Mathematical model for the Autonomous Nervous System**

The systematic description of the regulatory mechanisms of the ANS using mathematical models is an exciting area, briefly explored in this thesis. By incorporating physiological information about the kinetics of the neurotransmitters on the SAN the described model was able to properly predict the response of the ANS to an AOT. Future work will incorporate breathing in the baroreflex loop and study the origin of Mayer waves or 10s rhythm.

Mathematical models such as the one described, might also play an important role in another open issue: The problem of decoupling the activity of the sympathetic and parasympathetic branches of the ANS on the heart's activity. This has been the emphasis of the work by many researchers, however, proper models for the influence of the two branches of the ANS on the SAN are still not available.

Such models are particularly important as they will provide the basis to alternative ways to discriminate the contributions of the parasympathetic and sympathetic branches on the HRV. In fact, all the algorithms currently depending on HRV frequency analysis, including the ones described in this chapter, are based on the assumption that the frequency bands on the HRV directly reflect the activity of the two branches of the ANS. However, those frequency bands reflect the variations induced by the two branches, and not the activity of each branch itself. Proper models for the ANS and its influence of the SAN are thus necessary as well as proper decoupling methods.

### **Automatic Sleep Staging from limited sets of data**

A proper algorithm for reliable automatic sleep staging and/or sleep parameter computation, from limited sets of data, is highly desirable in sleep medicine. The described method tries to incorporate all the knowledge gained in the remaining chapters, concerning both behavioural and physiological data.

The performance of the algorithm, tested on a dataset of voluntary healthy individuals, is among the highest reported in the literature. The global accuracy, 78.3%, is not an impressive

---

value, however, it must be placed in perspective with the fact that the inter-scorer agreement in Hypnogram estimation is known to be only 83%. This poses an interesting challenge in the future development of sleep staging algorithms, whose performances must be assessed using, not only multiple subjects, but also multiple scorers.

The presented results are supported by a relatively small amount of subjects, all categorized under a "healthy" label. Further studies should include larger numbers of subjects, including individuals pre-diagnosed with sleep disorders.

In the authors opinion, the performance of the method will degrade when testing the algorithm in sleep-disordered subjects (assuming that the training was made with healthy subjects). In fact, preliminary results have shown that the feature selection procedure yields different feature arrays for healthy and disordered subjects. A number of methods might be implemented to overcome this limitation, among them a multi-model approach might yield interesting results, i.e. different models, trained for different pathologies, are tested for each subject and the model yielding a higher posterior probability is selected. The described algorithm, based on a HMM, assumes that the model parameters are constant during the night. This assumption can be modified under two different approaches.

Although sleep can be roughly characterized by a relatively stable state marked by stochastic transitions, some easily observable stimuli are known to be correlated with these transitions. Such an example are the changes in posture, analysed in Chapter 4 and shown to be highly correlated with wakefulness state and SW transitions; ambient noises and ambient lights. These informations are not contemplated in the implemented algorithm but could be included either in the observation model or using an Input-Output-Hidden Markov Model, whose parameters would change in the presence of any external stimuli.

The second approach is related with the intrinsic nature of the sleep cycle. As explained in Chapter 2 the sleep cycle has a well defined structure, where REM cycles tend to get longer along the night and NREM shorter. This characteristic is not implemented in the current model but a solution supported by a Input-Output-HMM could easily integrate this extra information.

### **8.0.5 Limitations and guidelines for portable sleep monitor applications**

The readily availability of devices with a large range of sensors and relatively low costs fostered the appearance of several devices and applications claiming to monitor sleep often with dubious validation. These non medical-grade devices might pose a hidden threat to the general public, by providing misleading results and/or postponing the seek of medical care. The control of these applications by regulatory laws is impractical, since they are valid tools for the casual curious user, however public campaigns for the awareness of sleep disorders should address this issue.

In the case of medical-grade devices, the American Academy of Sleep Medicine has an important role in the definition of standards and validation of new devices for portable sleep

## **Chapter 8. Conclusions and Future Work**

---

monitoring. In the authors opinion, these devices have an enormous potential and will play a fundamental role in the future of sleep medicine, contributing to the general awareness of the importance of sleep and to the improvement of sleep quality.

# A Actigraphy - Comparative methods

In this Appendix, two of the methods for SW discrimination listed in Table 4.1, are described, as well as the adaptations required for their use with the existing datasets. The two methods, here called Sadeh's [7] and Hedner's [109], were selected by their reported performance, particularly its *Sens* and *Spec* balance.

## A.1 Sadeh's algorithm

In [7] Sadeh *et al.* propose a scoring algorithm, using 60 seconds epochs, that linearly combines several features in the following discriminative function,

$$PS = \boldsymbol{\alpha} \boldsymbol{\theta}^T \quad (\text{A.1})$$

where  $\boldsymbol{\alpha}$  is a vector of adjustable parameters defined in [7] as

$$\boldsymbol{\alpha} = [7.601; -0.065; -1.08; -0.056; -0.703]. \quad (\text{A.2})$$

$\boldsymbol{\theta}$  is a vector of features extracted from the data expressed as

$$\boldsymbol{\theta} = [1; \mu; Nat; \sigma; LogAct] \quad (\text{A.3})$$

where  $\mu$  is the mean number of activity counts on a 11 minute window centred in the current epoch,  $Nat$  is the number of epochs with activity level equal to or higher than 50 but lower than 100 activity counts in a window of 11 minutes,  $\sigma$  is the standard deviation of the activity on the last 6 minutes and  $LogAct$  is the natural logarithm of the number of activity counts during the scored epoch plus 1.

A given epoch is scored as *sleep* if  $PS \geq 0$  and *wakefulness* otherwise.

## **Appendix A. Actigraphy - Comparative methods**

---

Since the initial algorithm was developed for a different Actigraph device and database, the 5 parameters from the discriminative function were optimized for the current data. The optimal parameters were found maximizing the cost function given by (??) leading to,

$$\boldsymbol{\alpha}^* = [4.097; -0.528; -0.51; -0.259; -1.65]. \quad (\text{A.4})$$

### **A.2 Hedner's algorithm**

In [109] Hedner *et al.* present a SW state estimation algorithm with focus on sleep apnea patients. The algorithm is divided in 4 distinct steps with the last one aiming at the detection of periodic movements, typical from apnea patients. Here, the last step is discarded and the algorithm is as follows:

1. Determination of the background movement activity of the patient throughout the night,  $\sigma$ .
2. Bandpass filter between 2 and 2.5 Hz, leading to a signal regarded as the energy of the activity.
3. For each 30 second epoch, values of energy below  $\sigma$  are discarded and the remaining energy is integrated using a 5-minute Hanning window. Values below a fixed threshold,  $\theta$  are scored as *sleep* and values above are scored as *wakefulness*.

The two parameters,  $\sigma$  and  $\theta$  were computed maximizing the cost function given by (??).

## B International Classification of sleep disorders

The ICSD-2 was published with the goal of standardizing definitions of sleep disorders and creating a systematic approach to diagnosis. It is widely used by clinicians and researchers worldwide, improving research efforts throughout the international community by adhering to a recognised set standards.

Table B.1 shows the complete list of sleep disorders included in the International Classification of Sleep Disorders-2 [57]. There are eight main categories as defined by the classification. The left hand column represents the category, the middle column the medical term for the sleep disorder and the right hand column contains any other alternative terms in common use.

Table B.1: International Classification of Sleep Disorders

Category/Sub-Category	Sleep Disorder	Alternative Name	
INSOMNIA	Adjustment Insomnia Psychophysiological Insomnia Paradoxical Insomnia Idiopathic Insomnia Insomnia Due to Mental Disorder Inadequate Sleep Hygiene Behavioral Insomnia of Childhood Insomnia Due to Drug or Substance Insomnia Due to Medical Condition Insomnia Not Due to Substance or Known Physiological Condition Physiological (Organic) Insomnia	Acute insomnia, short term insomnia  Sleep state misperception Primary insomnia	
SLEEP RELATED BREATHING DISORDERS	Central Sleep Apnea Syndromes  Obstructive Sleep Apnea Syndromes  Sleep Related Hypoventilation/Hypoxemic Syndromes	Primary Central Sleep Apnea Central Sleep Apnea Due to Cheyne Stokes Breathing Pattern Central Sleep Apnea Due to High-Altitude Periodic Breathing Central Sleep Apnea Due to Medical Condition Not Cheyne Stokes Central Sleep Apnea Due to Drug or Substance Primary Sleep Apnea of Infancy  Obstructive Sleep Apnea, Adult Obstructive Sleep Apnoea, Pediatric  Sleep Related Nonobstructive Alveolar Hypoventilation, Idiopathic Congenital Central Alveolar Hypoventilation Syndrome Sleep Related Hypoventilation/Hypoxemia Due to Medical Condition Sleep Related Hypoventilation/Hypoxemia Due to Pulmonary Parenchymal or Vascular Pathology Sleep Related Hypoventilation/Hypoxemia Due to Lower Airways Obstruction Sleep Related Hypoventilation/Hypoxemia Due to Neuromuscular and Chest Wall Disorders	OSA, sleep apnoea Child sleep apnea

## Appendix B. International Classification of sleep disorders

Table B.1: continued

Category/Sub-Category	Sleep Disorder	Alternative Name
	Other Sleep Related Breathing Disorder Sleep Apnea/Sleep Related Breathing Disorder, Unspecified	
HYPERSOMNIAS OF CENTRAL ORIGIN		
	Narcolepsy with Cataplexy Narcolepsy Without Cataplexy Narcolepsy Due to Medical Condition Narcolepsy Unspecified Idiopathic Hypersomnia With Long Sleep Time Idiopathic Hypersomnia Without Long Sleep Time Behaviorally Induced Insufficient Sleep Syndrome Hypersomnia Due to Medical Condition Hypersomnia Due to Drug or Substance Hypersomnia Not Due to Substance or Known Physiological Condition Physiological (Organic) Hypersomnia, Unspecified	Primary hypersomnia Primary hypersomnia  Nonorganic hypersomnia,NOS Organic hypersomnia,NOS
Recurrent Hypersomnia	Recurrent Hypersomnia Kleine-Levin Syndrome "Menstrual-Related Hypersomnia	Sleeping beauty syndrome
CIRCADIAN RHYTHM SLEEP DISORDERS		
	Circadian Rhythm Sleep Disorder, Delayed Sleep Phase Type  Circadian Rhythm Sleep Disorder, Advanced Sleep Phase Type Circadian Rhythm Sleep Disorder, Irregular Sleep-Wake Type Circadian Rhythm Sleep Disorder, Free-Running Type Circadian Rhythm Sleep Disorder, Jet Lag Type Circadian Rhythm Sleep Disorder, Shift Work Type Circadian Rhythm Sleep Disorder Due to Medical Condition Other Circadian Rhythm Sleep Disorder Other Circadian Rhythm Sleep Disorder Due to Drug or Substance	Delayed sleep phase disorder, delayed sleep phase syndrome Advanced sleep phase disorder Irregular sleep-wake rhythm Nontrained type Jet lag Shift work disorder  Circadian rhythm disorder, NOS
PARASOMNIAS		
Parasomnias usually associated with REM sleep	Disorders of arousal (from non-REM sleep) Confusional arousals Sleepwalking Sleep terrors  REM sleep behavior disorder (including parasomnia overlap disorder and status dissociatus) Recurrent isolated sleep paralysis Nightmare disorder	Somnambulism Night Terrors  REM sleep disorder RBD  Sleep paralysis Nightmares
Other Parasomnias	Sleep Related Dissociative Disorders Sleep Enuresis Sleep Related Groaning Exploding Head Syndrome Sleep Related Hallucinations Sleep Related Eating Disorders Parasomnia Unspecified Parasomnia Due to Drug or Substance Parasomnia Due to Medical Condition	Nocturnal enuresis / Bedwetting Catastrophes  SRED
SLEEP RELATED MOVEMENT DISORDERS		
	Restless Legs Syndrome Periodic Limb Movement Disorder Sleep Related Leg Cramps Sleep Related Bruxism Sleep Related Rhythmic Movement Disorder Sleep Related Movement Disorder, Unspecified Sleep Related Movement Disorder Due to Drug or Substance Sleep Related Movement Disorder Due to Medical Condition	Teeth grinding
ISOLATED SYMPTOMS, APPARENTLY NORMAL VARIANTS AND UNRESOLVED ISSUES		
	Long Sleeper Short Sleeper Snoring Sleep Talking Sleep Starts Benign Sleep Myoclonus of Infancy Hypnagogic Foot Tremor and Alternating Leg Muscle Activation During Sleep Propriospinal Myoclonus at Sleep Onset Excessive Fragmentary Myoclonus	Hypnic jerks

---

Table B.1: continued

Category/Sub-Category	Sleep Disorder	Alternative Name
OTHER SLEEP DISORDERS	Other Physiological (organic) Sleep Disorder Other Sleep Disorder Not Due to Substance or Known Physiological Condition Environmental Sleep Disorder	



# Bibliography

- [1] HR Colten and BM Altevogt. *Sleep disorders and sleep deprivation: an unmet public health problem*. 2006. (page 1)
- [2] Charlotte A Schoenborn and Patricia F Adams. Health behaviors of adults: United States, 2005-2007. Technical report, 2010. (page 1)
- [3] Damien Leger and SR Pandi-Perumal. Review of Sleep Disorders: Their Impact on Public Health. *Sleep*, 30(7):934, July 2007. (pages 1 and 20)
- [4] Avi Sadeh and Christine Acebo. The role of actigraphy in sleep medicine. *Sleep Medicine Reviews*, 6(2):113–124, May 2002. (pages 3, 20, 50, 51, and 52)
- [5] Avi Sadeh. The role and validity of actigraphy in sleep medicine: an update. *Sleep medicine reviews*, 15(4):259–67, Aug 2011. (pages 3, 20, 50, and 52)
- [6] Roger J. Cole, Daniel F. Kripke, William Gruen, and J. Christian Gillin. Automatic sleep-wake identification from wrist actigraphy. *Sleep*, pages 461–9, Oct 1992. (pages 3, 20, 53, and 54)
- [7] A Sadeh, K M Sharkey, and M a Carskadon. Activity-based sleep-wake identification: an empirical test of methodological issues. *Sleep*, 17(3):201–7, Apr 1994. (pages 3, 20, 53, 54, 73, 78, 126, and 135)
- [8] Sonia Ancoli-Israel, Roger Cole, Cathy Alessi, Mark Chambers, William Moorcroft, and Charles P Pollak. The role of actigraphy in the study of sleep and circadian rhythms. *Sleep*, 26(3):342–92, May 2003. (pages 3, 53, 55, and 74)
- [9] Juan Szajzel. Heart rate variability: a noninvasive electrocardiographic method to measure the autonomic nervous system. *Swiss medical weekly*, 134(35-36):514–22, September 2004. (page 3)
- [10] T Electrophysiology. *Heart rate variability. Standards of measurement, physiological interpretation, and clinical use*. 1996. (pages 3, 88, 96, 102, and 103)
- [11] Daniel T Schmitt, Phyllis K Stein, and Plamen Ch Ivanov. Stratification pattern of static and scale-invariant dynamic measures of heartbeat fluctuations across sleep stages in

## Bibliography

---

- young and elderly. *IEEE transactions on bio-medical engineering*, 56(5):1564–73, May 2009. (page 3)
- [12] Phyllis K Stein and Yachuan Pu. Heart rate variability, sleep and sleep disorders. *Sleep medicine reviews*, 16(1):47–66, Feb 2012. (pages 3, 91, and 92)
- [13] Aaron Lewicke, Edward Sazonov, Michael J Corwin, Michael Neuman, and Stephanie Schuckers. Sleep versus wake classification from heart rate variability using computational intelligence: consideration of rejection in classification models. *IEEE transactions on bio-medical engineering*, 55(1):108–18, Jan 2008. (pages 3, 100, and 108)
- [14] M.O. Mendez, M. Matteucci, S. Cerutti, F. Aletti, and A.M. Bianchi. *Sleep staging classification based on HRV: Time-variant analysis*, page 9–12. IEEE, Sep 2009. (pages 3, 100, and 117)
- [15] F. Yasuma. Respiratory Sinus Arrhythmia: Why Does the Heartbeat Synchronize With Respiratory Rhythm? *Chest*, 125(2):683–690, February 2004. (pages 3 and 90)
- [16] Jan W. Kantelhardt, Thomas Penzel, Sven Rostig, Heinrich F. Becker, Shlomo Havlin, and Armin Bunde. Breathing during rem and non-rem sleep: correlated versus uncorrelated behaviour. *Physica A: Statistical Mechanics and its Applications*, 319:447–457, Mar 2003. (pages 3 and 92)
- [17] Daniel J. Buysse, Charles F. Reynolds, Timothy H. Monk, Susan R. Berman, and David J. Kupfer. The Pittsburgh sleep quality index: A new instrument for psychiatric practice and research. *Psychiatry Research*, 28:193–213, 1989. (pages 3 and 19)
- [18] Daniel J Buysse. Diagnosis and assessment of sleep and circadian rhythm disorders. *Journal of psychiatric practice*, 11(2):102–15, March 2005. (page 3)
- [19] Stefan Silbernagl Agamemnon Despopoulos. *Color Atlas of Physiology*. Thieme, 5th edition, 2002. (pages 8, 9, 85, and 86)
- [20] A A Borbély. A two process model of sleep regulation. *Human neurobiology*, 1(3):195–204, January 1982. (page 9)
- [21] Peter Achermann. The two-process model of sleep regulation revisited. *Aviation, space, and environmental medicine*, 75:A37–A43, 2004. (page 9)
- [22] K Sakai and S Crochet. Role of dorsal raphe neurons in paradoxical sleep generation in the cat: no evidence for a serotonergic mechanism. *The European journal of neuroscience*, 13(1):103–12, January 2001. (page 10)
- [23] Narayana S Murali, Anna Svatikova, and Virend K Somers. Cardiovascular physiology and sleep. *Frontiers in bioscience : a journal and virtual library*, 8:s636–52, May 2003. (page 10)

- [24] Jonathan R L Schwartz and Thomas Roth. Neurophysiology of sleep and wakefulness: basic science and clinical implications. *Current neuropharmacology*, 6(4):367–78, December 2008. (page 10)
- [25] J E Sherin, J K Elmquist, F Torrealba, and C B Saper. Innervation of histaminergic tuberomammillary neurons by GABAergic and galaninergic neurons in the ventrolateral preoptic nucleus of the rat. *The Journal of neuroscience : the official journal of the Society for Neuroscience*, 18(12):4705–21, June 1998. (page 10)
- [26] John F. Davis, Derrick L. Choi, and Stephen C. Benoit. *Handbook of Behavior, Food and Nutrition*. Springer New York, 2011. (page 10)
- [27] T Porkka-Heiskanen, R E Strecker, M Thakkar, A A Bjorkum, R W Greene, and R W McCarley. Adenosine: a mediator of the sleep-inducing effects of prolonged wakefulness. *Science (New York, N.Y.)*, 276(5316):1265–8, May 1997. (pages 10 and 11)
- [28] Tarja Porkka-Heiskanen, Lauri Alanko, Anna Kalinchuk, and Dag Stenberg. Adenosine and sleep. *Sleep medicine reviews*, 6(4):321–32, August 2002. (page 10)
- [29] Carlos Blanco-Centurion, Man Xu, Eric Murillo-Rodriguez, Dmitry Gerashchenko, Anjelica M Shiromani, Rafael J Salin-Pascual, Patrick R Hof, and Priyattam J Shiromani. Adenosine and sleep homeostasis in the Basal forebrain. *The Journal of neuroscience : the official journal of the Society for Neuroscience*, 26(31):8092–100, August 2006. (page 11)
- [30] Anna V Kalinchuk, Anna-Sofia Urrila, Lauri Alanko, Silja Heiskanen, Henna-Kaisa Wigren, Maricel Suomela, Dag Stenberg, and Tarja Porkka-Heiskanen. Local energy depletion in the basal forebrain increases sleep. *The European journal of neuroscience*, 17(4):863–9, February 2003. (page 11)
- [31] Porkka Heiskanen and Anna V. Kalinchuk. Adenosine as a sleep factor. *Sleep and Biological Rhythms*, 9:18–23, February 2011. (page 11)
- [32] J R Pappenheimer, G Koski, V Fencl, M L Karnovsky, and J Krueger. Extraction of sleep-promoting factor S from cerebrospinal fluid and from brains of sleep-deprived animals. *Journal of neurophysiology*, 38:1299–1311, 1975. (page 11)
- [33] Teresa Paiva and Thomas Penzel. *Centro de Medicina do Sono*. Lidel, 1st edition, January 2011. (pages 11, 12, 13, 15, 16, and 18)
- [34] Mark Peplow. The Anatomy of Sleep. *Nature*, 497:8–9, 2013. (page 11)
- [35] I Capellini, C L Nunn, P McNamara, B T Preston, and R A Barton. Energetic constraints, not predation, influence the evolution of sleep patterning in mammals. *Functional ecology*, 22(5):847–853, October 2008. (page 12)

## Bibliography

---

- [36] E J Van Someren. More than a marker: interaction between the circadian regulation of temperature and sleep, age-related changes, and treatment possibilities. *Chronobiology international*, 17(3):313–54, May 2000. (page 12)
- [37] R J Berger and N H Phillips. Energy conservation and sleep. *Behavioural brain research*, 69(1-2):65–73, 1995. (page 12)
- [38] Daniela Cevolani and Pier Luigi Parmeggiani. Responses of extrahypothalamic neurons to short temperature transients during the ultradian wake-sleep cycle. *Brain Research Bulletin*, 37(3):227–232, 1995. (page 12)
- [39] Timothy K Revell and Stephen G Dunbar. The energetic savings of sleep versus temperature in the Desert Iguana (*Dipsosaurus dorsalis*) at three ecologically relevant temperatures. *Comparative biochemistry and physiology. Part A, Molecular & integrative physiology*, 148:393–398, 2007. (page 12)
- [40] Howard P. Roffwarg, Joseph N. Muzio, and William C. Dement. Ontogenetic Development of the Human Sleep-Dream Cycle. *Science*, 152:604–619, 1966. (page 12)
- [41] J. Lee Kavanau. (page 12)
- [42] J L Kavanau. Memory, sleep and the evolution of mechanisms of synaptic efficacy maintenance. *Neuroscience*, 79(1):7–44, July 1997. (page 12)
- [43] Lulu Xie, Hongyi Kang, Qiwu Xu, Michael J Chen, Yonghong Liao, Meenakshisundaram Thiagarajan, John O'Donnell, Daniel J Christensen, Charles Nicholson, Jeffrey J Iliff, Takahiro Takano, Rashid Deane, and Maiken Nedergaard. Sleep drives metabolite clearance from the adult brain. *Science (New York, N.Y.)*, 342(6156):373–7, October 2013. (page 12)
- [44] Teofilo L. Lee-Chiong. *Sleep: A comprehensive handbook*. Wiley, 2006. (pages 12 and 16)
- [45] C A Everson, B M Bergmann, and A Rechtschaffen. Sleep deprivation in the rat: III. Total sleep deprivation. *Sleep*, 12(1):13–21, February 1989. (page 12)
- [46] K. Spiegel, K. Knutson, R. Leproult, E. Tasali, and E. Van Cauter. Sleep loss: A novel risk factor for insulin resistance and Type 2 diabetes. *Journal of Applied Physiology*, 99:2008–2019, 2005. (page 12)
- [47] J E Gangwisch, S B Heymsfield, B Boden-Albala, R M Buijs, F Kreier, T G Pickering, A G Rundle, G K Zammit, and D Malaspina. Short sleep duration as a risk factor for hypertension: analyses of the first National Health and Nutrition Examination Survey. *Journal of the American Heart Association*, 47:833–839, 2006. (page 12)
- [48] Francesco P Cappuccio, Saverio Stranges, Ngianga-Bakwin Kandala, Michelle A Miller, Frances M Taggart, Meena Kumari, Jane E Ferrie, Martin J Shipley, Eric J Brunner, and Michael G Marmot. Gender-specific associations of short sleep duration with prevalent

- and incident hypertension: the Whitehall II Study. *Hypertension*, 50:693–700, 2007. (page 12)
- [49] Francesco Portaluppi and Ramón C Hermida. Circadian rhythms in cardiac arrhythmias and opportunities for their chronotherapy. *Advanced drug delivery reviews*, 59:940–951, 2007. (page 12)
- [50] Michelle A Miller and Francesco P Cappuccio. Inflammation, sleep, obesity and cardiovascular disease. *Current vascular pharmacology*, 5:93–102, 2007. (page 13)
- [51] J T Arnedt, G J Wilde, P W Munt, and A W MacLean. How do prolonged wakefulness and alcohol compare in the decrements they produce on a simulated driving task? Technical Report 3, Department of Psychology, Queen's University, Kingston, Ont., Canada. j\_todd\_arnedt@brown.edu, 2001. (page 13)
- [52] D F Dinges, F Pack, K Williams, K A Gillen, J W Powell, G E Ott, C Aptowicz, and A I Pack. Cumulative sleepiness, mood disturbance, and psychomotor vigilance performance decrements during a week of sleep restricted to 4-5 hours per night. *Sleep*, 20(4):267–277, 1997. (page 13)
- [53] Hans Berger. Über das Elektrenkephalogramm des Menschen. *Archiv für Psychiatrie und Nervenkrankheiten*, 87(1):527–570, December 1929. (page 13)
- [54] E Aserinsky and N Kleitman. Regularly occurring periods of eye motility, and concomitant phenomena, during sleep. *Science (New York, N.Y.)*, 118(3062):273–4, September 1953. (page 13)
- [55] E Aserinsky. The discovery of REM sleep. *Journal of the history of the neurosciences*, 5:213–227, 1996. (page 13)
- [56] M A Carskadon and William C Dement. Normal Human Sleep: an Overview. In *Principles and practice of sleep medicine*, pages 16–26. 2011. (pages 14 and 15)
- [57] American Academy of Sleep Medicine. *International Classification of Sleep Disorders, Version 2: Diagnostic and Coding Manual*. 2005. (pages 16, 18, and 137)
- [58] G Keklund and T Akerstedt. Objective components of individual differences in subjective sleep quality. *Journal of sleep research*, 6:217–220, 1997. (page 19)
- [59] Morin CM and Espie CA. *Insomnia: A clinical guide to assessment and treatment*. Kluwer Academic/Plenum, 2003. (page 19)
- [60] Miles I. *Sleep Questionnaire and Assessment of Wakefulness*. Butterworths, Boston, 1982. (page 19)
- [61] A. B. Douglass, R. Bornstein, Nino G. Murcia, S. Keenan, L. Miles, V. P. Zarcone, C. Guilleminault, and W. C. Dement. The Sleep Disorders Questionnaire. I: Creation and multivariate structure of SDQ. *Sleep*, 17(2):160–7, 1994. (page 19)

## Bibliography

---

- [62] Zulley J, Palombini L, Raab H, Ohayon MM, Guilleminault C. Validation of the sleep-eval system against clinical assessments of sleep disorders and polysomnographic data. *Sleep*, 22(7):925–30, 1999. (page 19)
- [63] E Hoddes, V Zarcone, H Smythe, R Phillips, and W C Dement. Quantification of sleepiness: a new approach. *Psychophysiology*, 10:431–436, 1973. (page 19)
- [64] M W Johns. A new method for measuring daytime sleepiness: the Epworth sleepiness scale. *Sleep*, 14:540–545, 1991. (page 19)
- [65] Michael Thorpy, Andrew Chesson, Sarkis Derderian, Gihan Kader, Richard Millman, Samuel Potolicchio, Gerald Rosen, and Patrick J Strollo. Practice parameters for the use of actigraphy in the clinical assessment of sleep disorders. american sleep disorders association. *Sleep (Rochester)*, 18(4):285–287, 1995. (pages 20, 50, 52, and 58)
- [66] Timothy Morgenthaler, Cathy Alessi, Leah Friedman, Judith Owens, Vishesh Kapur, Brian Boehlecke, Terry Brown, Andrew Chesson, Jack Coleman, Teofilo Lee-Chiong, Jeffrey Pancer, and Todd J Swick. Practice parameters for the use of actigraphy in the assessment of sleep and sleep disorders: an update for 2007. *Sleep*, 30(4):519–29, April 2007. (pages 20, 50, and 52)
- [67] A Sadeh, P J Hauri, D F Kripke, and P Lavie. The role of actigraphy in the evaluation of sleep disorders. *Sleep*, 18(4):288–302, May 1995. (pages 20, 50, and 51)
- [68] Stacia K Martin and Charmane I Eastman. Sleep logs of young adults with self-selected sleep times predict the dim light melatonin onset. *Chronobiology international*, 19:695–707, 2002. (page 20)
- [69] Sandrine Devot, Reimund Dratwa, and Elke Naujokat. Sleep/wake detection based on cardiorespiratory signals and actigraphy. *Conference proceedings : ... Annual International Conference of the IEEE Engineering in Medicine and Biology Society. IEEE Engineering in Medicine and Biology Society. Conference*, 2010:5089–92, Jan 2010. (pages 20, 100, and 115)
- [70] A. L. Loomis, E. N. Harvey, and G. A. Hobart. Cerebral states during sleep, as studied by human brain potentials. (page 21)
- [71] Clete a Kushida, Michael R Littner, Timothy Morgenthaler, Cathy a Alessi, Dennis Bailey, Jack Coleman, Leah Friedman, Max Hirshkowitz, Sheldon Kapen, Milton Kramer, Teofilo Lee-Chiong, Daniel L Loube, Judith Owens, Jeffrey P Pancer, and Merrill Wise. Practice parameters for the indications for polysomnography and related procedures: an update for 2005. *Sleep*, 28(4):499–521, April 2005. (page 21)
- [72] Mary A. Carskadon and Allan Rechtschaffen. Monitoring and Staging Human Sleep. In *Principles and Practice of Sleep Medicine*, pages 1359–1377. 2005. (page 21)

- [73] Richard B. Berry, Rita Brooks, Charlene E. Gamaldo, Susan M. Harding, Carole L. Marcus, and Bradley V. Vaughn. The AASM Manual for the Scoring of Sleep and Associated Events: Rules, Terminology and Technical Specifications. Technical report, American Academy of Sleep Medicine, 2013. (page 22)
- [74] Shannon S Sullivan and Clete A Kushida. Multiple sleep latency test and maintenance of wakefulness test. *Chest*, 134(4):854–61, October 2008. (page 22)
- [75] Jay W McLaren, Peter J Hauri, Siong-Chi Lin, and Cameron D Harris. Pupilometry in clinically sleepy patients. *Sleep medicine*, 3(4):347–52, July 2002. (page 23)
- [76] R. A. Fisher. THE USE OF MULTIPLE MEASUREMENTS IN TAXONOMIC PROBLEMS. *Annals of Eugenics*, 7(2):179–188, September 1936. (pages 27 and 28)
- [77] Vladimir N. Vapnik Bernhard E. Boser, Isabelle M. Guyon. A Training Algorithm for Optimal Margin Classifiers. *Proceedings of the fifth annual workshop on Computational learning theory*, pages 144–152, 1992. (page 29)
- [78] G Hadley. *Nonlinear and Dynamic Programming*. Addison-Wesley Pub. Co., 1st edition, 1964. (pages 32 and 64)
- [79] Emanuel Parzen. On Estimation of a Probability Density Function and Mode, 1962. (page 36)
- [80] C C Berry. The kappa statistic. *JAMA : the journal of the American Medical Association*, 268(18):2513–4, November 1992. (pages 40 and 112)
- [81] L.R. Rabiner. A tutorial on hidden Markov models and selected applications in speech recognition. *Proceedings of the IEEE*, 77(2):257–286, 1989. (page 43)
- [82] Andrew J. Viterbi. Error bounds for convolutional codes and an asymptotically optimum decoding algorithm. *IEEE Transactions on Information Theory*, 13(2):260–269, 1967. (page 44)
- [83] G Jean-Louis, H von Gizycki, F Zizi, A Spielman, P Hauri, and H Taub. The actigraph data analysis software: II. A novel approach to scoring and interpreting sleep-wake activity. *Perceptual and motor skills*, 85:219–226, 1997. (page 49)
- [84] Sonia Ancoli-Israel, Roger Cole, Cathy Alessi, Mark Chambers, William Moorcroft, and Charles P Pollak. The role of actigraphy in the study of sleep and circadian rhythms. *Sleep*, 26(3):342–92, May 2003. (pages 50, 51, and 54)
- [85] Michael Littner, Clete A Kushida, W McDowell Anderson, Dennis Bailey, Richard B Berry, David G Davila, Max Hirshkowitz, Sheldon Kopen, Milton Kramer, Daniel Loube, Merrill Wise, and Stephen F Johnson. Practice parameters for the role of actigraphy in the study of sleep and circadian rhythms: an update for 2002. *Sleep*, 26(3):337–41, May 2003. (page 50)

## Bibliography

---

- [86] Kenneth L Lichstein, Kristen C Stone, James Donaldson, Sidney D Nau, James P Soeffing, David Murray, Kristin W Lester, and R Neal Aguillard. Actigraphy validation with insomnia. *Sleep*, 29(2):232–9, February 2006. (pages 51 and 52)
- [87] M Montserrat Sánchez-Ortuño, Jack D Edinger, Melanie K Means, and Daniel Almirall. Home is where sleep is: an ecological approach to test the validity of actigraphy for the assessment of insomnia. *Journal of clinical sleep medicine : JCSM : official publication of the American Academy of Sleep Medicine*, 6:21–29, 2010. (page 51)
- [88] Vincenzo Natale, Giuseppe Plazzi, and Monica Martoni. Actigraphy in the assessment of insomnia: a quantitative approach. *Sleep*, 32:767–771, 2009. (page 51)
- [89] Annie Vallières and Charles M Morin. Actigraphy in the Assessment of Insomnia. *Sleep*, 26(7):902–6, 2003. (page 51)
- [90] Borge Sivertsen, Siri Omvik, Odd E Havik, Stale Pallesen, Bjorn Bjorvatn, Geir Hostmark Nielsen, Sivert Straume, and Inger Hilde Nordhus. A comparison of actigraphy and polysomnography in older adults treated for chronic primary insomnia. *Sleep*, 29(10):1353–8, Oct 2006. (pages 51, 53, and 54)
- [91] Martin A King, Marc-Olivier Jaffre, Emma Morrish, John M Shneerson, and Ian E Smith. The validation of a new actigraphy system for the measurement of periodic leg movements in sleep. *Sleep medicine*, 6:507–513, 2005. (page 51)
- [92] Emilia Sforza, Mathis Johannes, and Bassetti Claudio. The PAM-RL ambulatory device for detection of periodic leg movements: a validation study. *Sleep medicine*, 6:407–413, 2005. (page 51)
- [93] M Elbaz, G M Roue, F Lofaso, and M A Quera Salva. Utility of actigraphy in the diagnosis of obstructive sleep apnea. *Sleep*, 25:527–531, 2002. (page 51)
- [94] F Gagnadoux, X L Nguyen, D Rakotonanahary, S Vidal, and B Fleury. Wrist-actigraphic estimation of sleep time under nCPAP treatment in sleep apnoea patients. *The European respiratory journal : official journal of the European Society for Clinical Respiratory Physiology*, 23:891–895, 2004. (page 51)
- [95] H A Middelkoop, G J Lammers, B J Van Hilten, C Ruwhof, H Pijl, and H A Kamphuisen. Circadian distribution of motor activity and immobility in narcolepsy: assessment with continuous motor activity monitoring. *Psychophysiology*, 32:286–291, 1995. (page 51)
- [96] Helene Werner, Luciano Molinari, Caroline Guyer, and Oskar G Jenni. Agreement rates between actigraphy, diary, and questionnaire for children's sleep patterns. *Archives of pediatrics & adolescent medicine*, 162(4):350–8, April 2008. (page 51)
- [97] M J Chambers. Actigraphy and insomnia: a closer look. Part 1. *Sleep*, 17:405–408; discussion 408–410, 1994. (page 52)

- [98] Pedro Pires, Teresa Paiva, and Joao Sanches. Sleep/wakefulness state from actigraphy. In *Pattern Recognition and Image Analysis, IbPRIA'09*, pages 362–369, Berlin, Heidelberg, 2009. Springer-Verlag. (pages 52, 60, and 65)
- [99] C P Pollak, W W Tryon, H Nagaraja, and R Dzwonczyk. How accurately does wrist actigraphy identify the states of sleep and wakefulness? *Sleep*, 24(8):957–65, Dec 2001. (page 53)
- [100] Christine Acebo and Monique K LeBourgeois. Actigraphy. *Respiratory care clinics of North America*, 12(1):23–30, viii, Mar 2006. (page 53)
- [101] Jean Paquet, Anna Kawinska, and Julie Carrier. Wake Detection Capacity of Actigraphy During Sleep. *Ethics*, pages 14–17, 2007. (page 53)
- [102] Joelle Tilmanne, Jérôme Urbain, Mayuresh V Kothare, Alain Vande Wouwer, and Sanjeev V Kothare. Algorithms for sleep-wake identification using actigraphy: a comparative study and new results. *Journal of sleep research*, 18(1):85–98, Mar 2009. (pages 53, 54, and 55)
- [103] Stephanie L Sitnick, Beth L Goodlin-Jones, and Thomas F Anders. The use of actigraphy to study sleep disorders in preschoolers: some concerns about detection of nighttime awakenings. *Sleep*, 31:395–401, 2008. (page 53)
- [104] Lisa J. Meltzer, Hawley E. Montgomery-Downs, Salvatore P. Insana, and Colleen M. Walsh. Use of actigraphy for assessment in pediatric sleep research, 2012. (page 53)
- [105] Luciane De Souza, Ana Amelia Benedito silva, Maria Laura, Nogueira Pires, Dalva Poyares, Sergio Tufik, and Helena Maria Calil. Further validation of actigraphy for sleep studies. *Sleep*, 26(1):81–85, 2003. (page 53)
- [106] Warren W Tryon. Issues of validity in actigraphic sleep assessment. *Sleep*, 27(1):158–65, Feb 2004. (page 53)
- [107] Jesse Gale, T Leigh Signal, and Philippa H Gander. Statistical artifact in the validation of actigraphy. *Sleep*, 28(8):1017–8, Aug 2005. (page 53)
- [108] C a Kushida, a Chang, C Gadkary, C Guilleminault, O Carrillo, and W C Dement. Comparison of actigraphic, polysomnographic, and subjective assessment of sleep parameters in sleep-disordered patients. *Sleep medicine*, 2(5):389–96, Sep 2001. (page 54)
- [109] Jan Hedner, Giora Pillar, Stephen D Pittman, Ding Zou, Ludger Grote, and David P White. A novel adaptive wrist actigraphy algorithm for sleep-wake assessment in sleep apnea patients. *Sleep*, 27(8):1560–6, Dec 2004. (pages 54, 73, 78, 135, and 136)
- [110] Walter Karlen, Claudio Mattiussi, and Dario Floreano. Improving actigraph sleep/wake classification with cardio-respiratory signals. *Conference proceedings : Annual International Conference of the IEEE Engineering in Medicine and Biology Society.*, 2008:5262–5, Jan 2008. (page 54)

## Bibliography

---

- [111] Pierluigi Casale, Oriol Pujol, and Petia Radeva. Human activity recognition from accelerometer data using a wearable device. In *Proceedings of the 5th Iberian conference on Pattern recognition and image analysis*, IbPRIA'11, pages 289–296, Berlin, Heidelberg, 2011. Springer-Verlag. (page 54)
- [112] Reijo Takalo, Heli Hytti, and Heimo Ihalainen. Tutorial on univariate autoregressive spectral analysis. *Journal of clinical monitoring and computing*, 19(6):401–10, Dec 2005. (page 54)
- [113] Miroslav Kubat and Stan Matwin. Addressing the curse of imbalanced training sets: One-sided selection. *Proceedings of the Fourteenth International Conference on Machine Learning*, 1997. (page 55)
- [114] Alexandre Domingues, Teresa Paiva, and J Miguel Sanches. An actigraphy heterogeneous mixture model for sleep assessment. *Conference Proceedings of the International Conference of IEEE Engineering in Medicine and Biology Society*, 2012. (page 58)
- [115] Alexandre Domingues, Teresa Paiva, and J Miguel Sanches. Statistical characterization of actigraphy data for sleep/wake assessment. *7th International Workshop on Biosignal Interpretation.*, 2012. (page 58)
- [116] Jyrki Lötjönen, Ilkka Korhonen, Kari Hirvonen, Satu Eskelinen, Marko Myllymäki, and Markku Partinen. Automatic sleep-wake and nap analysis with a new wrist worn online activity monitoring device vivago WristCare. *Sleep*, 26(1):86–90, February 2003. (page 60)
- [117] Ondrej Adamec, Alexandre Domingues, Teresa Paiva, and J Miguel Sanches. Statistical characterization of actigraphy data during sleep and wakefulness states. *Conference proceedings: Annual International Conference of the IEEE Engineering in Medicine and Biology Society*, 2010:2342–5, Jan. (page 60)
- [118] V Gimeno, T Sagales, L Miguel, and M Ballarin. The statistical distribution of wrist movements during sleep. *Neuropsychobiology*, 38(2):108–12, January 1998. (page 60)
- [119] H Shinkoda, K Matsumoto, J Hamasaki, Y J Seo, Y M Park, and K P Park. Evaluation of human activities and sleep-wake identification using wrist actigraphy. *Psychiatry and clinical neurosciences*, 52(2):157–9, April 1998. (page 60)
- [120] A. P. Dempster, N. M. Laird, and D. B. Rubin. Maximum likelihood from incomplete data via the em algorithm. *Journal of the Royal Statistical Society. Series B*, 39(1):1–38, 1977. (page 62)
- [121] S. Kullback and R. A. Leibler. On Information and Sufficiency, 1951. (page 65)
- [122] Curtis R. Vogel. *Computational methods for inverse problems*. Frontiers in applied mathematics. 2002. (page 69)

- [123] Hirotugu Akaike. Fitting autoregressive models for prediction. 1969. (page 70)
- [124] J. Novovicova P. Pudil and J. Kittler. Floating search methods in feature selection. *Pattern Recognition Letters*, (15):1119–25, 1994. (page 70)
- [125] W Stephen and Jennifer R Spiro. Comparing different methodologies used in wrist actigraphy. *Sleep Review*, Summer:1–6, 2001. (page 74)
- [126] R J Salin-Pascual, T A Roehrs, L A Merlotti, F Zorick, and T Roth. Long-term study of the sleep of insomnia patients with sleep state misperception and other insomnia patients. *The American Journal of Psychiatry*, 149(7):904–908, 1992. (page 74)
- [127] Cristina Crespo, Mateo Aboy, Jose Ramon Fernandez, and Artemio Mojón. Automatic identification of activity rest periods based on actigraphy. *Medical & Biological Engineering & Computing*, 50(4):329–340, Mar 2012. (page 79)
- [128] Richard D Lane, Shari R Waldstein, Margaret A Chesney, J Richard Jennings, William R Lovallo, Peter J Kozel, Robert M Rose, Douglas A Drossman, Neil Schneiderman, Julian F Thayer, and Oliver G Cameron. The rebirth of neuroscience in psychosomatic medicine, Part I: historical context, methods, and relevant basic science. *Psychosomatic medicine*, 71(2):117–34, February 2009. (page 82)
- [129] John E Hall and Arthur C Guyton. *Guyton and Hall Textbook of Medical Physiology*. Saunders Elsevier, 12th edition, 2011. (pages 82, 83, 87, and 91)
- [130] Terry N Thrasher. Baroreceptors and the long-term control of blood pressure. *Experimental physiology*, 89(4):331–5, July 2004. (page 86)
- [131] T.F Itani and E. Koushanpour. In *Images of the Twenty-First Century. Proceedings of the Annual International Engineering in Medicine and Biology Society*, pages 288–289. IEEE, 1989. (page 86)
- [132] K M Spyer. Neural organisation and control of the baroreceptor reflex. *Reviews of physiology, biochemistry and pharmacology*, 88:24–124, January 1981. (page 86)
- [133] W Osterrieder, A Noma, and W Trautwein. On the kinetics of the potassium channel activated by acetylcholine in the S-A node of the rabbit heart. *Pflugers Archiv : European journal of physiology*, 386:101–109, 1980. (page 87)
- [134] W Trautwein and M Kameyama. Intracellular control of calcium and potassium currents in cardiac cells. *Japanese heart journal*, 27 Suppl 1:31–50, 1986. (page 87)
- [135] H F Brown, D DiFrancesco, and S J Noble. How does adrenaline accelerate the heart? *Nature*, 280:235–236, 1979. (page 87)
- [136] E H Hon and S T Lee. Electronic Evaluation of the Fetal Heart Rate. VIII. Patterns preceding fetal death, further observations. *American journal of obstetrics and gynecology*, 87:814–26, November 1963. (page 87)

## Bibliography

---

- [137] G G Berntson, J T Bigger, D L Eckberg, P Grossman, P G Kaufmann, M Malik, H N Nagaraja, S W Porges, J P Saul, P H Stone, and M W Van Der Molen. Heart rate variability: Origins, methods, and interpretive caveats. *Psychophysiology*, 34(6):623–648, 1997. (pages 88 and 91)
- [138] A Malliani, F Lombardi, and M Pagani. Power spectrum analysis of heart rate variability: a tool to explore neural regulatory mechanisms. *British heart journal*, 71(1):1–2, January 1994. (page 88)
- [139] B Pomeranz, R J Macaulay, M A Caudill, I Kutz, D Adam, D Gordon, K M Kilborn, A C Barger, D C Shannon, and R J Cohen. Assessment of autonomic function in humans by heart rate spectral analysis. *The American journal of physiology*, 248:H151–H153, 1985. (page 88)
- [140] M S Houle and G E Billman. Low-frequency component of the heart rate variability spectrum: a poor marker of sympathetic activity. *The American journal of physiology*, 276(1 Pt 2):H215–23, January 1999. (page 88)
- [141] Gari D Clifford. *Signal Processing Methods for Heart Rate Variability Analysis*. PhD thesis, St Cross College, 2002. (pages 88, 92, and 102)
- [142] George E Billman. The LF/HF ratio does not accurately measure cardiac sympatho-vagal balance. *Frontiers in physiology*, 4:26, January 2013. (page 88)
- [143] S Y Kim and D E Euler. Baroreflex sensitivity assessed by complex demodulation of cardiovascular variability. *Hypertension*, 29:1119–1125, 1997. (page 88)
- [144] K.D.; Moore E.N. Spear, J.F.; Kronhaus and R.P. Kline. The effect of brief vagal stimulation on the isolated rabbit sinus node. *American Heart Association*, 44:75–88, 1979. (pages 89, 94, 95, and 97)
- [145] R D Berger, J P Saul, and R J Cohen. Transfer function analysis of autonomic regulation. I. Canine atrial rate response. *The American journal of physiology*, 256:H142–H152, 1989. (page 89)
- [146] I Hill-Smith and R D Purves. Synaptic delay in the heart: an ionophoretic study. *The Journal of physiology*, 279:31–54, June 1978. (page 90)
- [147] B. Hille. *Ionic Channels of Excitable Membranes*, volume 42. Sunderland, MA, 2nd edition, 1992. (page 90)
- [148] M N Levy, T Yang, and D W Wallick. Assessment of beat-by-beat control of heart rate by the autonomic nervous system: molecular biology technique are necessary, but not sufficient. *Journal of cardiovascular electrophysiology*, 4(2):183–93, April 1993. (page 90)
- [149] Shoji Ito, Hiroshi Sasano, Nobuko Sasano, Junichiro Hayano, Joseph A Fisher, and Hiro-tada Katsuya. Vagal nerve activity contributes to improve the efficiency of pulmonary gas exchange in hypoxic humans. *Experimental physiology*, 91:935–941, 2006. (page 90)

- [150] Robert W Shields. Heart rate variability with deep breathing as a clinical test of cardiovagal function. *Cleveland Clinic journal of medicine*, 76 Suppl 2:S37–40, May 2009. (page 91)
- [151] Nobuko Sasano, Alex E Vesely, Junichiro Hayano, Hiroshi Sasano, Ron Somogyi, David Preiss, Kiyoyuki Miyasaka, Hirotada Katsuya, Steve Iscoe, and Joseph A Fisher. Direct effect of Pa(CO<sub>2</sub>) on respiratory sinus arrhythmia in conscious humans. *American journal of physiology. Heart and circulatory physiology*, 282:H973–H976, 2002. (page 91)
- [152] J J Goldberger, M W Ahmed, M A Parker, and A H Kadish. Dissociation of heart rate variability from parasympathetic tone. *The American journal of physiology*, 266:H2152–H2157, 1994. (page 91)
- [153] L. Bernardi, F. Keller, M. Sanders, P. S. Reddy, B. Griffith, F. Meno, and M. R. Pinsky. Respiratory sinus arrhythmia in the denervated human heart. *Journal of Applied Physiology*, 67:1447–1455, 1989. (page 91)
- [154] J P Saul, R D Berger, P Albrecht, S P Stein, M H Chen, and R J Cohen. Transfer function analysis of the circulation: unique insights into cardiovascular regulation. *The American journal of physiology*, 261:H1231–H1245, 1991. (page 91)
- [155] R. W. DeBoer, J. M. Karemaker, and J. Strackee. Hemodynamic fluctuations and baroreflex sensitivity in humans: a beat-to-beat model. *Am J Physiol Heart Circ Physiol*, 253(3):H680–689, September 1987. (pages 91 and 93)
- [156] Michael H Bonnet. Heart rate variability measures add a new dimension to the understanding of sleepiness. *Sleep*, 35(3):307–8, March 2012. (page 91)
- [157] F Jurysta, J-P Lanquart, V Sputaels, M Dumont, P-F Migeotte, S Leistedt, P Linkowski, and P van de Borne. The impact of chronic primary insomnia on the heart rate–EEG variability link. *Clinical neurophysiology : official journal of the International Federation of Clinical Neurophysiology*, 120(6):1054–60, June 2009. (page 91)
- [158] R S Leung and T D Bradley. Sleep apnea and cardiovascular disease. *American journal of respiratory and critical care medicine*, 164(12):2147–65, December 2001. (page 92)
- [159] H Otzenberger, C Gronfier, C Simon, A Charloux, J Ehrhart, F Piquard, and G Brandenberger. Dynamic heart rate variability: a tool for exploring sympathovagal balance continuously during sleep in men. *The American journal of physiology*, 275:H946–H950, 1998. (page 92)
- [160] Emilio Vanoli, Philip B. Adamson, Ba-Lin, Gian D. Pinna, Ralph Lazzara, and William C. Orr. Heart rate variability during specific sleep stages : A comparison of healthy subjects with patients after myocardial infarction. *Circulation*, 91(7):1918–1922, 1995. (page 92)
- [161] B V Vaughn, S R Quint, J a Messenheimer, and K R Robertson. Heart period variability in sleep. *Electroencephalography and clinical neurophysiology*, 94(3):155–62, Mar 1995. (page 92)

## Bibliography

---

- [162] L Toscani, P F Gangemi, a Parigi, R Silipo, P Ragghianti, E Sirabella, M Morelli, L Bagnoli, R Vergassola, and G Zaccara. Human heart rate variability and sleep stages. *Italian journal of neurological sciences*, 17(6):437–9, December 1996. (page 92)
- [163] S Elsenbruch, M J Harnish, and W C Orr. Heart rate variability during waking and sleep in healthy males and females. *Sleep*, 22(8):1067–71, Dec 1999. (page 92)
- [164] Francesco Versace, Manola Mozzato, Giuliano De Min Tona, Corrado Cavallero, and Luciano Stegagno. Heart rate variability during sleep as a function of the sleep cycle. *Biological Psychology*, 63(2):149–162, May 2003. (page 92)
- [165] M H Bonnet and D L Arand. Heart rate variability: sleep stage, time of night, and arousal influences. *Electroencephalography and clinical neurophysiology*, 102(5):390–6, May 1997. (page 92)
- [166] Daniel E. Vigo, Barbara Ogrinz, Li Wan, Evgeny Bersenev, Francis Tuerlinckx, Omer Van den Bergh, and André E. Aubert. Sleep-wake differences in heart rate variability during a 105-day simulated mission to mars. *Aviation, Space, and Environmental Medicine*, 83(2):125–130, Feb 2012. (page 92)
- [167] S. J. Redmond, P. Chazal, C. O'Brien, S. Ryan, W. T. McNicholas, and C. Heneghan. Sleep staging using cardiorespiratory signals. *Somnologie - Schlafforschung und Schlafmedizin*, 11(4):245–256, Oct 2007. (pages 92, 100, and 117)
- [168] José Santos. A baroreflex control model using head-up tilt test. Master's thesis, Instituto Superior Técnico, 2008. (page 93)
- [169] V. Saks, P. Dzeja, U. Schlattner, M. Vendelin, A. Terzic, and T. Wallimann. Cardiac system bioenergetics: metabolic basis of the frank-starling law. *Journal of Physiology*, 571:253–273, 2006. (page 93)
- [170] Virginie Le Rolle, Alfredo I. Hernández, Pierre-Yves Richard, and Guy Carrault. An Autonomic Nervous System Model Applied to the Analysis of Orthostatic Tests. *Modelling and Simulation in Engineering*, 2008(i):1–15, 2008. (page 93)
- [171] M. Diaz-Insua and M. Delgado. Modeling and simulation of the human cardiovascular system with bond graph: A basic development. *Computers in Cardiology 1996*, 1996. (page 93)
- [172] A L Bardou, P M Auger, P J Birkui, and J L Chassé. Modeling of cardiac electrophysiological mechanisms: from action potential genesis to its propagation in myocardium. *Critical reviews in biomedical engineering*, 24:141–221, 1996. (page 93)
- [173] Thomas Heldt, Eun B Shim, Roger D Kamm, and Roger G Mark. Computational modeling of cardiovascular response to orthostatic stress. *Journal of applied physiology (Bethesda, Md. : 1985)*, 92:1239–1254, 2002. (page 93)

- [174] Arie M. Van Roon, Lambertus J.M. Mulder, Monika Althaus, and Gijsbertus Mulder. Introducing a baroreflex model for studying cardiovascular effects of mental workload. *Psychophysiology*, 41:961–981, 2004. (page 93)
- [175] M Ursino. Interaction between carotid baroregulation and the pulsating heart: a mathematical model. *The American journal of physiology*, 275(5 Pt 2):H1733–47, November 1998. (page 93)
- [176] M Ursino, A Fiorenzi, and E Belardinelli. The role of pressure pulsatility in the carotid baroreflex control: a computer simulation study. *Computers in biology and medicine*, 26(4):297–314, July 1996. (page 93)
- [177] M Ursino. A mathematical model of the carotid baroregulation in pulsating conditions. *IEEE transactions on bio-medical engineering*, 46(4):382–92, April 1999. (page 93)
- [178] A.R. Mejia-Rodriguez, M.J. Gaitan-Gonzalez, S. Carrasco-Sosa, and A. Guillen-Mandujano. Time varying heart rate variability analysis of active orthostatic and cold face tests applied both independently and simultaneously. *Computers in Cardiology*, 36:361–364, 2009. (pages 95 and 96)
- [179] A Steptoe and C Vögele. Cardiac baroreflex function during postural change assessed using non-invasive spontaneous sequence analysis in young men. *Cardiovascular research*, 24:627–632, 1990. (pages 95 and 96)
- [180] G Cybulski and W Niewiadomski. Influence of age on the immediate heart rate response to the active orthostatic test. *Journal of physiology and pharmacology : an official journal of the Polish Physiological Society*, 54(1):65–80, March 2003. (page 96)
- [181] R Vetter, J M Vesin, P Celka, and U Scherrer. Observer of the human cardiac sympathetic nerve activity using noncausal blind source separation. Technical report, 1999. (page 98)
- [182] Jongyoon Choi Jongyoon Choi and R. Gutierrez-Osuna. Using Heart Rate Monitors to Detect Mental Stress. *2009 Sixth International Workshop on Wearable and Implantable Body Sensor Networks*, 2009. (page 98)
- [183] H J Burgess, J Trinder, Y Kim, and D Luke. Sleep and circadian influences on cardiac autonomic nervous system activity. *The American journal of physiology*, 273(4 Pt 2):H1761–8, Oct 1997. (page 99)
- [184] Xi Long and Pedro Fonseca. Time-frequency analysis of heart rate variability for sleep and wake classification. (November):11–13, 2012. (page 100)
- [185] a M Bianchi, L Mainardi, E Petrucci, M G Signorini, M Mainardi, and S Cerutti. Time-variant power spectrum analysis for the detection of transient episodes in hrv signal. *IEEE transactions on bio-medical engineering*, 40(2):136–44, Feb 1993. (page 100)

## Bibliography

---

- [186] Giulia Tacchino, Sara Mariani, Matteo Migliorini, and Anna M Bianchi. Optimization of time-variant autoregressive models for tracking rem - non rem transitions during sleep. page 2236–2239, 2012. (page 100)
- [187] K Kesper, S Canisius, T Penzel, T Ploch, and W Cassel. Ecg signal analysis for the assessment of sleep-disordered breathing and sleep pattern. *Medical and biological engineering and computing*, 50(2):135–44, Feb 2012. (page 100)
- [188] Matteo Matteucci, Vincenza Castronovo, Luigi Ferini-Strambi, Sergio Cerutti, and Anna Maria Bianchi. Sleep staging from heart rate variability : time-varying spectral features and hidden markov models. *International Journal of Biomedical Engineering and Technology*, 3(3/4):246–263, 2010. (pages 100 and 115)
- [189] Tim Willemen, Dorien Van Deun, Vincent Verhaert, Marie Vandekerckhove, Vasileios Exadaktylos, Johan Verbraecken, Sabine Van Huffel, Bart Haex, and Jos Vander Sloten. An evaluation of cardio-respiratory and movement features with respect to sleep stage classification. *IEEE journal of biomedical and health informatics*, PP(99):1, September 2013. (pages 100 and 117)
- [190] Walter Karlen, Claudio Mattiussi, and Dario Floreano. Improving actigraph sleep/wake classification with cardio-respiratory signals. *Conference proceedings : Annual International Conference of the IEEE Engineering in Medicine and Biology Society. IEEE Engineering in Medicine and Biology Society. Conference*, 2008:5262–5, Jan 2008. (page 100)
- [191] Stephen J Redmond and Conor Heneghan. Cardiorespiratory-based sleep staging in subjects with obstructive sleep apnea. *IEEE transactions on bio-medical engineering*, 53(3):485–96, Mar 2006. (pages 100 and 117)
- [192] Devy Widjaja, Elke Vlemincx, and Sabine Van Huffel. Stress classification by separation of respiratory modulations in heart rate variability using orthogonal subspace projection \*. page 6123–6126, 2013. (page 104)
- [193] Miguel Almeida and Ricardo Vigário. Source separation of phase-locked subspaces. In *Proceedings of the 8th International Conference on Independent Component Analysis and Signal Separation*, ICA '09, pages 203–210, Berlin, Heidelberg, 2009. Springer-Verlag. (page 104)
- [194] Sebastian Canisius, Thomas Ploch, Volker Gross, Andreas Jerrentrup, Thomas Penzel, and Karl Kesper. Detection of sleep disordered breathing by automated ECG analysis. *Conference proceedings : ... Annual International Conference of the IEEE Engineering in Medicine and Biology Society. IEEE Engineering in Medicine and Biology Society. Conference*, 2008:2602–5, January 2008. (page 117)
- [195] Juha M Kortelainen, Martin O Mendez, Anna Maria Bianchi, Matteo Matteucci, and Sergio Cerutti. Sleep staging based on signals acquired through bed sensor. *IEEE*

- Transactions on Information Technology in Biomedicine*, 14(3):776–785, 2010. (page 117)
- [196] Richard S Rosenberg and Steven Van Hout. The American Academy of Sleep Medicine inter-scorer reliability program: sleep stage scoring. *Journal of clinical sleep medicine : JCSM : official publication of the American Academy of Sleep Medicine*, 9(1):81–7, January 2013. (page 117)
- [197] S. Pitchers K. Van Dam and M. Barnard. In *Proceedings of Wireless World Research Forum*. (page 120)
- [198] Hao, Yang, Foster, and Robert. Wireless body sensor networks for health-monitoring applications. *Physiological Measurement*, 29(11):R27–R56, November 2008. (page 120)
- [199] Benoît Latré, Bart Braem, Ingrid Moerman, Chris Blondia, and Piet Demeester. A survey on wireless body area networks. *Wireless Networks*, 17(1):1–18, November 2010. (pages 120, 121, and 122)
- [200] Practice parameters for the use of portable recording in the assessment of obstructive sleep apnea. Standards of Practice Committee of the American Sleep Disorders Association. *Sleep*, 17(4):372–7, June 1994. (page 122)
- [201] Nancy A Collop, W McDowell Anderson, Brian Boehlecke, David Claman, Rochelle Goldberg, Daniel J Gottlieb, David Hudgel, Michael Sateia, and Richard Schwab. Clinical guidelines for the use of unattended portable monitors in the diagnosis of obstructive sleep apnea in adult patients. Portable Monitoring Task Force of the American Academy of Sleep Medicine. *Journal of clinical sleep medicine : JCSM : official publication of the American Academy of Sleep Medicine*, 3(7):737–47, December 2007. (page 123)
- [202] Nancy A Collop, Sharon L Tracy, Vishesh Kapur, Reena Mehra, David Kuhlmann, Sam A Fleishman, and Joseph M Ojile. Obstructive sleep apnea devices for out-of-center (OOC) testing: technology evaluation. *Journal of clinical sleep medicine : JCSM : official publication of the American Academy of Sleep Medicine*, 7(5):531–48, October 2011. (page 123)
- [203] Joachim Behar, Aoife Roebuck, João S Domingos, Elnaz Gederi, and Gari D Clifford. A review of current sleep screening applications for smartphones. *Physiological measurement*, 34:R29–46, 2013. (page 124)
- [204] Abu Saleh Mohammad Mosa, Illhoi Yoo, and Lincoln Sheets. A Systematic Review of Healthcare Applications for Smartphones, 2012. (page 124)
- [205] A Roebuck, V Monasterio, E Gederi, M Osipov, J Behar, A Malhotra, T Penzel, and G D Clifford. A review of signals used in sleep analysis. *Physiological measurement*, 35(1):R1–R57, December 2013. (page 124)

## Bibliography

---

- [206] Shahid Mohammed Daly Jonathan Miranda Pureza Andre Hallack Niclas Palmius Stradling John Clifford Gari D Behar Joachim, Roebuck Aoife. An Evidence Based Android OSA Screening Application. In *Computing in Cardiology conference*, volume 40, pages 257–260, 2013. (page 124)
- [207] Zephyr-technology. <http://www.zephyr-technology.com/>. (page 125)
- [208] Ana L. N. Fred, José Guerreiro, Raúl Martins, Hugo Silva, and A. Lourenço. BITalino: A Multimodal Platform for Physiological Computing. In *Proc International Conf. on Informatics in Control, Automation and Robotics*, 2013. (page 126)
- [209] Dirk Cysarz, Roland Zerm, Henrik Bettermann, Matthias Frühwirth, Maximilian Moser, and Matthias Kröz. Comparison of respiratory rates derived from heart rate variability, ECG amplitude, and nasal/oral airflow. *Annals of biomedical engineering*, 36(12):2085–94, December 2008. (page 126)
- [210] Justin Boyle, Niranjan Bidargaddi, Antti Sarela, and Mohan Karunanithi. Automatic detection of respiration rate from ambulatory single-lead ECG. *IEEE transactions on information technology in biomedicine : a publication of the IEEE Engineering in Medicine and Biology Society*, 13:890–896, 2009. (page 126)
- [211] Ann M Berger, Kimberly K Wielgus, Stacey Young-McCaughan, Patricia Fischer, Lynne Farr, and Kathryn A Lee. Methodological challenges when using actigraphy in research. *Journal of pain and symptom management*, 36(2):191–9, August 2008. (page 126)
- [212] E Juulia Paavonen, Mika Fjällberg, Maija-Riikka Steenari, and Eeva T Aronen. Actigraph placement and sleep estimation in children. *Sleep*, 25(2):235–7, March 2002. (page 126)
- [213] J.J. Van Hiltten, H.A.M. Middelkoop, S.I.R. Kuiper, C.G.S. Kramer, and R.A.C. Roos. Where to record motor activity: an evaluation of commonly used sites of placement for activity monitors. 1993. (page 126)
- [214] D. Bensamoun, R. David, D. Alexandre, V. Marie, and P. Robert. Comparative study of postural recognition from four actigraphs during activities of daily living. *European Psychiatry*, 28, 2013. (page 126)
- [215] Patrick S. Hamilton and Willis J. Tompkins. Quantitative Investigation of QRS Detection Rules Using the MIT/BIH Arrhythmia Database. *IEEE Transactions on Biomedical Engineering*, BME-33(12):1157–1165, December 1986. (page 102)
- [216] G.D. Clifford, P.E. McSharry, and L. Tarassenko. Characterizing artefact in the normal human 24-hour RR time series to aid identification and artificial replication of circadian variations in human beat to beat heart rate using a simple threshold. In *Computers in Cardiology*, pages 129–132. IEEE, 2002. (page 102)